Adaptation of Target Load Functions for RAINS simulations of time delays of recovery caused by European reduction alternatives of acidifying compounds

Final Report

Service Contract N^{o} 070501/2004/380217/MAR/C1

Bilthoven, 06 February 2006

Netherlands Environmental Assessment Agency (MNP)
Unit for European Air Quality and Sustainability

Coordination Center for Effects (CCE)
J.-P.Hettelingh[1]
M.Posch
J.Slootweg

[1] j.p.hettelingh@mnp.nl; MNP-LED/CCE (PB24), www.mnp.nl/cce, P.O.Box 303, 3720 AH Bilthoven, The Netherlands

Contents

Acknowledgements

The methods and resulting maps contained in this report have partly been supported under service contract Service Contract N^{o} 070501/2004/380217/MAR/C1.

The results were co-produced under the workplan of the Effects Programme of the UNECE Convention on Long-range Transboundary Air Pollution (LRTAP-Convention), involving many institutions and individuals throughout Europe.

Part of the results described in this report were presented at the twenty fourth Session of the Working Group on Effects (Geneva, 31 August- 2 September 2005) and described in the CCE Status Report 2005 presented to the twenty third meeting of the Executive Body (Geneva 12-15 December 2005) of the LRTAP-Convention.

In addition the Coordination Center for Effects of the Netherlands Environmental Assessment Agency (MNP) associated with RIVM thanks the following:

- The Directorate for Climate Change and Industry of the Dutch Ministry of Housing, Spatial Planning and the Environment and Mr. J. Sliggers in particular for their continued support,
- The Working Group on Effects, the Task Force of the International Co-operative Programme on the Modelling and Mapping of Critical Levels and Loads and Air Pollution Effects, Risks and Trends for their collaboration and assistance,
- The EMEP Steering Body for its collaboration,
- The UNECE secretariat of the Convention on Long-range Transboundary Air Pollution for its valuable support, including the preparation of official documentations,

Abstract

European Critical Loads and Dynamic Modelling

The analysis of air pollution impacts on environment and health becomes ever more important for the support of air pollution policies also because the health risk op particulate matter has recently become more recognised . A number of air pollution abatement agreements will be reviewed and possibly revised in the near future. These include the UNECE Protocol to Abate Acidification, Eutrophication and Ground Level Ozone, the EC's National Emissions Ceiling Directive and Thematic Strategy for Air Pollution. In support of the review of the first two agreements the report provides updated European maps of critical loads for acidification and eutrophication as well as novel results regarding the temporal delay of damage or recovery of acidification. While decreasing since the 1980s, the exceedance of critical loads for acidification remains a European-wide issue. 'Acid rain' may seem yesterday's problem, but the risk of acidification of ecosystems continues to demand attention. Based on data provided by 14 countries, 95% of the European forest soils are estimated to recover by 2030 provided depositions of sulphur and nitrogen are sufficiently reduced below critical loads. It is noted that the exceedance of critical loads for eutrophication, and allied risks for biodiversity, remain high and widespread.

Keywords: acidification, atmospheric deposition, CCE background database, critical loads, eutrophication, exceedances.

Preface

This report describes the results of the call for data on critical loads on acidification and eutrophication and novel outcomes with European applications of dynamic models addressing time delays of recovery from acidification or damage caused by the latter.

In its 17th session in December 1999, the Executive Body of the Convention '... underlined the importance of ... dynamic modelling of recovery' (ECE/EB.AIR/68 p. 14, para. 51. b) to enable the assessment of time delays of recovery in regions where critical loads stop being exceeded and time delays of damage in regions where critical loads continue to be exceeded.

The Working Group on Effects (WGE), at its 23rd session (Geneva, 1-3 September 2004), approved the proposal made at the 20th Task Force meeting of the ICP-M&M (Laxenburg, 27-28 May 2004) to issue a call for data on critical loads for acidification and eutrophication, and for data on dynamic modelling of acidification (EB.AIR/WG.1/2004/2 para. 57c).

The Commission of the European Communities emphasized the importance of the response to the call for data, in particular by the EU Member States. The outcomes of the call are not only used for the support of policy processes under the Convention (possible revision process of the Gothenburg Protocol), but also have the potential to support the Clean Air for Europe (CAFE) programme under the European Commission (preparation of the revision of the National Emission Ceilings directive).

The CCE issued the call on 24 November 2004, setting the deadline to 28 February 2005. In addition to information provided in the Mapping Manual (www.icpmapping.org), also a detailed instruction document had been compiled by the CCE and distributed to the National Focal Centres and also made available on the CCE website (before 1 May 2005 www.mnp.nl/cce).

The objective of the call, in accordance to the medium-term work plan of the WGE, was to produce an updated database on critical loads and dynamic modelling results which could be made available for use in integrated assessment modelling to support European air pollution abatement policies.

Under service contract N° 070501/2004/380217/MAR/C1 the following objectives have been covered and fulfilled:

(1) Have developed methods for the translation of scientific knowledge on time delays of recovery (i.e. embedded in Target Load Functions) provided by National Focal Centres to the CCE, both under the CLRTAP, to indicators for use in RAINS, such as Target Load Isolines on the RAINS resolution of 50x50 km^2 EMEP grid cells (*see chapter 2 and Appendix A of this report*)

(2) Have developed appropriate and feasible ecosystem indicators, e.g. based on Target loads, Damage Delay Time (DDT) or Recovery Delay Time (RDT), in support of the work done by the team that is developing Cost-Benefit analysis of CAFE, lead by AEA Technology. As discussed with the Cost Benefit Analysis (CBA) team, specific attention will be given to provide an ecosystem specific break down of results (*chapter 2 and chapter 4 of this report)*

(3) Have interacted with, and provided to, the IIASA-RAINS team the data (or appropriate parameters derived thereof) for an update of the RAINS effects module to include updated critical loads for acidification and eutrophication and dynamic effects of acidification in EMEP grid cells. Results described in this report have been presented to - and taken note of - by the 23rd session of the Working Group on Effects (see document EB.AIR/WG.1/2005/10 in accordance with Task 6 of the Service contract), after which they have been released to the Centre for Integrated Assessment Modelling. The results have also been presented to the Task Force on Integrated Assessment Modelling (TFIAM, *Gothenburg, 8-9 December 2005*)

(4) Advise, as appropriate, on the possible use of RAINS environmental impact indicators, i.e. (1) critical load exceedances, (2) ecosystem protection, and (3) time delays of damage or recovery for carrying out CBA of air pollution issues, in particular in the Clean Air for Europe (CAFE) Programme. The possible use of these indicators is subject to the suitability of CBA methodologies, which are being developed elsewhere under CAFÉ (*see chapter 4 and Appendix B of this report*)

Chapter 1 serves as an executive summary including critical loads for acidification, eutrophication, exceedance maps and dynamic modelling of time delays of acidification impact changes. Chapter 2 analyses the data on critical loads and dynamic modelling submitted by National Focal Centres including an inter-country comparison of data statistics. Chapter 3 describes the latest CCE background database for calculating critical loads for forest soils in Europe. This database is used to provide critical loads in countries that did not submit any data. Chapter 4 summarizes recent CCE work to identify so-called impact factors that describe the relationship between marginal emission changes and changes in the area exceeded. This chapter particularly addresses the application in the optimization model of the RAINS model. Further development of such indicators including quantitative results using the CCE background database is described in Appendix B. The report is completed with Appendix A, which is a reprint of the 'instructions' provided to the NFCs to assist in their response to the call for data.

1 Status of European Critical Loads and Dynamic Modelling

Jean-Paul Hettelingh, Maximilian Posch, Jaap Slootweg

1.1 Acidification and eutrophication: background

The Working Group on Effects, at its 23rd session (Geneva, 1-3 September 2004), approved the proposal made at the 20th Task Force meeting of the ICP-M&M (Laxenburg, 27-28 May 2004) to issue a call for data on critical loads for acidification and eutrophication, and for data on dynamic modelling of acidification (EB.AIR/WG.1/2004/2 para. 57c).

The objective of the call, in accordance to the medium-term work plan of the WGE was to produce an updated database on critical loads and dynamic modelling results which could be submitted to Task Force on Integrated Assessment Modelling (TFIAM).

At the meeting of the Working Group on Effects the representative of the Commission of the European Communities emphasized the importance of the response to the call for data, in particular by the EU member states. The outcomes of the call are not only used for the support of policy processes under the Convention (possible revision process of the Gothenburg Protocol), but also have the potential to support the Clean Air for Europe (CAFE) programme under the European Commission (preparation of the revision of the National Emission Ceilings directive).

The CCE issued the call on 24 November 2004, setting the deadline to 28 February 2005. In addition to information provided in the Mapping Manual (www.icpmapping.org), also detailed instructions had been compiled by the CCE and distributed to the National Focal Centres. It was also made available on the CCE website (www.mnp.nl/cce) and can be found in Appendix A.

The following sections provide a summary of the results of the call for data on critical loads for acidification and eutrophication and dynamic modelling variables, including exceedance maps. A more detailed overview and analysis of national data submissions regarding critical loads and dynamic modelling variables is presented in Chapter 2, whereas country reports can be found in Part II of this report.

1.2 Response to the call for data

In 2005 fourteen parties under the Convention submitted updated data on critical loads of acidity and of nutrient-N, while 13 countries provided dynamic modelling data. Considering earlier submissions of Parties Table 1-1 gives an overview of the year in which the latest update by a NFC was recorded.

The critical loads consist of four basic variables which were asked to be submitted and which were used to support the Gothenburg Protocol. These variables are the basis for the maps used in the effect modules of the European integrated assessment modelling effort: (a) the maximum allowable deposition of S, $CL_{max}(S)$, i.e. the highest deposition of S which does not lead to 'harmful effects' in the case of zero nitrogen deposition, (b) the minimum critical load of nitrogen, $CL_{min}(N)$ to ensure sufficient nitrogen for plant uptake including nitrogen immobilisation (c) the maximum 'harmless' acidifying deposition of N, $CL_{max}(N)$, in the case of zero sulphur deposition, and (d) the critical load of nutrient N, $CL_{nut}(N)$, preventing eutrophication of ecosystems.

Table 1-1. Overview of the year in which a Party submitted the latest update on critical loads for acidification, eutrophication and dynamic modelling data.

	Critical loads for Acidification based on data of:		Critical loads for eutrophication based on data of:		Dynamic Modelling data based on data of:	
Austria (AT)		2005		2005		2005
Belgium (BE)[1]	2003[1]		2003[1]		-	
Bulgaria (BG)		2005		2005		2005
Belarus (BY)		2005		2005	-	
Switzerland (CH)		2005		2005		2005
Cyprus (CY)	2004		2004		-	
Czech Rep. (CZ)		2005		2005		2005
Germany (DE)		2005		2005		2005
Denmark (DK)	2004		2004		-	
Estonia (EE)	2001		2001		-	
Spain (ES)	1997		1997		-	
Finland (FI)	2004		2004		-	
France (FR)		2005		2005		2005
United Kingd. (GB)		2005	2004			2005
Croatia (HR)	2003		2003		-	
Hungary (HU)	2004		2004		2004	
Ireland (IE)		2005		2005		2005
Italy (IT)		2005		2005		2005
Moldava (MD)	1998		1998		-	
Netherlands (NL)		2005		2005		2005
Norway (NO)		2005		2005		2005
Poland (PL)		2005		2005		2005
Russia (RU)	1998		1998		-	
Sweden (SE)		2005		2005		2005
Slovakia (SK)	2003		2003		-	
Total # parties	11	14	11	14	1	13

[1]The last update of data from Wallonia is of 2001

Dynamic modelling results submitted in 2005 may be different to the results of 2004 also because depositions of acidifying compounds had to be used which were now computed with the Unified Model on an EMEP50 grid (see Simpson et al., 2003).

1.3 Critical load maps

This section contains maps of critical loads for ecosystems within 50×50 km^2 EMEP (EMEP50) grid cells. The maps are based on updated national contributions from 14 countries. For other countries the most recent data submission was used as listed in Table 1-1. For countries that never submitted critical loads data the European background database (see Chapter 4) has been used.

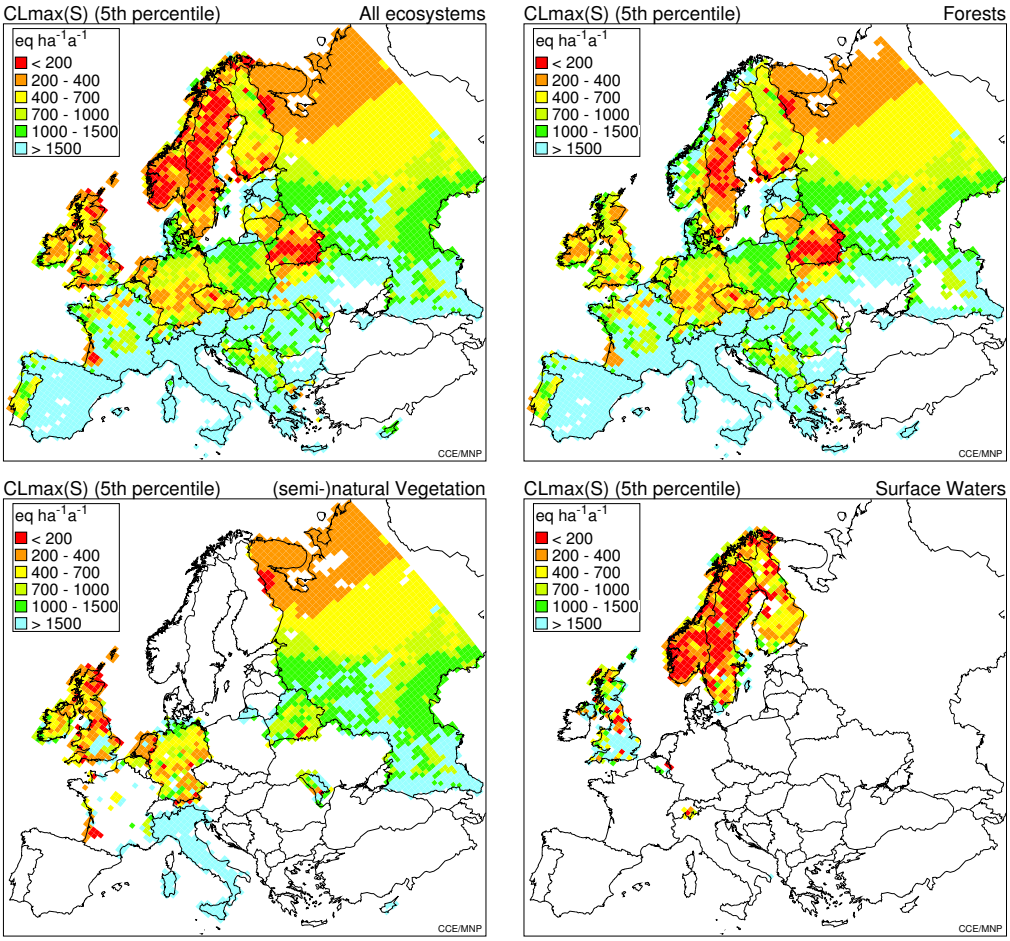

Figure 1.1. The 5th percentiles of the critical loads for acidity for all ecosystems (top left), forests (top right), semi-natural vegetation (bottom left) and surface waters. The maps present these quantities on the EMEP50 grid.

Figure 1.1 shows 5th percentile maps of $CL_{max}(S)$ for all ecosystems combined (top-left), forest ecosystems (top-right), semi-natural vegetation (bottom-left) and aquatic ecosystems. Low critical loads below 200 eq ha^{-1}a^{-1} (red shaded) show up north of 50^o latitude. In Sweden low critical loads reflect highly sensitive forest and aquatic ecosystems. In Belarus low deposition values are needed to protect forests and natural vegetation. In south-western France low critical loads exist for semi-natural vegetation.

Figure 1.2 shows analogous maps for $CL_{nut}(N)$. Low values of the 5th percentile (below 400 eq ha^{-1}a^{-1}) occur particularly for forest soils in most of Europe.

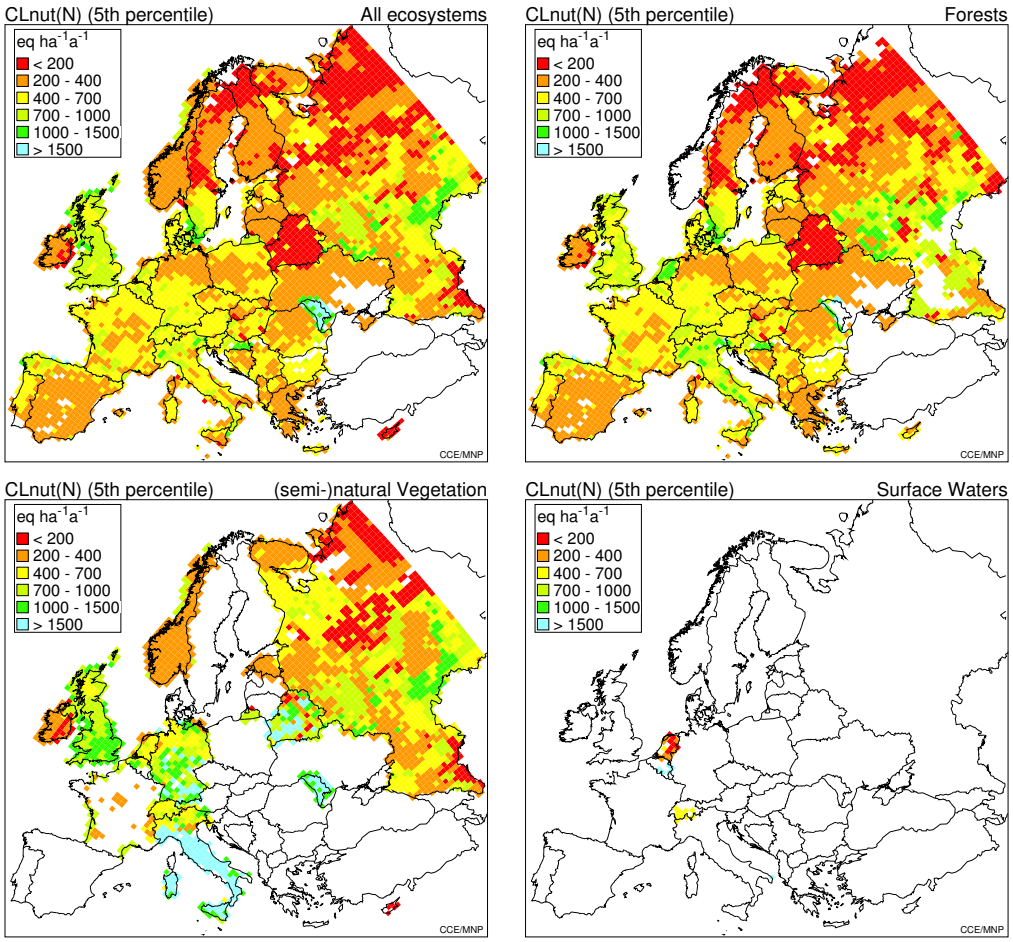

Figure 1.2 The 5th percentiles of the critical loads of nutrient nitrogen for all ecosystems (top left), forests (top right), semi-natural vegetation (bottom left) and surface waters. The maps present these quantities on the EMEP50 grid.

1.4 Robustness of critical load submissions

Figure 1-3 provides a comparison of the statistics of the national focal centre submissions since 1998 until the year in which the NFC made its last update. The minimum, 5th, 25th (lower quartile), 50th, 75th (upper quartile), 95th percentiles and the maximum of the critical loads of each country that submitted data are shown in an analogy to the well known 'Box and Whisker plot', i.e. a 'diamond plot'. A diamond plot offers some visual advantages, e.g. when diamonds are overlaid.

Statistics of $CL_{max}(S)$ are on the left ranging over an interval of 0 to 4000 eq $ha^{-1}a^{-1}$, while $CL_{nut}(N)$ (right) ranges from 0 to 2000 eq $ha^{-1}a^{-1}$. If we focus on the submission of this year and 2004 the following can be said. Compared to 2004 the median values (shown as vertical line dividing a 'diamond') of $CL_{max}(S)$ in 2005 increased in Austria, Switzerland, the Czech Republic, France, Norway and Poland, while decreasing in Belarus, Germany, the Netherlands and Sweden. The median value of data for $CL_{nut}(N)$ in 2005 revealed an increase for submissions from Austria, Bulgaria, Belarus, Germany, France, Italy, Poland and Sweden while the median decreased in the Czech Republic, Ireland and the Netherlands.

The striking increase of Austrian critical loads submitted in 2005 in comparison to earlier submissions is the result of replacing the entire database by another one due to improved knowledge on base cation weathering.

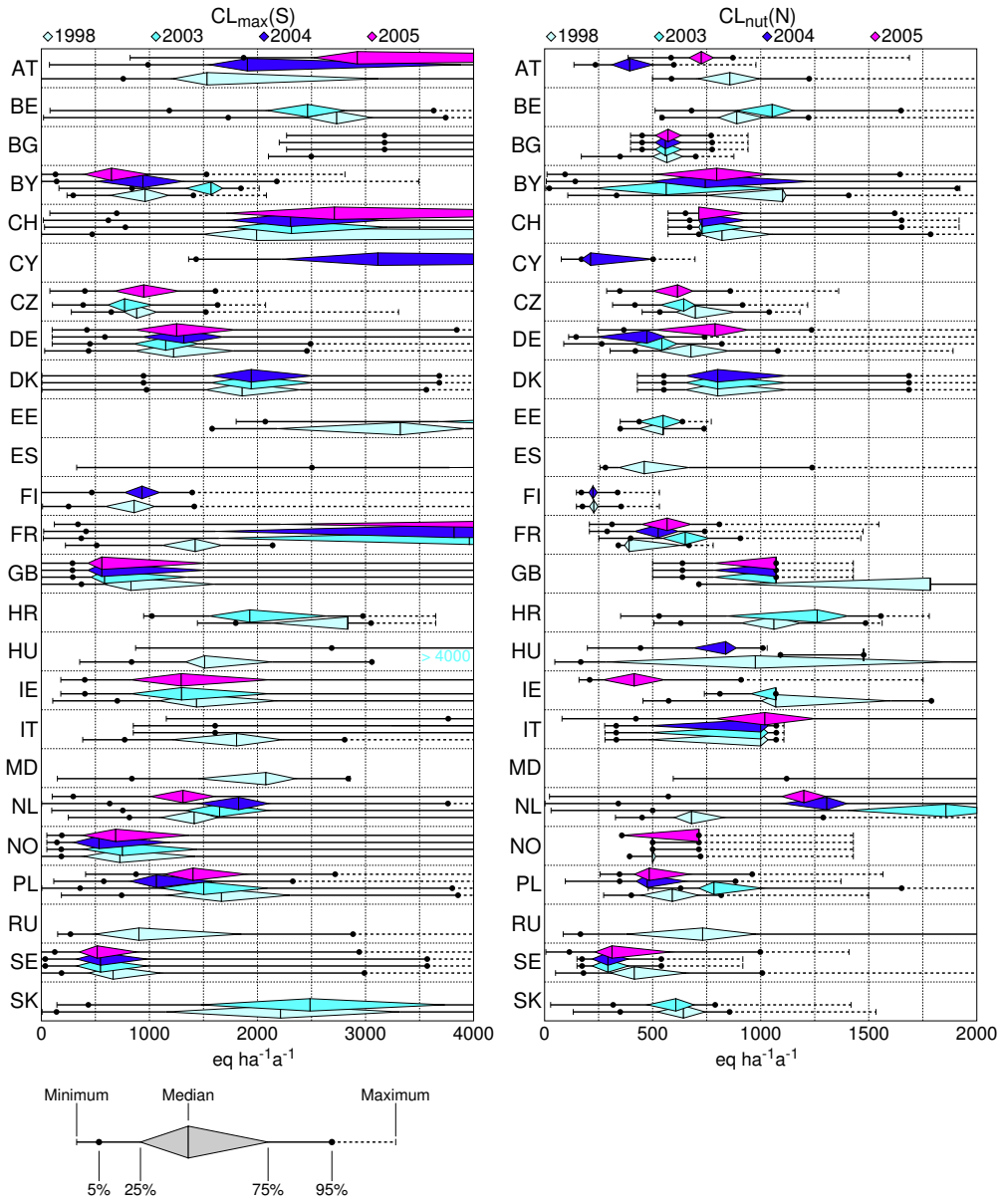

Figure 1-3. Diamond plot of the minimum (left extreme), 5th (left dot), 25th (left corner of diamond), 50th (vertical line in the diamond), 75th (right corner), 95th (right dot) percentiles and maximum (right extreme) critical loads of $CL_{max}(S)$ (left) and $CL_{nut}(N)$ (right) for the national data of (or before) 1998 (light blue), 2003 (turquoise), 2004 (dark blue) and 2005 (purple), respectively.

Inspecting the range of critical loads submitted since 1998 (which have been used for the support of the Gothenburg protocol) we can see that the last recorded NFC submission of the 5th percentile $CL_{max}(S)$ was markedly lower than in 1998 for Belgium, Belarus, the Czech Republic, France, Croatia, Ireland, United Kingdom, the Netherlands and Sweden while the median shifted downwards since 1998 in Belgium, Belarus, United Kingdom, Croatia, Ireland, the Netherlands, Poland and Sweden. Finally, it can be concluded that the $CL_{max}(S)$ values between the 25th and 75th percentile ('the diamond') generally show a cluster between 1998 and the last recorded submission. This is most striking in most of the country data of which the median in 2005 has shifted within a range of about 500 eq $ha^{-1}a^{-1}$ from the median in 1998. With respect to $CL_{nut}(N)$ the 5th percentile of the last recorded submission decreased with respect to the 1998 data in Belarus, Switzerland, the Czech Republic, Germany, France, Croatia, Ireland, Norway, Sweden and Slovakia. Also for $CL_{nut}(N)$ submissions of data in the range between the 25th and 75th percentile a clustering tendency can be remarked between 1998 and the latest recorded year for most of the countries. This tendency does not contradict the preliminary assertion that critical loads data have been robust over time.

1.5 Critical load exceedances and robustness

The term exceedance in this section refers to the 'average accumulated exceedance' (AAE). The AAE is the area-weighted average of exceedances (accumulated over all ecosystem points) in a grid cell, and not only the exceedance of the most sensitive ecosystem. See Posch *et al.* (2001) for the mathematical formulation. An AAE may be computed for all ecosystem categories within a grid cell, but also for one single ecosystem category (such as a forest) in a grid cell for which data points are submitted by an NFC. The European database of critical loads (both submitted and from the back ground database) covers 5,918,115 km^2 of ecosystem area (see Table 1-2) part of which is covered by ecosystems of 25 Parties under the LRTAP Convention that have submitted data over the past 15 years (1,654,876 km^2 is covered by critical loads data from the EU25 of which 18 Member States submitted data).

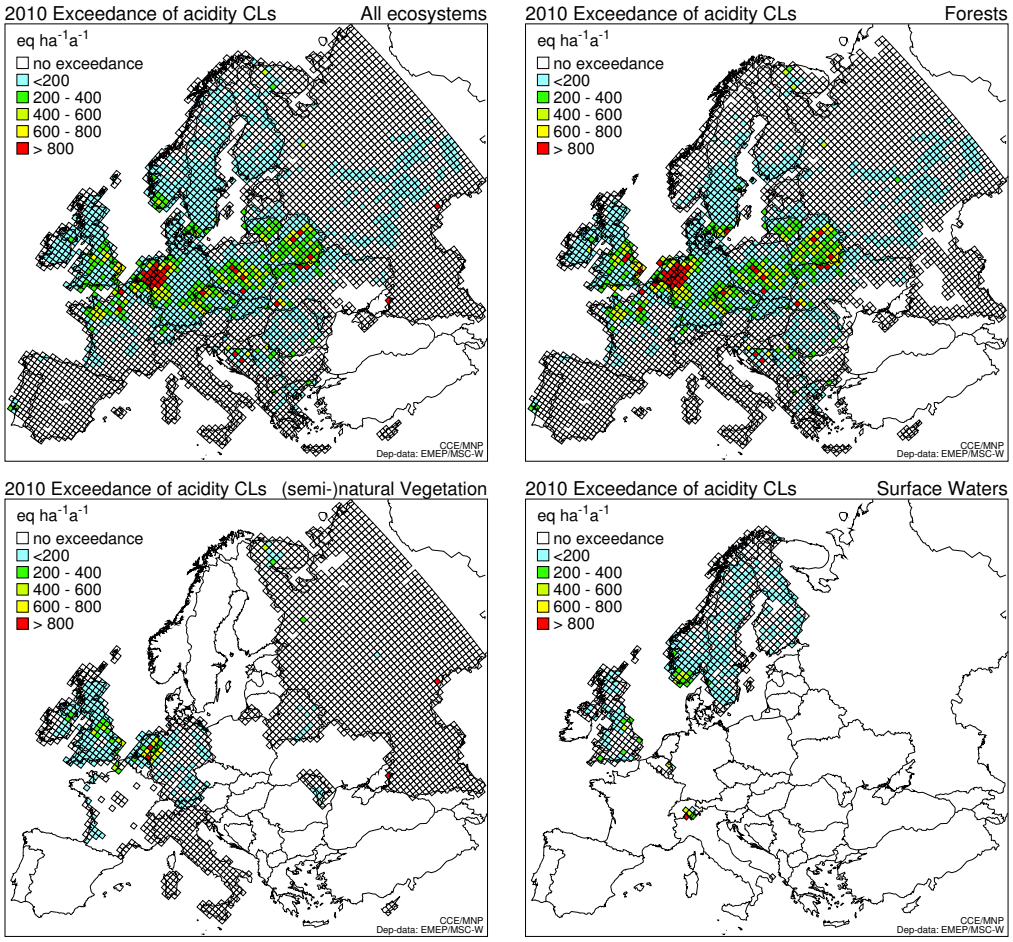

Figure 1-4. Average Accumulated Exceedance for acidity for all ecosystems (top left), forests (top right), vegetation (bottom left) and surface water using acid deposition computed by the EMEP Unified Model for 2010 using the CCE critical loads database of 2005

Figure 1-4 shows the AAE of acidity with the highest values occurring for exceedances in forest soils mostly north of 50^o latitude and for vegetation on the border of the Netherlands and Germany and in the east of the United Kingdom.

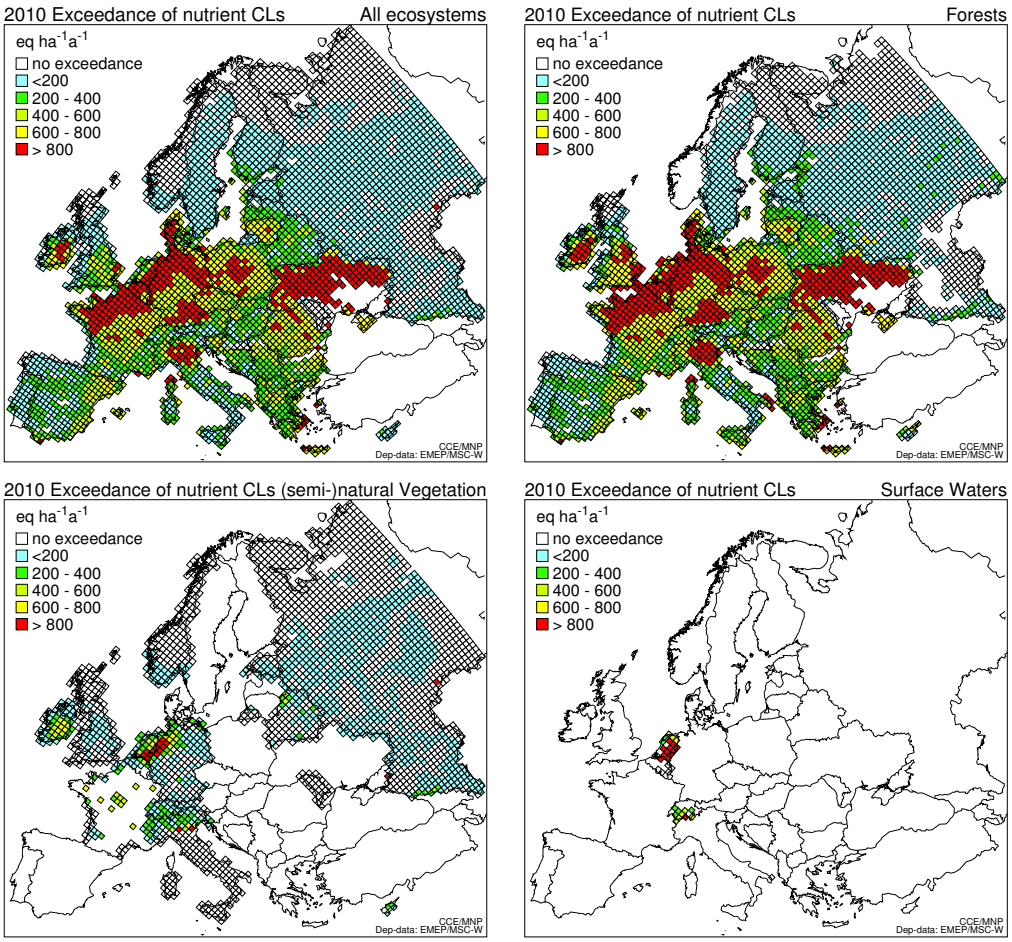

Figure 1-5. Average Accumulated Exceedance for eutrophication for all ecosystems (top left), forests (top right), vegetation (bottom left) and surface water using deposition of oxidized and reduced nitrogen computed by the EMEP Unified Model for 2010 using the CCE critical loads database of 2005

.

Figure 1-5 shows the AAE of critical loads of nutrient nitrogen. It reveals that submitted data on the critical load of nutrient nitrogen focuses on forest soils (top right). The highest exceedances are south of 58^{o} latitude with peaks in a broad coastal area between northern France and Denmark as well as in the north of Italy. Semi natural vegetation at risk occurs mostly in the border area between the Netherlands and Germany.

Figures 1-4 and 1-5 illustrate the spatial variation of the AAE. The cross border variation of exceedances was shown in Hettelingh et al. (2004) to change in particular due to the application of the EMEP Unified Model which replaced the lagrangian model results. We will not repeat the comparison here between the exceedances computed with the lagrangian and Unified Model. Suffices to say that it was shown that the spatial distribution of exceedances computed with the Unified Model was robust (areas with high exceedances under the lagrangian remained high under the Unified Model) but that the magnitude of the exceedances increased.

In Figure 1-6 we focus on the influence of the change of acidity critical load since 1998 on the national distribution of exceedances with particular attention on the occurrence of high national exceedances (the median and 95th percentile of the exceedance distribution in each country).

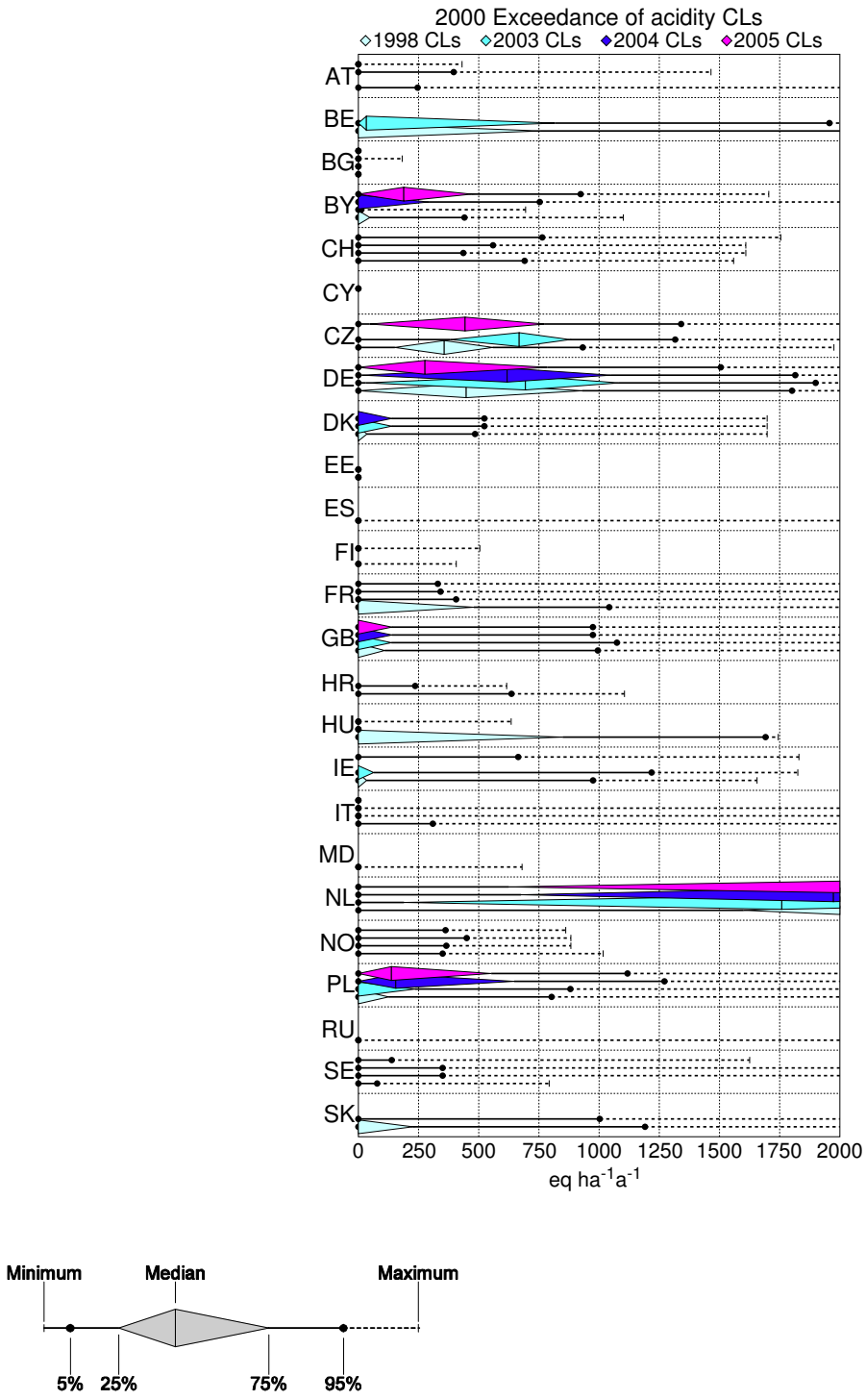

Figure 1-6. Diamond plot of national exceedances for acidity computed with critical load databases from 1998 until 2005, or the latest recorded submission of a National Focal Centre using depositions computed with the EMEP Unified Model and acidifying emissions of 2000.

Figure 1-6 shows that the median of the exceedances with recent critical loads (purple diamonds) compared to the median using 1998 critical loads (light blue) increased in Belarus, the Czech Republic, the Netherlands and in Poland. In the other countries the median exceedance is zero or decreased somewhat in comparison to the distribution of exceedances in 1998 as can be seen for Germany. Since the 1998 submission, the 95th percentile

(the right dot) of the distribution of exceedances increased in Belarus (about +483 eq ha^{-1} a^{-1}), the Czech Republic (about +409 eq ha^{-1} a^{-1}), Poland (about +316 eq ha^{-1} a^{-1}), Sweden (about +61 eq ha^{-1} a^{-1}) and the Netherlands (about +255 eq ha^{-1} a^{-1}). Exceedances in the Netherlands are the highest in comparison to other countries that submitted critical load data. A decrease between 1998 and 2005 of the 95th percentile exceedance is seen in Austria (about -246 eq ha^{-1} a^{-1}), Switzerland (about -73), Germany (about -296 eq ha^{-1} a^{-1}) and France (about -711 eq ha^{-1} a^{-1}).

Finally, Figure 1-7 displays the temporal development since 1940 of the Average Accumulated Exceedance of critical loads for acidity on all European ecosystems (top left) and of the ecosystem area percentage that is unprotected by acid deposition (top right). The development of the AAE illustrates the marked decrease of AAE especially on forest soils (brown graph). In 1985 about 60% of the forest soils (broadly distributed in Europe) and more than 40% of the surface waters (in northern Europe in particular) are unprotected. In 2010 these percentages become reduced below 20%. From Figure 1-4 it can be seen that the exceeded forest ecosystems in 2010 are located in about one third of the EMEP grid cells covering pan-Europe.

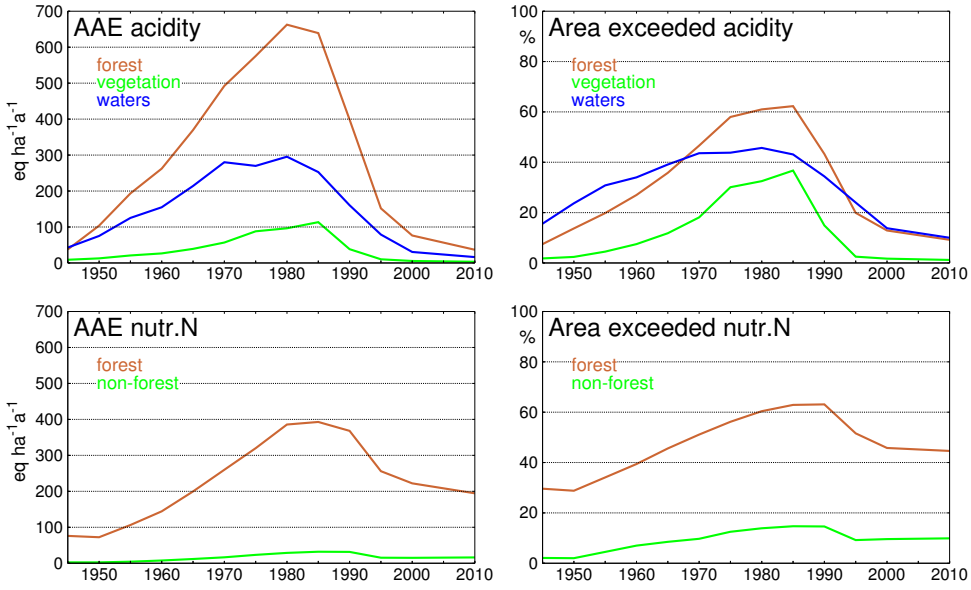

Figure 1-7. The Temporal development between 1945 and 2010 of the Average Accumulated Exceedance (AAE) of critical loads for acidity on all European ecosystems (top left), of the ecosystem area percentage that is exceeded by acid deposition (top right), of the AAE for eutrophication (bottom left) and % of areas unprotected from eutrophication (bottom right).

Figure 1-7 also shows that natural vegetation continues to be at risk of acid deposition after 1995 mostly in Germany, the Netherlands and in the United Kingdom (see Figure 1-4).

With respect to European forest ecosystems at risk of eutrophication, Figure 1-7 (bottom graphs) illustrates that the European AAE has decreased from about 400 to 200 eq ha^{-1} a^{-1} between 1985 and 2010 (bottom left graph). In terms of areas this implies (bottom right map) a reduction of unprotected areas from more than 60% in 1985 to about 45% in 2010. Note that about 10% of natural vegetation remains at risk of nutrient nitrogen as of about 1995. The latter also holds for surface waters, data for which are too limited to produce a meaningful plot from a European point of view.

1.6 Dynamic modelling[2]

Dynamic modelling and terminology

Important dynamic modelling results for possible use by the TFIAM are so-called target loads. A target load is the deposition (path) which ensures recovery by having the prescribed chemical (or, ideally, biological) criterion (e.g., the Al:Bc ratio) be met in a given year and maintained thereafter. The variety of deposition paths to reach a target load is numerous. We restrict to deposition pathways that are characterised by three numbers (years): (i) the protocol year, (ii) the implementation year, and (iii) the target year (see Figure 1-8). The protocol year for dynamic modelling is the year up to which the deposition path is assumed to be known and cannot be changed any more. This can be the present year or a year in the (near) future, for which emission reductions are already agreed. As *protocol year* countries were requested to use 2010, the year for which the Gothenburg Protocol and the EU NEC Directive are expected to be in place. The *implementation year* for dynamic modelling is the year in which all reduction measures to reach the final deposition (the target load) are assumed to be implemented *relative to a new protocol or directive.*

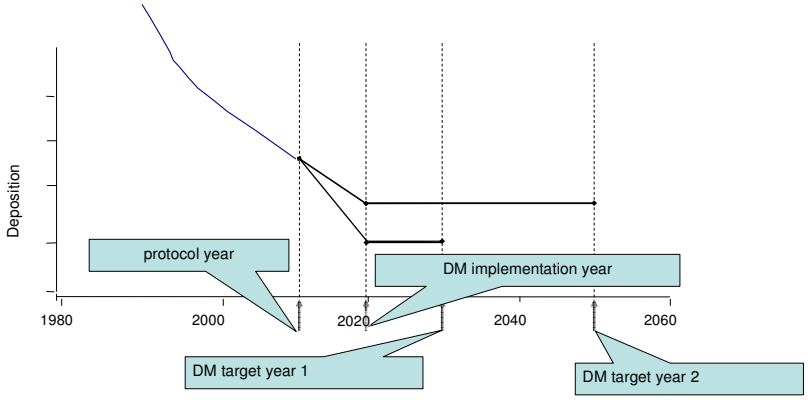

*Figure 1-8. Schematic representation of deposition paths leading to target loads by dynamic modelling (DM), characterised by three key years. (i) The year up to which the (historic) deposition is fixed (**protocol year**); (ii) the year in which the emission reductions leading to a target load are implemented (**DM implementation year**); and (iii) the years in which the chemical criterion is to be achieved (**DM target years**) (Source: Posch et al., 2003).*

Between the protocol year and the implementation year deposition is assumed to change linearly. After consultation with the chairmen of the ICP M&M, the WGE, the Working Group on Strategies and Review (WGSR) and other Convention representatives, 2020 was chosen as a preliminary implementation year and 2030 and 2050 as *target year.* A target year for dynamic modelling is the year in which the chemical criterion (e.g., the Al:Bc ratio) is met (for the first time). For scientific and technical purposes countries were also requested to submit a target load for 2100.

In addition to information on target loads and target years, National Focal Centres (NFCs) were also requested to ensure consistency between critical loads and dynamic modelling. This implies that each ecosystem-record in the critical load database should contain data that can be used to compute critical loads and to run the dynamic model. However, to maintain important statistical information on the (distribution of) sensitivity of ecosystems within an EMEP grid cell, NFCs were requested not to leave out records for which only critical loads and no dynamic modelling data are available. Deposition data are based on the Unified Model of EMEP (Simpson et al., 2003). However, no historical data based on the Unified Model of EMEP is yet available. Therefore, the ratio in 2000 of the magnitude of depositions generated by the lagrangian model (on 150×150 km^2; Schöpp et al., 2003; EMEP,

[2] Part of this work is supported by the European Commission under Service Contract 070501/2004/380217/MAR/C1

1998) to those from the new EMEP Unified Model (on 50×50 km^2) were used as a basis to scale the historical lagrangian deposition trends between 1880 and 2000.

Dynamic modelling results

A geographical representation of the areas for which we received target loads to ensure recovery in 2030, 2050 and 2100 is shown in Figure 1-9. Target loads have been set equal to critical loads in areas which are 'safe', i.e. where critical loads are not exceeded or critical limits niot violated (see Table 2-2 columns 7, 11, 15) and in areas where target loads have not been computed. A map showing grid cells in which target loads have been computed is given in Chapter 2 (see Fig 2-2). Target loads are set to 0 in areas where they are infeasible.

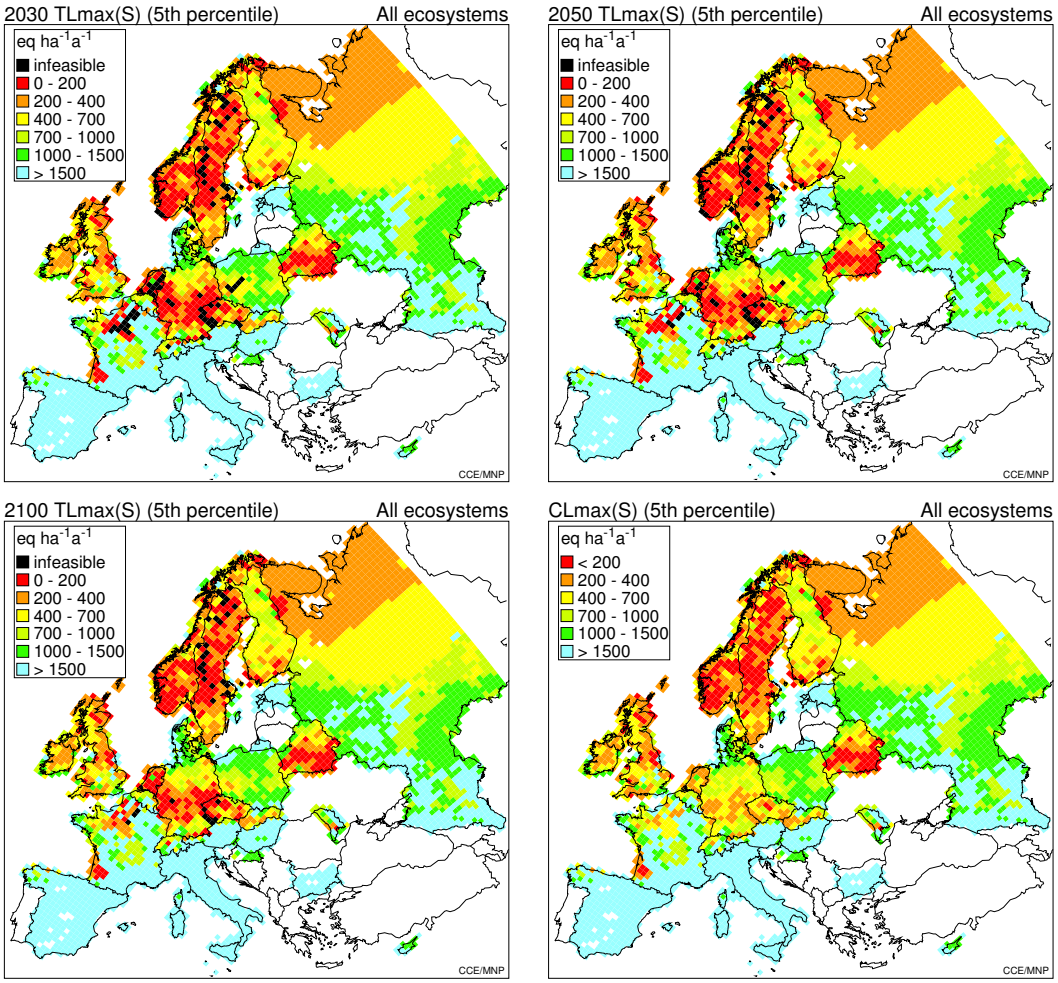

Figure 1-9. Location and magnitude of target loads that lead to recovery of 95% of the ecosystem area in 2030 (upper left), 2050 (upper right) and 2100 (lower left). For comparison the 5% map of CLmax(S) is shown as well.

Comparison of target load maps to the critical load map in Figure 1-9 shows grid cells where the 5th percentile target load values are lower than critical loads values (lower-right map) e.g. in the Czech Republic, France, Germany, the Netherlands, Poland and Sweden. Grid cells where target loads are equal to critical loads include areas for which dynamic modelling was not performed. Other general remarks that can be made with respect to Figure 1-9 are the following. Firstly, a target load which is identified to reach a recovery in 2100 is higher (or at critical load) than the target load set to meet recovery in an earlier year. This can be seen in a number of grids when comparing the shading-class of target load values in 2100 (Figure 1-9, bottom-left map) to the same grids in 2030 (Figure 1-9, top-left map). Secondly, one should be aware that intervals are used in Figure 1-9 to identify a colour for displaying the value of the 5th percentile target load in a grid cell. When comparing target load values in a late year (e.g. 2100) to an earlier year (e.g. 2030) colour changes only occur when the 5th percentile target

load value jumps from an interval of high values to one with lower values. Finally, note that ecosystems which are subject to the risk of (very) small exceedances will tend to have target load values that will not significantly vary over target years.

We were able to compute Recovery Delay Times (RDT) under the Base Line Current Legislation (BL-CLE) scenario of which the deposition files became available from IIASA in the autumn of 2005 as result of the assessment of the CAFE programme. It turned out in the CLRTAP-domain that 29.2% (25.7% in EU25) of the area which is not safe now could recover in the future, i.e. 20.2% (21.9%) before 2030, 20.7% (22.5%) before 2050 and 22.3% (24.2) before 2100. We conclude that another 6.9% (1.5 %) of the area which is not safe at present would recover after 2100. Deposition levels would need to be reduced further to either increase the area that recovers before 2100, or to bring closer the year of recovery. How much depositions should be reduced below BL-CLE deposition patterns depends on the year in which recovery is aimed to occur, i.e. on the target load required to obtain recovery in that year. In doing this we found that about 95% of the ecosystems which is not safe now could recover already in 2030 if acid deposition is sufficiently reduced in 2020 (implementation year). This does include ecosystems for which acid deposition needs to be reduced below critical loads. In chapter 2 a more detailed analysis of dynamic modelling elements is provided.

Figure 1-10 shows a comparison on a country scale between target loads and critical loads in the form of diamond-graphs.

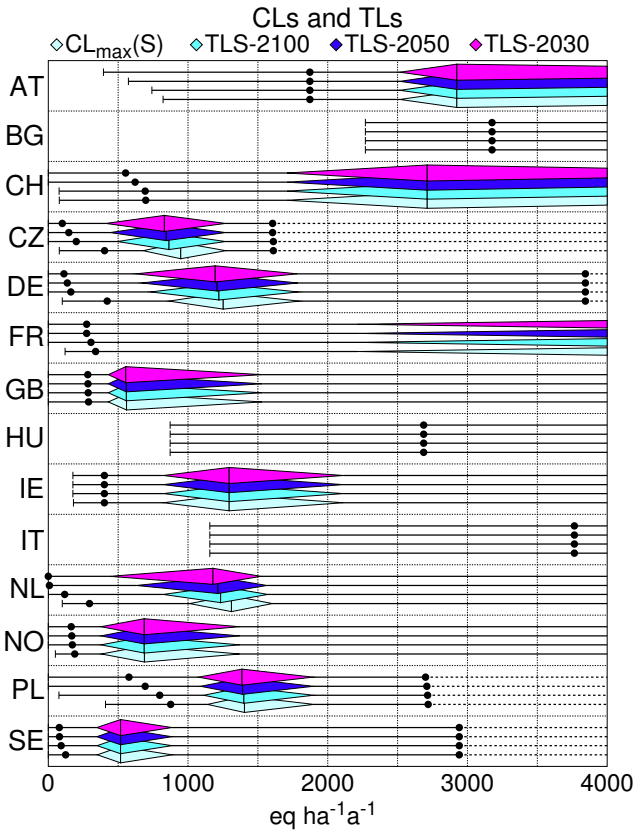

Figure 1-10. Diamond plot of the distribution of critical loads (light blue) and target load distributions in 2100 (turquoise), 2050 (dark blue) and 2030 (purple).

Figure 1-10 confirms that a marked differentiation between the 5th percentile values (left dot) of target loads and critical loads are in Switzerland, the Czech Republic, Germany, France, the Netherlands, Poland and Sweden. A decrease of the median values can be seen in the Czech Republic, Germany and the Netherlands in particular.

Finally, Table 1-2 provides an overview of trends from 1980 to 2010 of non-protected area in each country, including critical loads from the CCE European background database (EU-DB) for countries that did not ever submit data.

Deposition fields for 1980-2010 were provided by EMEP/MSC-W. The ecosystem area in the CLRTAP domain which is at risk from acidification (left part of Table 1-2) reduces from about 48% (48.6% in the EU25) in 1980 to about 6% (11% in the EU25) in 2010. For the risk of eutrophication (right part of Table 1-2) the percentages go from about 38% (80.5% in the EU25) to 28% (60% in the EU25). The persisting broad European areas that are unprotected from eutrophication point to the requirement of using dynamic models to improve knowledge of the delays by which damage from excessive nitrogen could occur.

Table 1-2. Exceedances of the critical load for acidification (left) and for eutrophication (right) as % of the European ecosystem area for which critical loads are available (including the CCE back ground database), using depositions computed with the EMEP-Unified Model (Simpson et al., 2003) from 1980 to 2010 on the basis of the BL_CLE scenario (totals include Andorra, Liechtenstein and San Marino).

country	$CL_{max}(S)$ Ecoarea	Area NOT protected from acidification (%)			
-	(km^2)	1980	1990	2000	2010
AL	6,334	0.9	0.9	0.0	0.0
AT	35,745	35.2	16.7	1.0	0.3
BA	10,241	70.4	65.3	52.7	45.2
BE	7,282	99.2	96.3	51.3	24.8
BG	52,032	0.0	2.7	0.0	0.0
BY	107,841	96.0	91.1	63.7	58.4
CH	11,792	59.4	38.7	19.2	13.2
CY	4,434	-	-	0.0	0.0
CZ	11,178	99.4	99.3	78.6	47.1
DE	104,186	94.6	93.3	61.7	41.5
DK	3,136	98.4	94.8	31.6	8.2
EE	21,416	0.0	0.0	0.0	0.0
ES	85,175	4.3	2.9	1.0	0.1
FI	265,919	39.0	15.6	1.5	1.0
FR	180,102	24.5	21.3	14.7	7.9
GB	77,129	75.4	67.1	33.9	16.5
GR	9,288	11.3	15.2	10.5	6.8
HR	6,931	96.7	80.7	10.7	1.2
HU	10,448	10.0	5.3	0.2	0.0
IE	8,933	41.0	33.6	24.6	12.9
IT	125,477	1.2	0.0	0.0	0.0
LT	17,651	92.5	89.7	76.6	68.1
LU	821	99.9	78.7	33.2	22.2
LV	27,321	56.3	46.8	24.7	14.8
MD	11,985	37.5	22.7	2.7	2.7
MK	5,068	47.4	47.4	42.9	17.3
NL	7,295	87.6	86.7	84.7	81.7
NO	386,692	42.4	33.8	15.5	11.3
PL	88,383	99.9	97.3	57.5	38.8
PT	21,221	10.0	12.4	10.8	4.6
RO	62,807	67.7	49.5	7.2	5.8
RU	3,516,432	46.4	24.3	1.1	1.1
SE	517,818	58.7	45.3	13.7	7.8
SI	5,264	70.1	51.2	2.2	0.0
SK	19,253	80.1	71.5	24.4	13.5
UA	63,600	93.1	82.1	27.8	22.7
YU	21,307	53.6	52.8	42.8	30.5
EU25	1,654,876	48.6	38.7	17.8	11.0
CLRTAP	5,918,115	48.1	31.2	8.5	6.1

country	$CL_{nut}(N)$ Ecoarea	Area NOT protected from eutrophication (%)			
-	(km^2)	1980	1990	2000	2010
AL	6,334	100.0	100.0	100.0	99.9
AT	35,745	99.8	99.8	97.2	87.8
BA	10,241	99.9	99.9	99.7	99.6
BE	7,282	97.5	97.1	95.1	93.8
BG	52,032	100.0	100.0	99.0	99.3
BY	107,841	75.8	76.0	58.6	59.9
CH	22,790	91.4	90.9	81.6	71.8
CY	4,434	-	-	89.1	89.0
CZ	11,178	100.0	100.0	99.5	98.6
DE	104,186	99.0	98.7	97.6	96.8
DK	3,136	100.0	100.0	93.8	85.4
EE	22,377	99.9	99.8	45.2	34.0
ES	85,175	72.2	82.3	87.9	81.6
FI	239,507	77.1	74.7	36.0	28.3
FR	180,102	98.4	98.6	97.9	97.2
GB	73,649	40.9	35.9	28.5	24.0
GR	9,288	100.0	100.0	100.0	100.0
HR	7,009	75.3	68.8	52.5	44.0
HU	10,448	100.0	100.0	98.5	87.5
IE	8,933	86.7	86.1	88.3	85.1
IT	125,477	76.9	78.1	71.3	65.1
LT	17,651	100.0	100.0	100.0	100.0
LU	821	100.0	100.0	100.0	100.0
LV	27,321	100.0	100.0	97.9	96.4
MD	11,985	0.2	0.2	0.1	0.1
MK	5,068	100.0	100.0	100.0	100.0
NL	4,334	98.1	98.1	94.3	90.5
NO	317,025	10.5	9.7	3.1	1.5
PL	88,383	99.5	99.3	97.8	97.0
PT	21,221	81.9	92.4	94.4	92.1
RO	62,807	100.0	100.0	99.1	99.5
RU	3,516,432	19.0	21.7	11.2	12.4
SE	223,771	56.6	55.1	17.6	10.3
SI	5,264	100.0	100.0	100.0	100.0
SK	19,253	100.0	100.0	100.0	99.6
UA	63,600	100.0	100.0	100.0	100.0
YU	21,307	100.0	100.0	100.0	100.0
EU25	1,328,936	80.5	80.4	65.2	60.5
CLRTAP	5,533,584	38.2	39.9	28.5	28.0

1.7 Conclusions

In 2005 fourteen parties under the LRTAP Convention submitted updated data on critical loads of acidity and of nutrient-N, while 13 countries (10 EU countries) provided dynamic modelling data for acidification. Including results of 2004 dynamic modelling data are available for 14 parties under the Convention (11 EU Member States). Critical load exceedances were computed with depositions computed with the EMEP Unified Model. Results reveal that still 8.5% of the ecosystem area in pan-Europe and 17.8% in the EU25 are still at risk of acidification in 2000. For eutrophication the risk stretches over an even larger area covering 28.5% and 65.2%, respectively. Dynamic modelling of the risk for acidification indicates that about 95% of the ecosystems concerned could recover already in 2030 if acid deposition is sufficiently reduced in 2020. This does include ecosystems for which acid deposition needs to be reduced below critical loads. It is recommended that dynamic modelling should be carried out for the remaining unprotected pan-European area for which results are not yet available to identify areas that can become protected in one of the target years. The persisting high exceedances of critical loads for eutrophication point to the requirements of using dynamic models to improve knowledge on time delays of damage and recovery.

References

EMEP (1998) Transboundary acidifying air pollution in Europe, MSC-W Status Report 1998 – Parts 1 and 2. EMEP/MSC-W Report 1/98, Norwegian Meteorological Institute, Oslo, Norway

Hettelingh J-P, Posch M, Slootweg J (2004) Status of European critical loads and dynamic modelling, in: Hettelingh JP, Posch M, Slootweg J (eds.), Critical loads and dynamic modelling results, CCE Progress Report, 2004. RIVM Report 259101014, Bilthoven, The Netherlands, pp .9-20, www.mnp.nl/cce

Posch M, Hettelingh J-P, De Smet PAM (2001) Characterization of critical load exceedances in Europe. *Water, Air and Soil Pollution* **130**: 1139-1144.

Posch M, Hettelingh J-P, Slootweg J (eds) (2003) Manual for dynamic modelling of soil response to atmospheric deposition. Coordination Center for Effects, RIVM Report 259101012, Bilthoven, Netherlands, pp.71 www.mnp.nl/cce

Schöpp W, Posch M, Mylona S, Johansson M (2003) Long-term development of acid deposition (1880–2030) in sensitive freshwater regions in Europe. Hydrol Earth Syst Sci 7: 436–446

Simpson D, Fagerli H, Jonson JE, Tsyro S, Wind P, Tuovinen, JP (2003) Transboundary Acidification Eutrophicationand Ground Level Ozone in Europe, Part 1 Unified EMEP Model Description, EMEP Status Report 2003, EMEP-Report 1/2003-PART I, Norwegian Meteorological Institute, Oslo, Norway

Tarrasón L, Jonson JE, Fagerli H, Benedictow A, Wind P, Simpson D, Klein H (2003) Transboundary Acidification Eutrophication and Ground Level Ozone in Europe, Part III: Source-receptor relationships. EMEP Report 1/2003-PART III, Norwegian Meteorological Institute, Oslo, Norway

UBA (2004) Manual on methodologies and criteria for modelling and mapping critical loads & levels and air pollution effects, risks and trends. UNECE Convention on Long-range Transboundary Air Pollution, Federal Environmental Agency (Umweltbundesamt), Berlin www.icpmapping.org

2 Summary of National Data

Jaap Slootweg, Maximilian Posch, Maarten van 't Zelfde*

*Institute of Environmental Sciences (CML), Leiden, the Netherlands

2.1 Introduction

The Working Group on Effects (WGE) '… approved calls for data for … critical loads of acidification and eutrophication and target loads (in early 2005)' (EB.AIR.WG.1.2004.2.e). In this call, with a deadline of 28 February 2005, the Coordination Center for Effects (CCE) requested National Focal Centres (NFCs) to submit data with only a few changes/additions since the previous call (compare with Hettelingh et al., 2004); *inter alia*:

- The implementation year changed from 2015 to 2020;
- The values of several output variables from dynamic modelling for 5 key years and 2 different scenarios ('Gothenburg' and 'Background') were requested;
- The computation of Damage Delay Times (DDT) and Recovery Delay Times (RDT) was requested;
- Updated software provided by the CCE enabled NFCs to perform consistency checks on their data before submission.

The full text of the 'Instructions for Submitting Critical Loads and Dynamic Modelling Data', which was sent to the NFCs with the call for data, is reproduced in Appendix A.

This Chapter reports on the results of the call for data (critical loads and dynamic modelling results) and shows statistical analyses of some of the most interesting variables.

2.2 National responses

A total of 14 countries updated their critical loads (CLs), and all except one also updated and extended their dynamic modelling (DM) results. Of these, the Czech Republic, Ireland and Switzerland submitted DM data for the first time. Altogether, critical load data are now available from 25 NFCs, and from these 14 have provided dynamic modelling results. Table 1-1 in Chapter 1 shows the most recent submission date for each NFC. Table 2-1 shows details about the 14 submissions following this call for data. The table lists the number of records and the total area covered for each ecosystem type. The EUNIS ecosystem classification system was applied by all countries, and for this overview the numbers are aggregated to EUNIS level 1.

Table 2-1 Type and number of ecosystem records for which data were provided in this call for data.

Country	Country Area (km^2)	EUNIS level 1	Acidity CLs		Nutrient N CLs		Dynamic Modelling	
			# ecosyst	Area (km^2)	# ecosyst	Area (km^2)	# ecosyst	Area (km^2)
Austria	83,858	Forest	496	35,745	496	35,745	496	35,745
Belarus	207,595	Forest	8,631	93,305	8,631	93,305		
		Grassland	1,779	15,257	1,779	15,257		
		Wetlands	100	773	100	773		
		total	10,510	109,334	10,510	109,334		
Bulgaria	110,994	Forest	87	52,032	87	52,032	83	47,887
Czech Republic	78,866	Forest	2,257	11,178	2,257	11,178	2,257	11,178
France	543,965	Forest	3,840	170,657	3,840	170,657	3,840	170,657
		Grassland	81	1,580	81	1,580	80	1,553
		Wetlands	67	5,123	67	5,123	67	5,123
		Other	156	2,741	156	2,741	156	2,741
		total	4,144	180,102	4,144	180,102	4,143	180,074
Germany	357,022	Forest	100,954	100,954	100,954	100,954	100,954	100,954
		Grassland	1,520	1,520	1,520	1,520	1,520	1,520

Country	Country Area (km^2)	EUNIS level 1	Acidity CLs		Nutrient N CLs		Dynamic Modelling	
			# ecosyst	Area (km^2)	# ecosyst	Area (km^2)	# ecosyst	Area (km^2)
		Shrub	310	310	310	310	310	310
		Wetlands	1,195	1,195	1,195	1,195	1,195	1,195
		Other	2,16	216	216	216	216	216
		total	104,195	104,195	104,195	104,195	104,195	104,195
Ireland	70,273	Forest	17,242	4,254	17,242	4,254	17,242	4,254
		Grassland	6,895	2,050	6,895	2,050	6,895	2,050
		Shrub	6,847	2,631	6,847	2,631	6,847	2,631
		total	30,984	8,936	30,984	8,936	30,984	8,936
Italy	301,336	Forest	714	89,560	714	89,560	714	89,560
		Grassland	185	23,027	185	23,027	185	23,027
		Shrub	210	12,822	210	12,822	210	12,822
		Water	1	6	1	6	1	6
		Other	19	463	19	463	19	463
		total	1,129	125,878	1,129	125,878	1,129	125,878
Netherlands	41,526	Forest	90,155	5,635	42,686	2,668	76,222	4,764
		Grassland	14,112	880	14,112	880	10,135	633
		Shrub	5,675	355	5,675	355	5,540	346
		Wetlands	1,637	104	1,637	104	1,101	69
		Water			417	5		
		Other	5,148	322	5,148	322	3,839	240
		total	116,727	7,295	69,675	4,334	96,837	6,052
Norway	323,759	Forest	662	67,011				
		Water	2,324	322,150			131	20,535
		Other			35,418	318,762		
		total	2,986	389,161	35,418	318,762	131	20,535
Poland	312,685	Forest	88,383	88,383	88,383	88,383	88,383	88,383
Sweden	449,964	Forest	25,442	225,264	25,442	225,264	542	24,400
		Water	3,084	284,819			234	6,724
		total	28,526	510,084	25,442	225,264	776	31,124
Switzerland	41,285	Forest	260	11,612	9,886	9,886	260	11,612
		Grassland			9,488	9,488		
		Shrub			1,640	1,640		
		Wetlands			1,727	1,727		
		Water	100	180	49	49		
		total	360	11,792	22,790	22,790	260	11,612
United Kingdom	243,307	Forest	150,208	19,748	151,815	19,896		
		Grassland	99,451	20,010	119,062	21,897		
		Shrub	78,550	24,669	78,985	24,785		
		Wetlands	18,682	5,455	19,079	5,506		
		Water	1,717	7,790			320	1,190
		Other			10,299	2,119		
		total	348,608	77,672	379,240	74,204	320	1,190
Grand Total	3,166,435		739,392	1,711,786	774,750	1,361,137	329,994	672,790

Figure 2-1 shows the same information in the form of bar charts, with the coverage of the different ecosystems relative to the total country area. The figure clearly shows that forests are the most widely used ecosystem, and that dynamic modelling is sometimes applied to a subset only, for which enough input data are available at a national scale. Finally, note that in Sweden the sum of ecosystem areas exceeds the area of Sweden itself. In general this can occur when National Focal Centres submit critical loads for overlapping ecosystems. This was decided in consultation with National Focal Centres under the International Cooperative Programme on Modelling and Mapping of the LRTAP Convention to meet the requirement of integrated assessment communities to be able to use critical loads for the assessment of the risk of individual rather than lumped ecosystems.

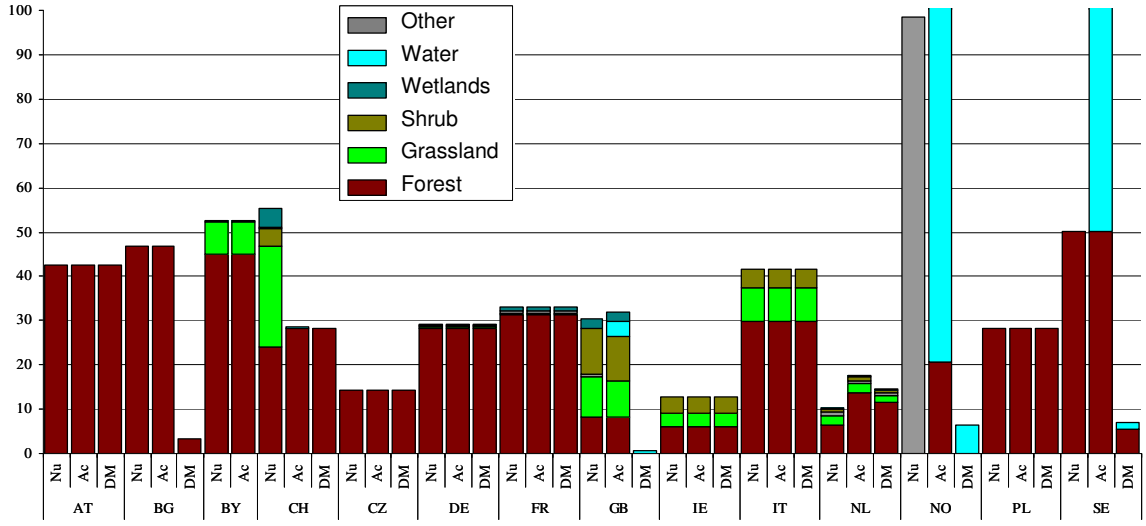

Figure 2-1. National distributions of ecosystem types for which data have been submitted for acidification (Ac), eutrophication (Nu) and dynamic modelling (DM).

The spatial coverage of Europe with critical load and dynamic model calculations can be seen in Figure 2-2 for all 25 NFCs. It shows that the dynamic modelling effort is concentrated in areas with the highest CL exceedances (mainly central and north-western Europe).

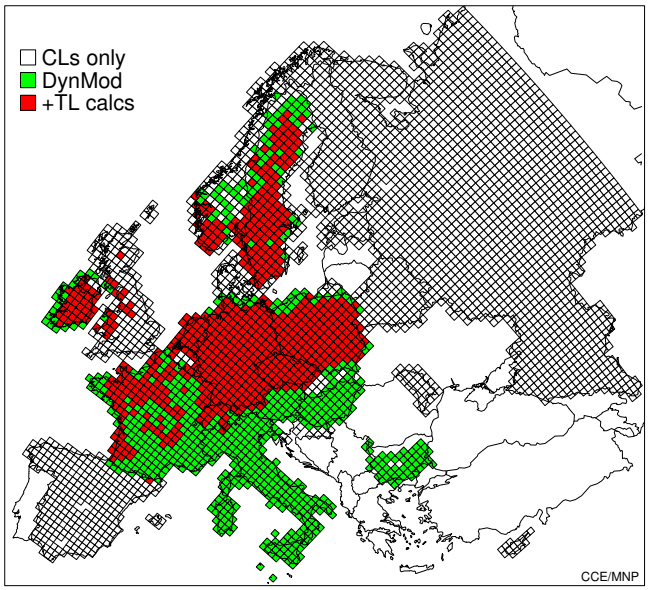

Figure 2-2. Map displaying the EMEP50 grid cells for which critical loads have are available from national submissions (25 NFCs). Coloured (green and red) cells indicate that also dynamic modelling has been performed (for at least one ecosystem); red cells that also target loads have been calculated.

A key quantity in determining a critical load is the chemical criterion linking soil (water) chemistry to the 'harmful effects on specified sensitive elements of the environment'. Figure 2-3 summarizes the critical values that NFCs selected in their critical load calculation. The area plotted is relative to the total area of all submitted ecosystems with a maximum critical load for sulphur. Not plotted are the following criteria:

- [ANC], which has been used for all aquatic ecosystems;
- Base saturation, used for the remaining 29% of Cypriot forest, and shrubs (57 %).

'Other' or 'missing' criteria. An increasing number of ecosystems is considered to be limited by different, or a combination of two or more criteria.

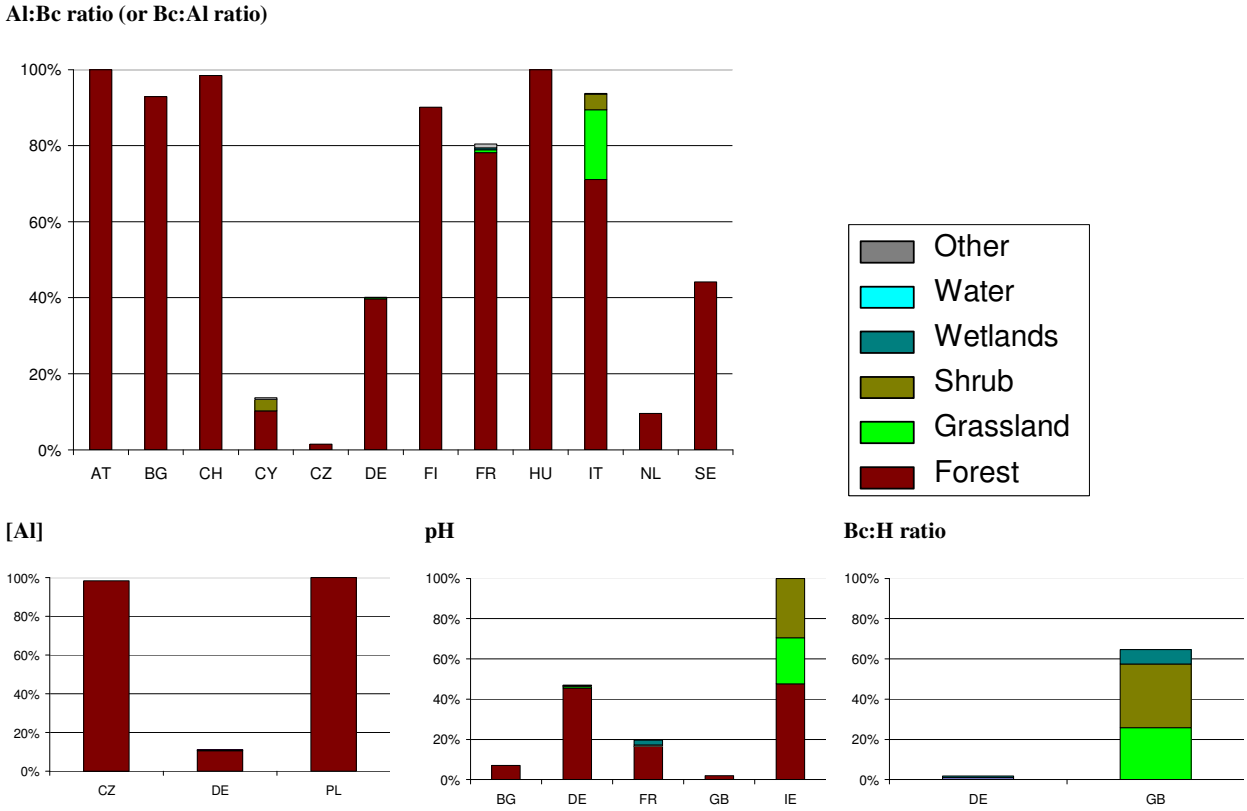

Figure 2-3. Area, relative to the total area of submitted ecosystems for acidity, for a selection of chemical criteria, broken down by ecosystem types.

2.3 Critical load maps and distributions

All 2005 national submissions contained critical loads for nutrient nitrogen, $CL_{nut}(N)$. Figure 2-4 shows the critical load in two ways. On the left are maps of CLnut(N) for the 5th, 25th, and 50th percentile in the 50×50 km EMEP grid cells, and on the right the cumulative distribution functions for each country, separately for 3 ecosystem classes, are plotted. The black dashed line, with the legend 'EU-DB', gives the distribution of CLnut(N) as computed with the European background database held at the CCE. This dataset is described in Chapter 4. EU-DB contains only data on forests, and thus only the national contribution for forest (the brown line) should be compared with it. The numbers at the right of the CDFs is the number of ecosystem records for the indicated ecosystem type.

Most of the sensitive areas in the 5th percentile also show sensitive in the 25th and even in the map showing the median values. The CDFs show relatively steep functions, also demonstrating this phenomenon. This means that reductions in these areas, if exceeded, are likely to be efficient. The 5th percentile is also shown in Figure 1-3 (Chapter 1), where it is mapped next to the 5th percentile for subsets of ecosystem types: forests, (semi-) natural vegetation and surface waters.

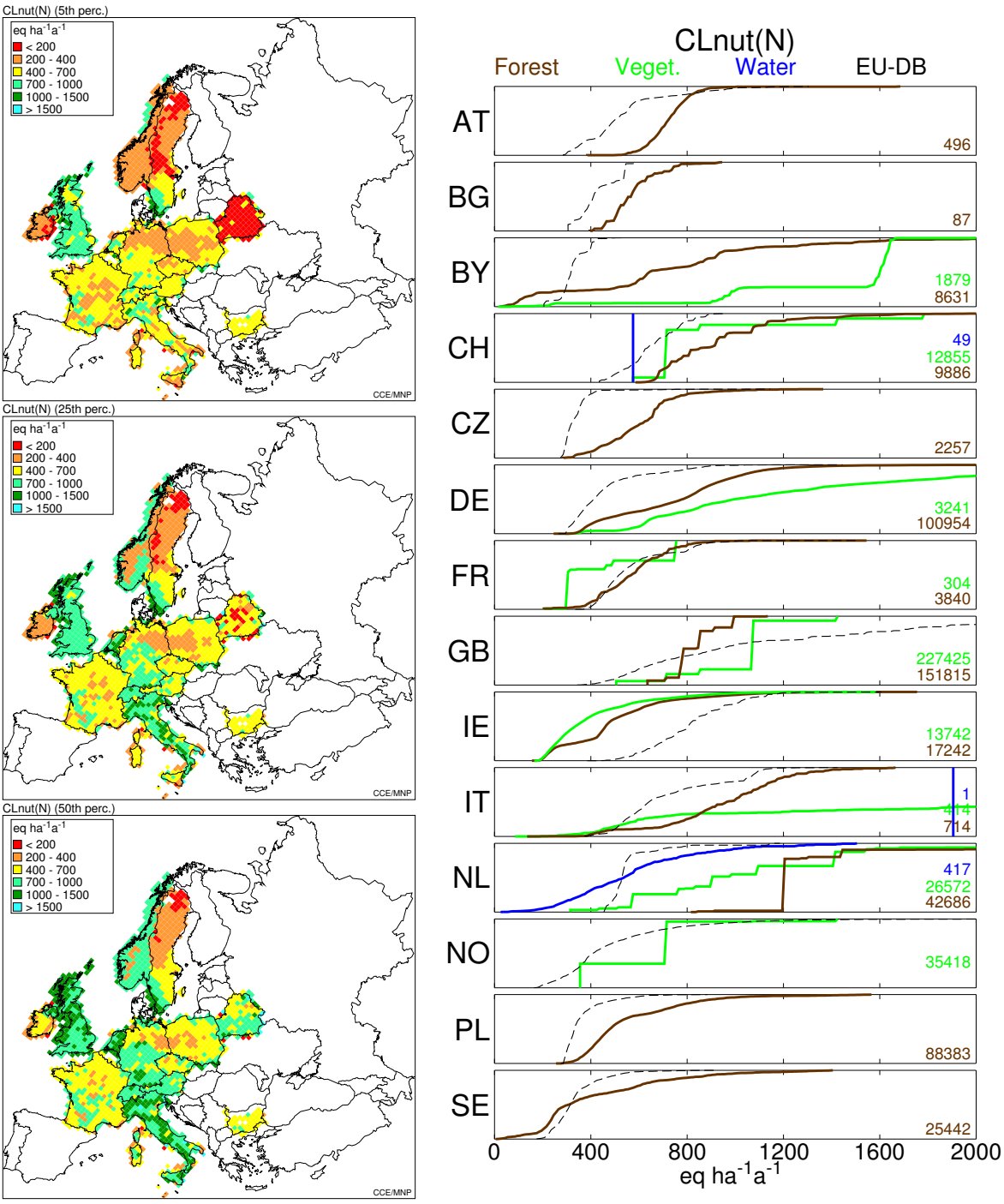

Figure 2-4. Critical loads of nutrient nitrogen from the 14 NFCs which responded to the last call The EMEP50 maps of the 5th, 25th and 50th percentile on the left and the cumulative distributions for 3 ecosystem classes on the right (EU-DB=European background data base).

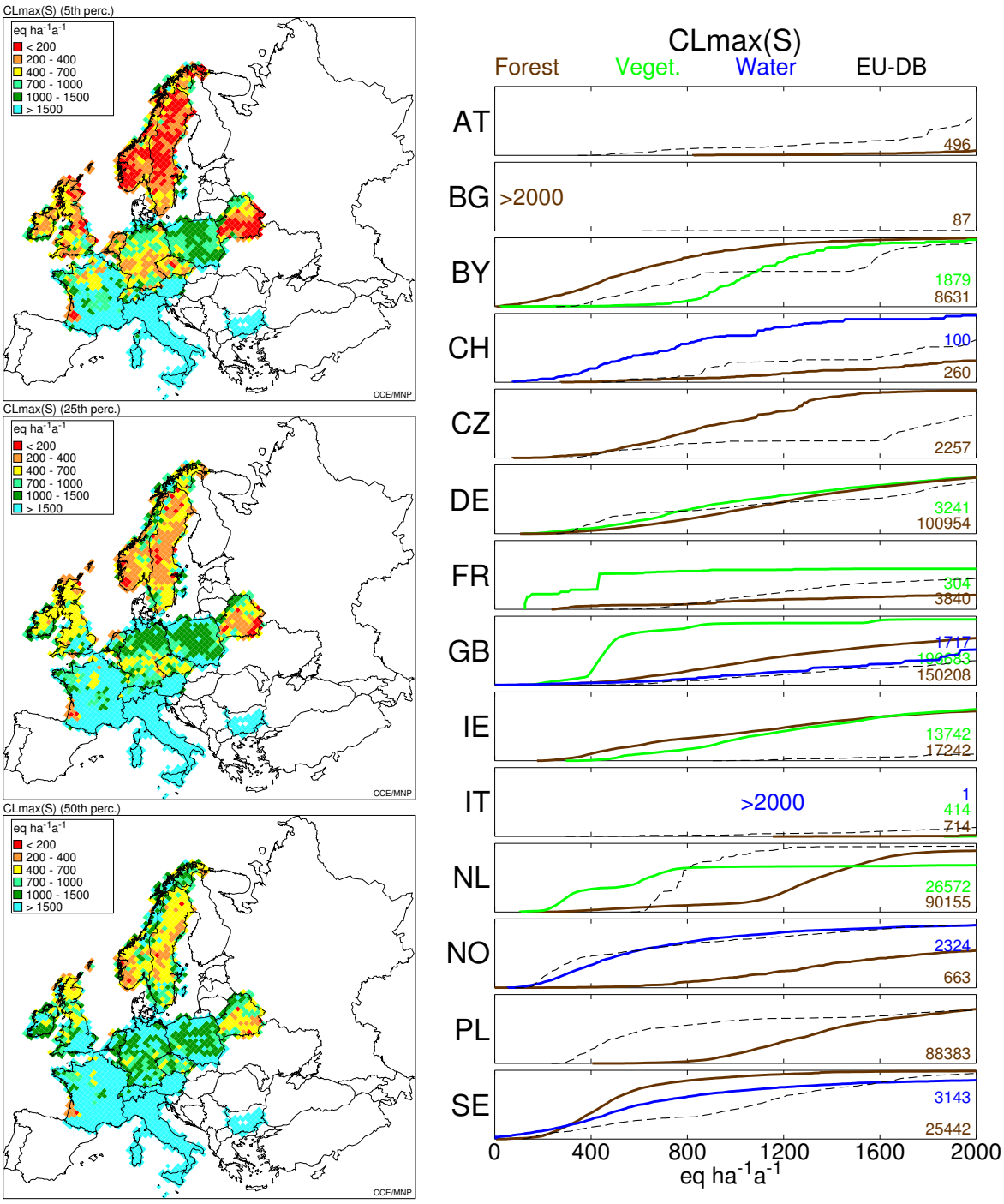

Figure 2-5. Maximum critical loads of sulphur from the 14 NFCs which responded to the last call The EMEP50 maps of the 5th, 25th and 50th percentile on the left and the cumulative distributions for 3 ecosystem classes on the right (EU-DB=European background data base).

In Figure 2-5 the same maps and functions are displayed for the maximum critical load of sulphur, $CL_{max}(S)$, chosen as a representative quantity for the acidity critical load function. The Figure shows that the ecosystems most sensitive to acidification are mostly located in the Nordic countries and Scotland.

Finally, in Figure 2-6 these maps and functions are shown for the minimum critical load of N, $CL_{min}(N)$. This quantity, which also is part of the critical load function of acidity, is (in most cases) the sum of net N uptake by vegetation and the long-term immobilisation of N. The maps and graphs show that this quantity has a much more narrow distribution than $CL_{max}(S)$.

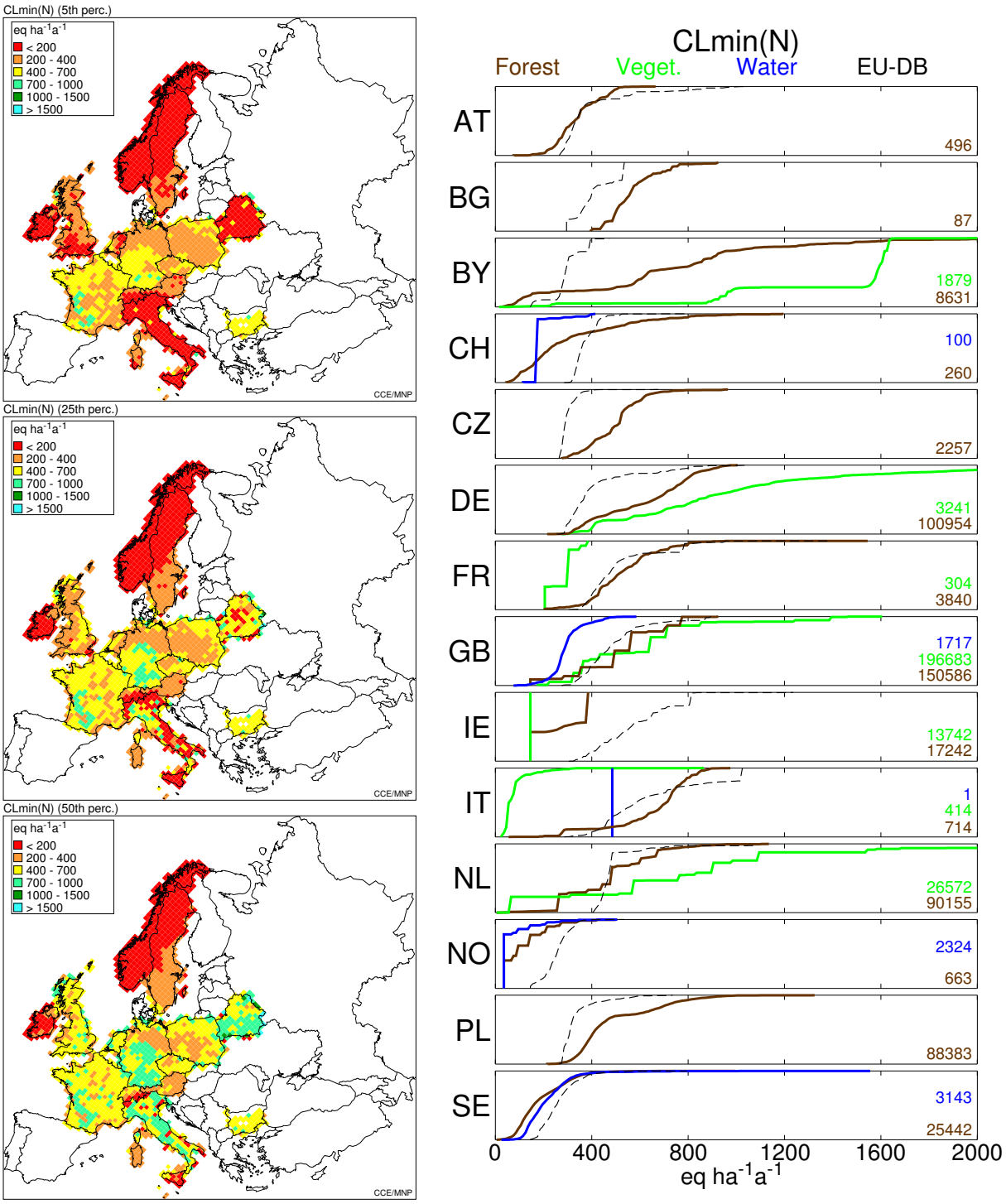

Figure 2-6. Minimum critical load of nitrogen from the 14 NFCs which responded to the last call The EMEP50 maps of the 5th, 25th and 50th percentile on the left and the cumulative distributions for 3 ecosystem classes on the right (EU-DB=European background data base).

2.4 Input variables for critical loads and dynamic modelling

The soil and other site specific parameters, which are used in critical load and dynamic model calculations, have been asked in the call for data to enable consistency checks and inter-country comparisons. In most cases the differences between counties can easily be explained, and it is the hope of the CCE that some differences or peculiarities in distributions shown in this section may lead to improvements in future data submissions.

Important element fluxes in the Simple Mass Balance (SMB) model are weathering, leaching, uptake and N immobilisation. A basic variable is the amount of water percolating through the root zone, Q_{le}. Its CDFs are shown for the countries that submitted data, separately for forests, semi-natural vegetation and surface waters. All CDFs shown in this section also display as a thin black dashed line the respective variable of the European background data base (see Chapter 4).

As can be seen in Figure 2-7, some countries show quite high values for Q_{le}, close to the annual precipitation, which could hint to at inconsistencies in the evapotranspiration calculations. Not all countries modelled denitrification, f_{de}, as a fraction of the net N input, but used an absolute amount of N denitrified N_{de}; thus no respective CDFs are shown for those countries (e.g. the United Kingdom

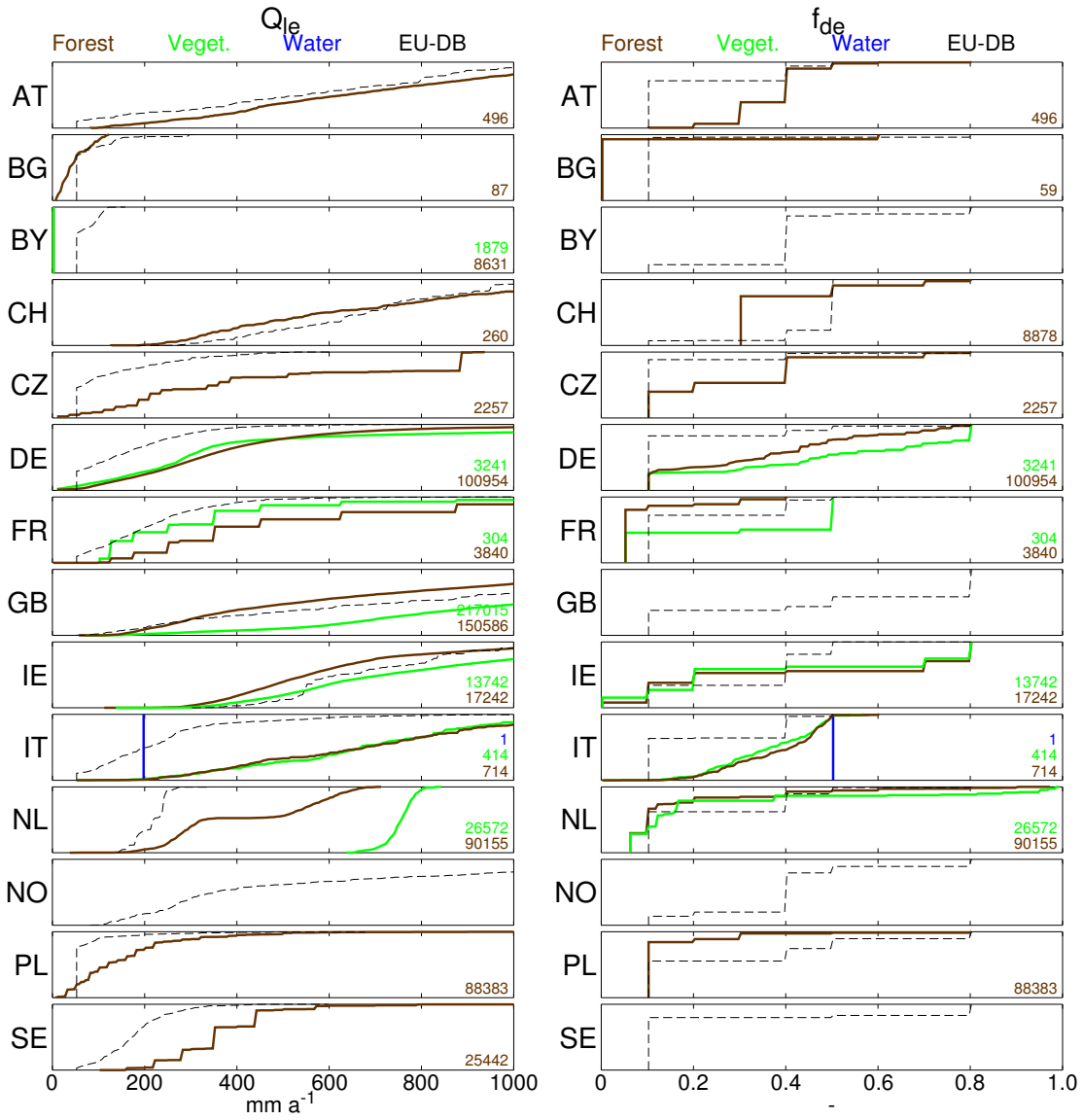

Figure 2-7. The CDFs of the amount of water percolating through the root zone, (Q_{le}, left) and the fraction of nitrogen denitrified in the soil (f_{de}, right) (EU-DB=European background data base).

Figure 2-8 shows the national CDFs of the acceptable leaching fluxes (left) and the N immobilisation fluxes. Whereas in the European background data base a constant value of 1 kg N $ha^{-1}a^{-1}$ (about 71.43 eq $ha^{-1}a^{-1}$); the upper limit suggested in the Mapping Manual) is used for the whole of Europe, NFCs have chosen very different – and in general larger – amounts on a national scale.

.

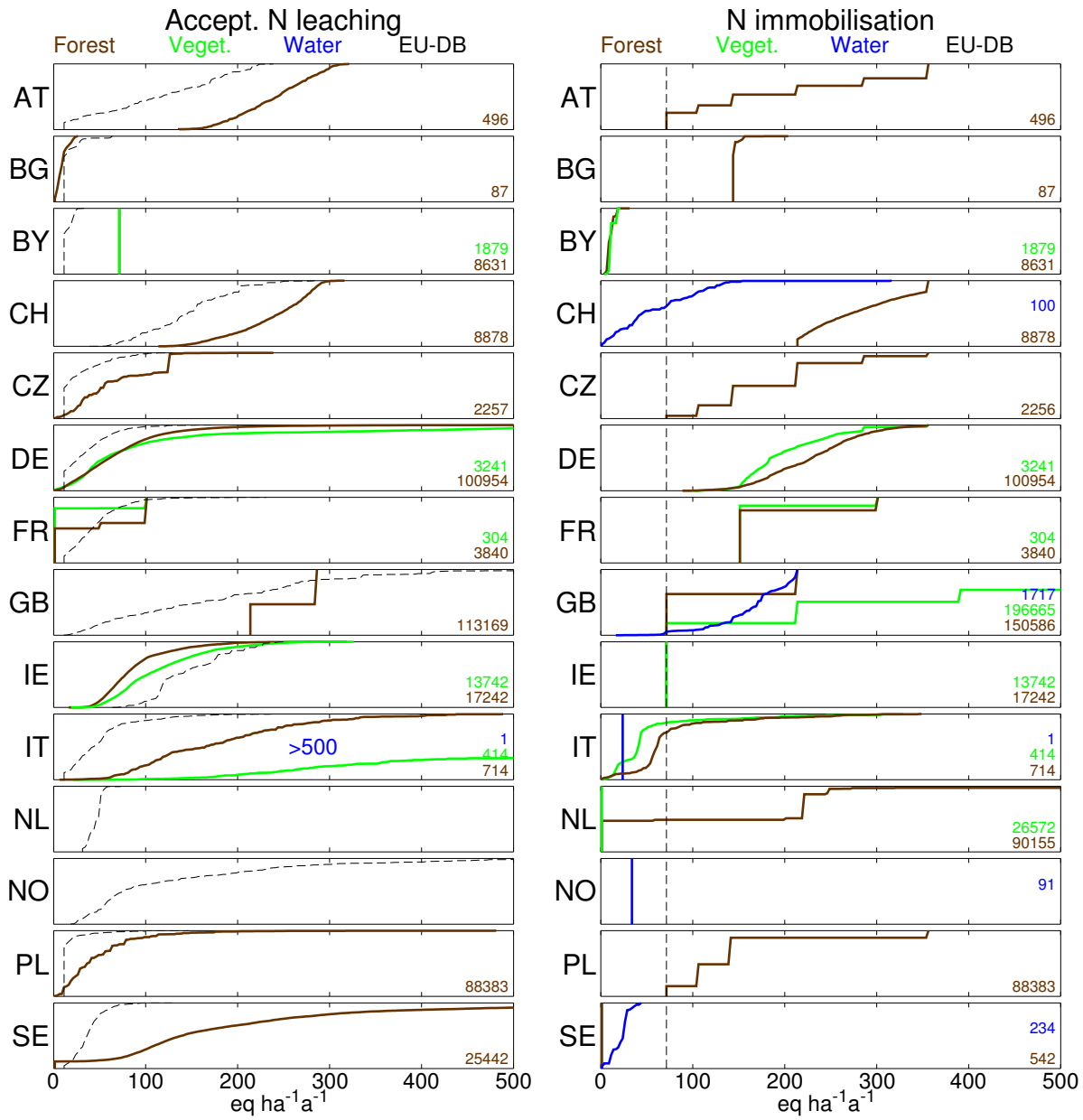

Figure 2-8. The CDFs of the acceptable amount of nitrogen leached per year from the soil ($N_{le(acc)}$, left), and the N immobilisation fluxes (right) (EU-DB=European background data base).

Figure 2-9 shows the correlation between nitrogen and base cation uptake for forests, vegetation, and waters (catchments). Plant and tree species have quite characteristic contents for nitrogen and the base cations in stem, branches, leaves and roots (Jacobsen et al., 2002). The amount of matter removed from the area can vary due to species and harvesting practises, but the ratio between nitrogen and the sum of base cations should reflect the mentioned specific contents. The grey lines in Figure 2-9 show the upper and lower limit of this ratio, using the numbers from Table 5.8 of the Mapping Manual (UBA, 2004). The top line is represents the content-ratio for oak, including branches, and the lower is for beech, stems only. It is remarkable that so many plots are outside of these lines, up to a few hundreds of equivalents. For areas, in which nitrogen uptake exceeds base cation uptake, the removal (harvest) of biomass would help combat acidification, a notion not everyone would agree with.

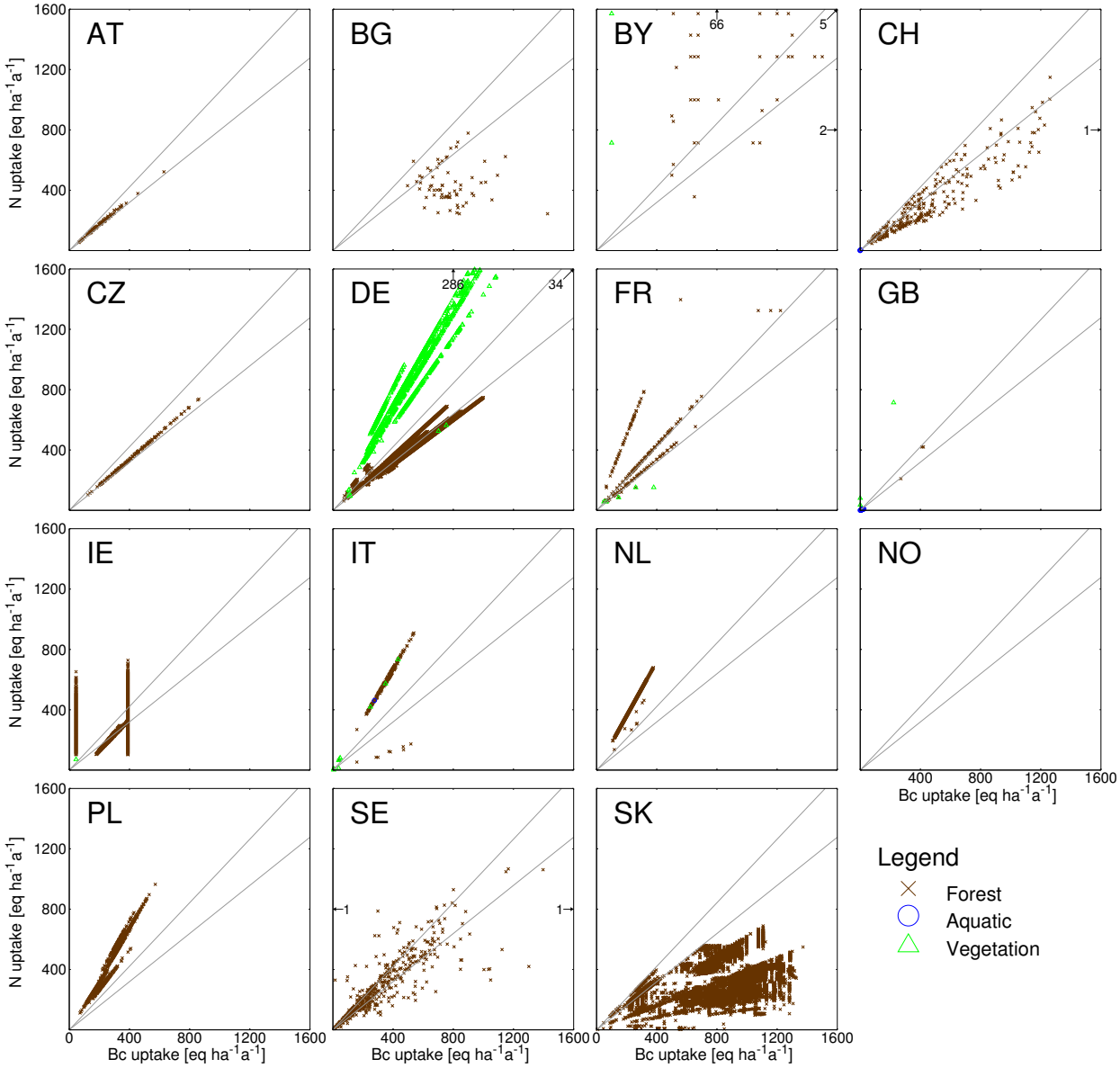

Figure 2-9. Net base cation uptake versus nitrogen uptake. The grey lines indicate the range given in the Mapping Manual.

The cumulative distributions of the total base cation weathering fluxes are shown for all submitting countries in Figure 2-10. Compared to last year's submission (see Hettelingh et al., 2004) Austria, Belarus and Switzerland have updated their values for weathering.

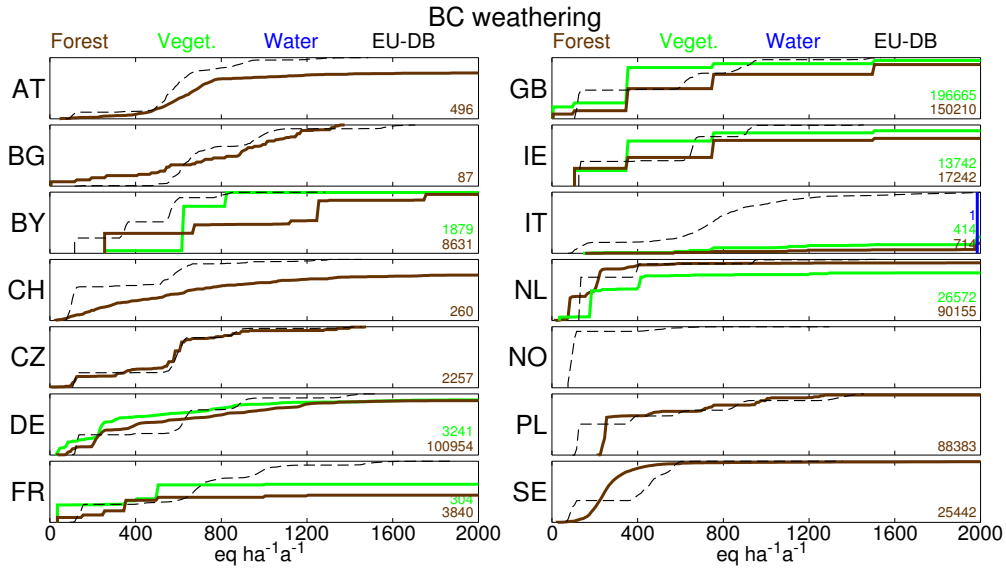

Figure 2-10. The CDFs of base cation weathering (BC= Ca+Mg+K+Na; EU-DB=European background data base).

Several countries have made use of the base cation deposition data that was made available by EMEP (Van Loon et al., 2005). Figure 2-11 shows of a map of the EMEP data on the left, and to the right a map of the average base cation deposition of the most recent submission of all NFCs. EMEP made also data available for deposition on forests. This explains why the maps differ, even for the countries that used the EMEP data. Both maps show sea salt corrected base cation depositions. For the national submissions that contained the individual ions, chloride is used as a tracer. Since the EMEP dataset does not contain chloride, it was assumed to have the same ratio to Na as in sea water. This might be the reason for the striking difference between the maps.

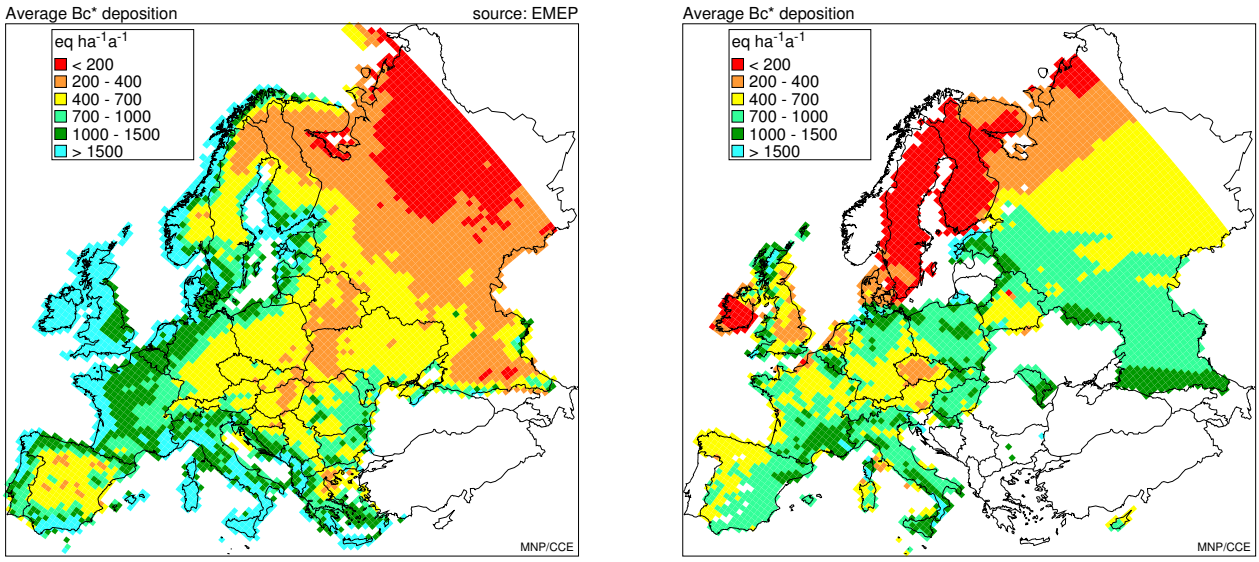

Figure 2-11. Sea salt corrected base cation deposition derived from EMEP data (left) and sea salt corrected base cation deposition submitted by NFCs, averaged over the EMEP50 grid (right).

In addition to variables used in critical load calculations, also variables only needed for dynamic modelling have been asked from the NFCs. In Figure 2-12 the cumulative distributions of the soil bulk density (left) and the cation exchange capacity (CEC) are displayed for each country that submitted new data. Bulk densities are quite low in some countries, hinting at a large proportion of organic soils. CEC values are in expected an expected range for all countries; and the rough estimates of the background database (dashes line) do not always agree with national estimates/measurements.

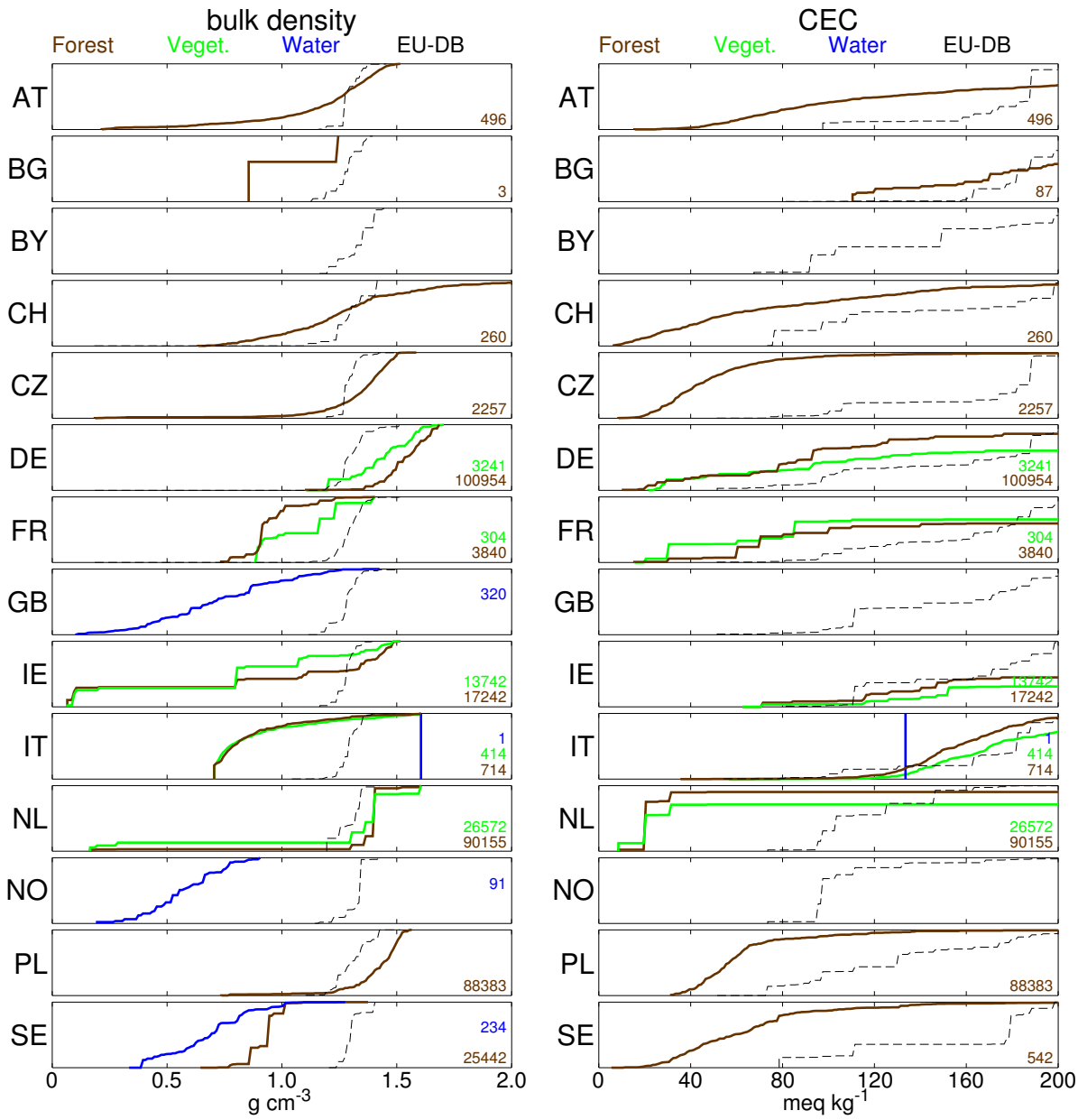

Figure 2-12. Cumulative distributions of bulk density (left) and cation exchange capacity (right) (EU-DB=European background data base).

Not only *input* variables used in critical load calculations and dynamic modelling, but also dynamic modelling *output* was asked for some key variables in a few years (1990, 2010, 2030, 2050 and 2100). Figure 2-13 shows national cumulative distribution functions of the molar [Al]:[Bc] ratio in the soil solution or surface water for the years 1990, 2010, 2030 and 2050 for two scenarios: (a) keeping the Gothenburg Protocol deposition constant after 2010 (right) and reducing deposition linearly to background values between 2010 and 2020 (right graphs in Figure 2-13). Obviously, the CDFs are identical for 1990 and 2010 in both sets of graphs; after that, however, a much faster and more widespread recovery, i.e. lower values, can be observed for the 'background scenario'. But even under this extreme scenario not all ecosystems recover, i.e. reach a value below one, before 2050. The figure also shows that in many countries the values for 2050 are (very) close to those for 2030. This reaching of a steady state is due to the fact depositions do not change after 2010 (for 'Gothenburg') or 2020 (for 'Background').

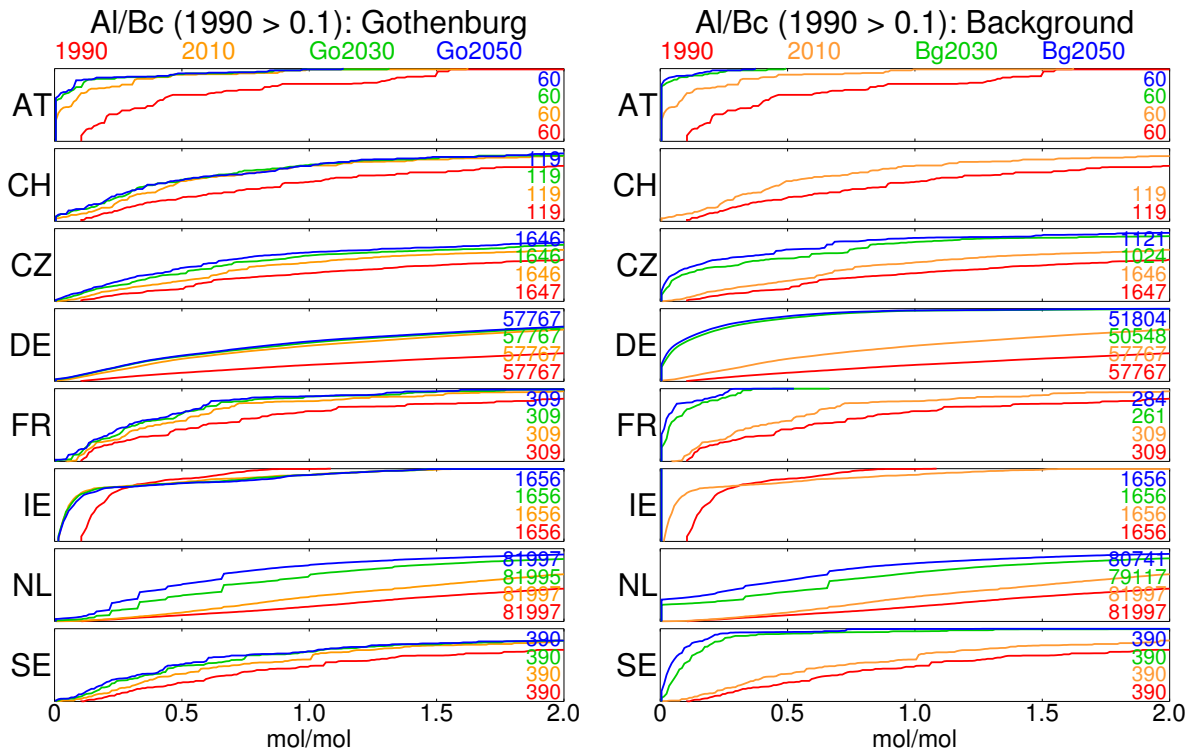

Figure 2-13. Molar Al:Bc ratio for 1990, 2010 (assuming the Gothenburg Protocol implementation) and for 2030 and 2050 with (a) deposition kept constant after 2010 (left) and (b) reducing deposition to background level into 2020 and keeping it constant thereafter (right) (only the sites with an Al:Bc ratio greater than 0.1 are plotted).

In Figure 2-14 the C:N ratio in the topsoil in the year 2010 is plotted versus the N concentration in the soil solution in the same year. The C:N ratio in the VSD model (and other dynamic models) controls the immobilisation of N in the soil (above the constant value used in CL calculations) and decreases over time. Thus one could expect an increase in N leaching for lower C:N ratios; but this seems not to be the case for the Dutch data.

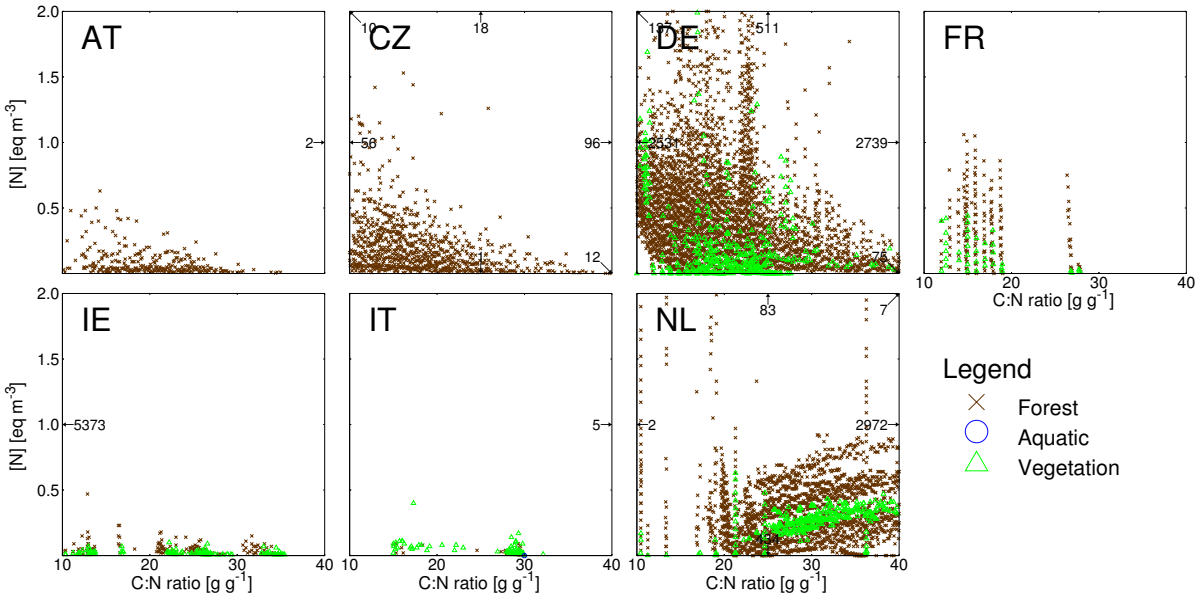

Figure 2-14. C:N ratio versus nitrogen concentration in the soil solution for 2010 (assuming the implementation of the Gothenburg Protocol).

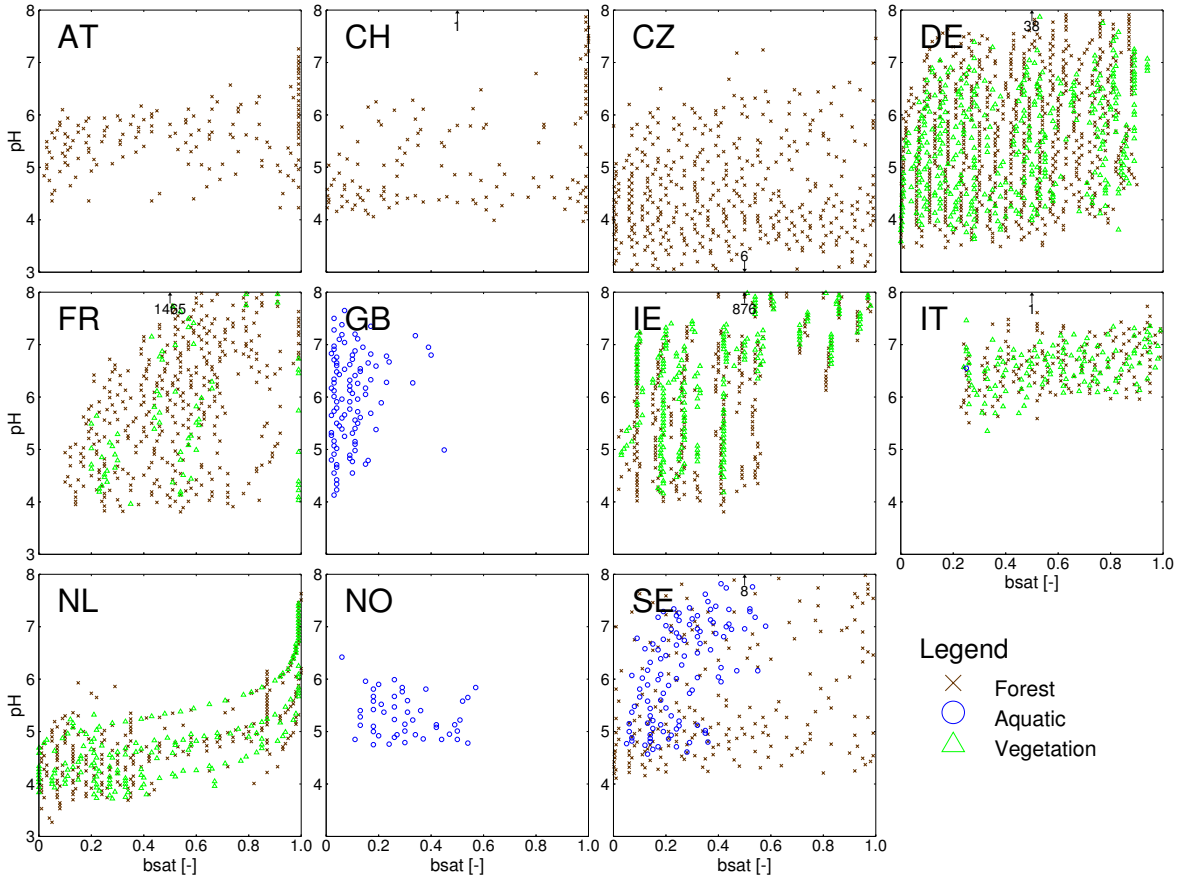

Figure 2-15. pH versus base saturation in 2050 with depositions kept constant after 2010 (Gothenburg).

In Figure 2-15, two other variables, i.e. pH and base saturation are plotted against each other for the year 2050 (with constant Gothenburg deposition after 2010). Except for the Netherlands, in none of the shown countries can one discern the S-shaped pattern, which has been documented in simple dynamic models (see, e.g. Reuss, 1983; De Vries et al., 1989). However, one has to bear in mind that Figure 2-15 shows the pH-base saturation relationship for many different sites at one given point in time, whereas in those references, this pattern is documented for single sites over time.

2.5 Damage delay and recovery times

Comparing critical loads to depositions, i.e. computing exceedances, can tell whether an ecosystem will be at risk or will be safe at some point in time, but it does not provide any insight when this will happen. To this end, dynamic models have to be applied. To get insight into, e.g., the length of the period between the occurrence of exceedance and the violation of the chemical criterion (the risk of damage), NFCs were also requested to compute these so-called damage delay times (DDT) and their counterpart in case of no-longer-being-exceeded, the recovery delay times (RDT), both when keeping the deposition after 2010 at the 2010 level (BL-CLE scenario reflecting the implementation of the Gothenburg Protocol and the EC NEC Directive). In Appendix A these quantities are explained in more detail, and in Figure 2-16 the possible cases are summarised in which an DDT or RDT exists as well as their relationship to target loads (TLs). In summary, it has to be noted that: (a) a damage delay exists only if there is exceedance of critical loads in the specified year, but non-violation of the chemical criterion; and (b) recovery can only occur if there is non-exceedance of critical loads in the specified year, but the criterion is still violated. In the other two possible cases – (c) exceedance and violation of the criterion, and (d) non-exceedance and non-violation – the system is ‘damaged’ or ‘safe’, respectively.

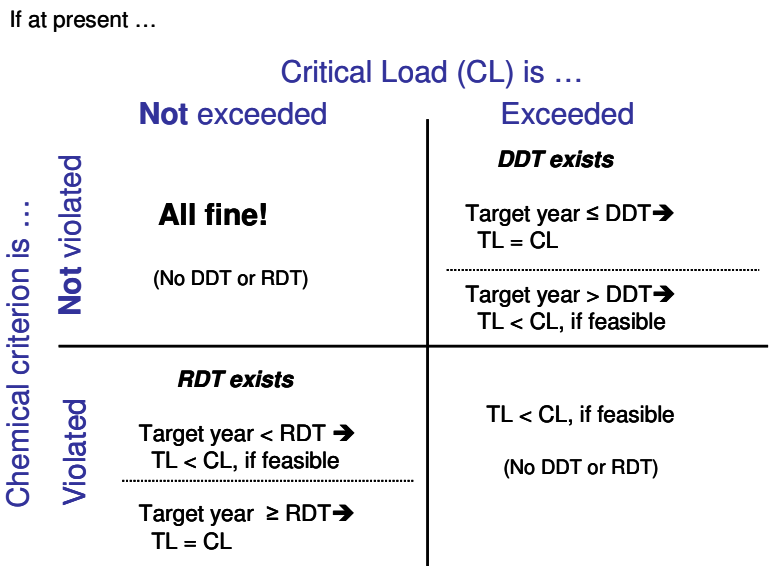

Figure 2-16. Summary of the cases in which damage or recovery delay can occur for all possible combinations of critical load (non-)exceedance and criterion (non-)violation. Also the connections with the existence of a target load are shown.

The cumulative distributions (CDFs) of the recovery and damage delay times between 2010 and 2100, as submitted by the NFCs, are shown in Figure 2-17. It is important to note that 100% in these distributions does not mean 100% of the ecosystems, but 100% of the cases for which the respective quantity exists; and the number of ecosystem to which this applies are also shown in Figure 2-17. From Table 2-1 the reader can infer how this numbers relate to the total number of ecosystems; and columns 5 and 6 in Table 2-2 below show for each country the percentage of ecosystem area for which a RDT or DDT, respectively exists. These percentages refer to the ecosystem area in a country, which is 'not safe' (column 4), i.e. the area of those ecosystems for which the critical load is exceeded or the criterion is (still) violated, or both.

The majority of the CDFs in Figure 2-17 are quite flat between 2010 and 2100, implying that most of the recovery/damage happens before 2010 and/or after 2100. This rather unexpected bimodality of the ecosystems involved, i.e. either recovering/deteriorating very fast or very slowly, certainly merits further investigations.

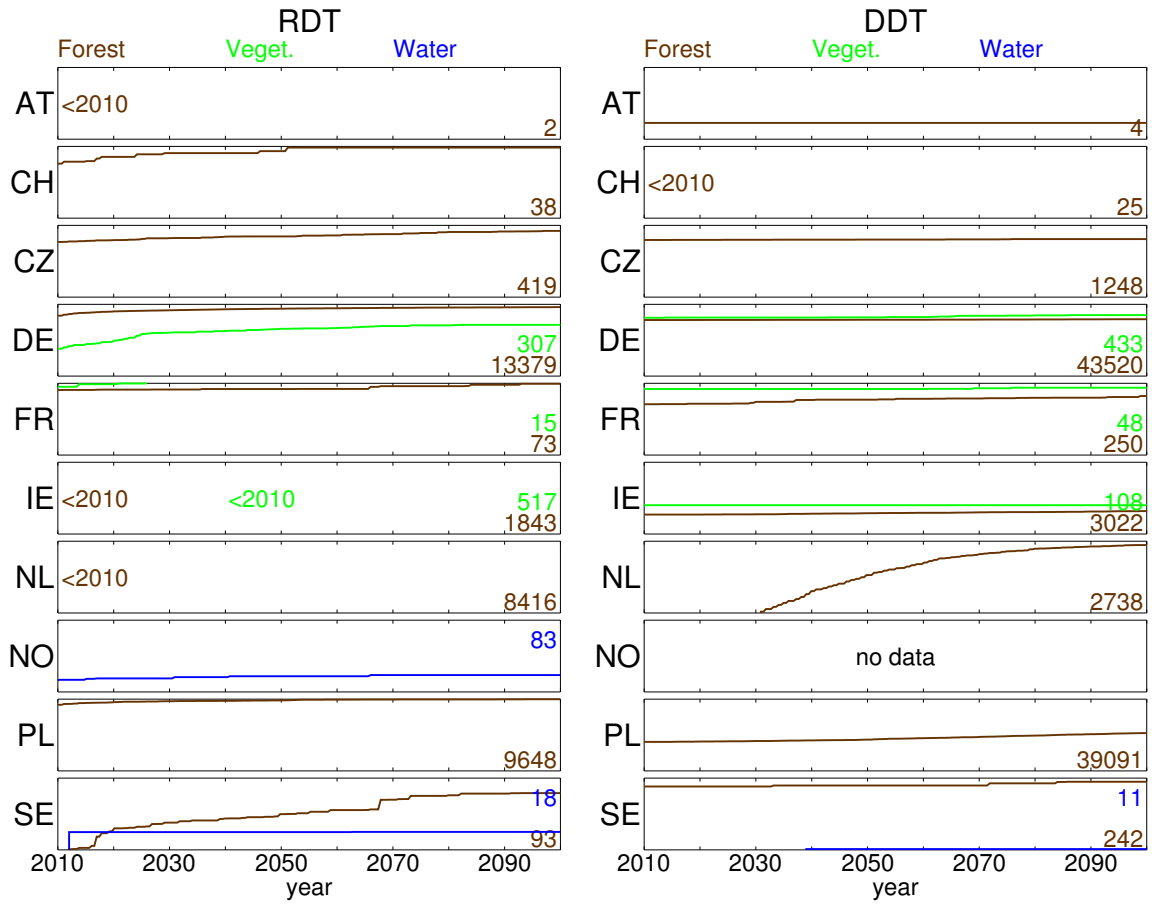

Figure 2-17. Cumulative distributions of recovery (RDT) and damage (DDT) delay times between 2010 and 2100 and three ecosystem classes, as computed by 10 NFCs.

2.6 Target loads for acidification

The emphasis of the last call for data with respect to dynamic modelling was on the calculation of target loads of acidity (sulphur and acidifying nitrogen). A target load (TL) for an ecosystem is a future deposition (path) which, when met, guarantees that the ecosystem is 'safe' – i.e. non-exceeded and chemical criterion met – from a pre-specified year, the target year, onwards. In contrast to the critical load, a target load is not unique – it depends on the target year – and it is not an ecosystem property, but, of course, depends on them. As with critical loads, since both sulphur and nitrogen contribute to acidity, there exists, for a given target year, not a single target load, but a *target load function* (TLF). Since, for a given target year, there are potentially infinite many possible deposition paths to reach the target, for the work under the LRTAP Convention, the deposition path leading to the target load has been uniquely defined by the Protocol year, the implementation year and the target year – see Chapter one (especially Figure 1-1) for details. Fore general overview over dynamic modelling and further details see also chapter 6 of the Mapping Manual (UBA, 2004).

Target load functions of acidity are not available for all ecosystems for which there are critical load functions in the data base. The reasons are either that a country has not carried out dynamic modelling at all, or within a country target load calculations are performed only for a subset of the ecosystems, often due to the lack of the additional information needed to carry out dynamic modelling. To make the target load data set completely compatible with the critical load data set, the following steps have been taken:

(a) If no target loads have been calculated for an ecosystem, the target load function has been set equal to the critical load function.

(b) If the target load computed is greater than the critical load, the critical load is taken (minimum of TLF and CLF). This guarantees that an ecosystem remains safe also after the target year.

(c) If a target load is not feasible for a given target year, i.e. even reducing N and S deposition to zero does not make the ecosystem 'safe' in that year, the target load is set to zero; TLF =(0,0).

To map the full information contained in the target load functions on a European scale is virtually impossible. Therefore, as is routinely done with critical load functions, we look at the maximum S target load, $TL_{max}(S)$, which is the pendant to the maximum critical load of sulphur, $CL_{max}(S)$. In Figure 1-9 of Chapter 1 the 5^{th} percentile in every EMEP50 grid cell of $TL_{max}(S)$ for the three target years 2030, 2050 and 2100 is mapped together with a map showing $CL_{max}(S)$. A comparison of the maps shows that (a) there are grids were more than 5% of the ecosystem area have a non-feasible target load (black grid cells), and (b) on a European scale the magnitude of the target loads does not change significantly as a function of the target year. Furthermore, since we set the target loads equal to critical loads and since the majority of ecosystems is not (or no longer) exceeded by the BL-CLE scenario, the target load maps are close to the critical load map for large areas. The similarity of the overall TLF set and the CLF set can also be seen from Figure 1-10 (Chapter 1), which shows these data per country as so-called diamond plots, a simplified form of displaying and comparing cumulative distributions (CDFs).

Further information on the dynamic modelling results on a country basis is summarised in Table 2-2. The Table is organized as follows. A country's ecosystem area (km^2), for which critical loads of acidity have been computed, is provided in column 2. In column 3 the ecosystem area is given for which dynamic modelling was performed. The last two rows of the table give the results for the EU25 (of which 12 NFCs have provided dynamic modelling data) and all NFCs ('LRTAP'; 14 countries with DM data).

Most relevant for the work under the LRTAP Convention is the area where critical loads are exceeded. This area turns out to include most of the countries that submitted dynamic modelling data. The area at risk of acidification in 2000 within the geographic domain of the Convention and of the EU25 covers 579,975 km^2 and 345,869 km^2, respectively. For part of that area dynamic models were applied. Of that area 168,661 km^2 and 153,828 km^2 turned out *not to be safe* in the LRTAP and EU25 domain, respectively (Table 2-2, column 4), meaning that the critical loads are exceeded *or* that the critical limit is violated (or both).

In the following results for the LRTAP-domain will be used as a reading guide of Table 2-2, with results applying to the EU25-domain given in brackets. Column 5 shows the percentage of the non-safe ecosystem area (given in column 4) for which a Recovery Delay Time (RDT) can be computed under the BL-CLE (Gothenburg) scenario. This is the case in areas where the critical load is at present no longer exceeded, but the critical limit is still violated (see also Figure 2-16). Column 5 tells us that in the LRTAP-domain 29.2% (25.7% in EU25) of the area, which is not safe at present, would recover in the future without further measures. In fact, BL-CLE depositions cause 20.2% (21.9%) to recover already before 2030 (see column 7), while 20.7% (22.5%) recover before 2050 (column 11), and finally by 2100 BL-CLE depositions will lead to a recovery of 22.3% in the LRTAP-domain and 24.2 in the EU25 domain (column 15). Comparing column 15 (2100) to column 5 we conclude that 6.9% (1.5 %) of the area which is not safe now would recover only after 2100. Deposition levels would need to be reduced to either increase the area that recovers before 2100, or to bring closer the year of recovery. How much depositions should be reduced in comparison to BL-CLE deposition patterns depends on the year in which recovery is aimed to occur, i.e. on the target load required to obtain recovery in that year. The percentage of the European area for which target loads for recovery can be identified in 2030, 2050 and 2100 are provided in columns 9, 13 and 17, respectively.

Table 2-2. Country statistics on delay times and dynamic modelling submissions for all 25 NFCs.

1	2	3	4	5	6	7	8	9	10	11	12	13	14	15	16	17	18
Country	CLaci	DynMod	NOT safe	RDT	DDT	**2030**				**2050**				**2100**			
-	km^2	km^2	km^2	%	%	safe	TL=CL	TLFs	n.f.	safe	TL=CL	TLFs	n.f.	safe	TL=CL	TLFs	n.f.
AT	35,745	35,745	334	31.0	53.4	31	36.4	32.6	0	31	36.4	32.6	0	31	36.4	32.6	0
BE	7,282	-	-	-	-	-	-	-	-	-	-	-	-	-	-	-	-
BG	52,032	4,7887	0	0	0	0	0	0	0	0	0	0	0	0	0	0	0
BY	107,843	-	-	-	-	-	-	-	-	-	-	-	-	-	-	-	-
CH	11,792	11,612	2,650	14.8	0	9	24.5	63.8	2.7	10.7	24.5	62.1	2.7	13.7	26.3	59.9	0
CY	4,534	-	-	-	-	-	-	-	-	-	-	-	-	-	-	-	-
CZ	11,178	11,178	8,004	27.1	14.9	22.2	13.6	59.2	4.9	22.9	13.6	60.9	2.6	25	13.6	60.7	0.7
DE	104,195	104,195	57,639	23.7	16.7	21.6	17.2	58.7	2.5	22.2	16.7	59	2.1	22.7	16.5	59.4	1.5
DK	3,149	-	-	-	-	-	-	-	-	-	-	-	-	-	-	-	-
EE	21,450	-	-	-	-	-	-	-	-	-	-	-	-	-	-	-	-
ES	85,225	-	-	-	-	-	-	-	-	-	-	-	-	-	-	-	-
FI	266,830	-	-	-	-	-	-	-	-	-	-	-	-	-	-	-	-
FR	180,102	180,074	21,510	38.9	15.3	35.8	16	43.5	4.7	36	16	46	2	38.6	16	44.1	1.3
GB	77,673	1,190	401	83.8	0	16.2	7	59.2	17.6	16.2	11.2	58	14.6	16.2	16.4	53.9	13.6
HR	6,931	-	-	-	-	-	-	-	-	-	-	-	-	-	-	-	-
HU	10,448	10,448	0	0	0	0	0	0	0	0	0	0	0	0	0	0	0
IE	8,936	8,936	1,542	42.3	41.7	42.3	44.3	13.4	0	42.3	44.3	13.4	0	42.3	44.5	13.1	0
IT	125,878	125,878	0	0	0	0	0	0	0	0	0	0	0	0	0	0	0
MD	11,985	-	-	-	-	-	-	-	-	-	-	-	-	-	-	-	-
NL	7,295	6,052	3,984	1.3	4.3	0	14.2	71.7	14.2	0.2	14.7	77	8.1	1.3	14.3	84.4	0
NO	389,161	20,535	12,183	76.5	0	0	7.5	87.6	4.9	0	11.3	84.9	3.8	0	13	86.4	0.7
PL	88,383	88,383	48,739	19.8	47.8	19.2	47.5	32	1.2	19.5	47.5	32.9	0.2	19.8	46.7	33.5	0
RU	3,517,134	-	-	-	-	-	-	-	-	-	-	-	-	-	-	-	-
SE	519,341	31,124	11,676	38.5	8.8	13.9	2.4	52.3	31.4	17.1	2.4	49.4	31.1	29.1	2.2	41	27.8
SK	19,227	-	-	-	-	-	-	-	-	-	-	-	-	-	-	-	-
EU25	1,576,871	603,204	153,828	25.7	25.6	21.9	25.5	47.5	5	22.5	25.4	48.2	3.9	24.2	25	47.8	2.9
CLRTAP	5,673,748	683,237	168,661	29.2	23.4	20.2	24.2	50.7	5	20.7	24.3	51.1	3.9	22.3	24.2	50.8	2.7

Column 6 gives the percentage of the area for which a Damage Delay Time (DDT) can be computed. This is the case in areas where the critical load is already exceeded but the critical limit is not yet violated (see also Figure 2-16). In Europe 23.4% (25.6%) of the non-safe ecosystem area (column 4) will be damaged in the future at deposition levels under the BL-CLE scenario.

Column 7 gives the percentage of the area that will be safe (critical limit not violated and deposition not exceeding critical loads) in 2030 under the BL-CLE scenario, i.e. 20.2% (21.9%). Column 8 lists the percentages of areas at risk (not safe) where target loads for recovery in 2030 equals the critical loads, i.e. 24.2% in the LRTAP domain and 25.5% in the EU25 domain. Target loads lower than critical loads (column 9) are found for 50.7% (47.5%) of the ecosystem area which is not safe in 2000 (column 4). The European area for which no target loads can be found, i.e. for which even zero deposition would not lead to recovery in 2030, cover 5% (5%) (column 10). We conclude that the area which is – and would become – safe in 2030 (columns 7+8+9) is about 95% (95%) of the areas which are not safe now (column 4).

Finally, columns11–14 and 15–18 provide the analogous information for 2050 and 2100, respectively. It can be seen that the European area for which target loads can be identified in 2050 (column 12) is 24.3% (25.4%). In comparison to 2030 this implies an increment of 0.1% (0.1%). The area for which target loads can be identified need not necessarily be larger than a previous year. This can be seen when we compare column 17 to column 13. The difference of about 0.4% depicts the area for which a target load was required to establish recovery in 2030, but which can recover in 2100 under BL-CLE depositions. This can be seen from the fact that the areas defined as 'safe' (columns 7, 11 and 15) increase from 2030 to 2100, whereas the area for which target loads are non feasible (columns 10, 14 and 18) go down in the same period.

It is difficult to compare a large number of critical load and target load functions in a single plot. Therefore we restrict such a comparison to the maximum critical load of sulphur, $CL_{max}(S)$, and the corresponding quantity for target loads, $TL_{max}(S)$. Figure 2-18 shows for each of the 11 countries, for which TLFs have been calculated, in a so-called 'windmill plot' four correlations, namely between $TL_{max}(S)$ for the target years 2030 and 2050 (top right quadrants), between $TL_{max}(S)$ for 2050 and 2100 (bottom right), $TL_{max}(S)$ for 2100 and $CL_{max}(S)$ (botton left), and $CL_{max}(S)$ and $TL_{max}(S)$ for 2030 (top left quadrants). The different symbols refer to three ecosystem classes (forests, semi-natural vegetation and surface waters). The axes extend to 2000 eq/ha/a in all four directions, and the small numbered arrows indicate the number of ecosystems above this value in the respective direction(s).

A look at Figure 2-18 confirms that target loads for the different target years are fairly close to each other in many countries and for a majority of the ecosystems, and close to the critical loads as well. An extreme case is Ireland (IE) in which target loads for all years and critical loads hardly differ. An interesting case is Sweden (SE) where surface water target and critical loads are very close to each other, whereas the forest TLs, which are similar for the different target years, differ vastly from critical loads. The earlier a target year, the more stringent the target load (if it exists at all!); therefore the data points in Figure 2-18 should all lie on one side of the respective 1:1-line (diagonal), and deviations from this rule should be carefully looked into. This type of figure allows a quick assessment both of the correctness and difference in target loads and their relationship to critical loads.

References

De Vries W, Posch M, Kämäri J (1989) Simulation of the long-term soil response to acid deposition in various buffer ranges. Water, Air and Soil Pollution 48: 349-390

Hettelingh J-P, Posch M, Slootweg J (eds) (2004) Critical loads and dynamic modelling results. CCE Progress Report 2004, Coordination Center for Effects, RIVM Report 259101014, Bilthoven, Netherlands, 134 pp www.mnp.nl/cce

Jacobsen C, Rademacher P, Meesenburg H, Meiwes KJ (2002) Element contents in tree compartments – Literature study and data collection (in German). Report, Niedersächsische Forstliche Versuchsanstalt, Göttingen, Germany, 80 pp.

Reuss JO (1983) Implications of the calcium-aluminum exchange system for the effect of acid precipitation on soils. Journal of Environmental Quality 12(4): 591-595

UBA (2004) Manual on methodologies and criteria for modelling and mapping critical loads & levels and air pollution effects, risks and trends. Umweltbundesamt Texte 52/04, Berlin. www.icpmapping.org

Van Loon M, Tarrasón L, Posch M (2005) Modelling base cations in Europe. EMEP/MSC-W & CCE Note 2/05, Norwegian Meteorological Institute, Oslo, 58 pp

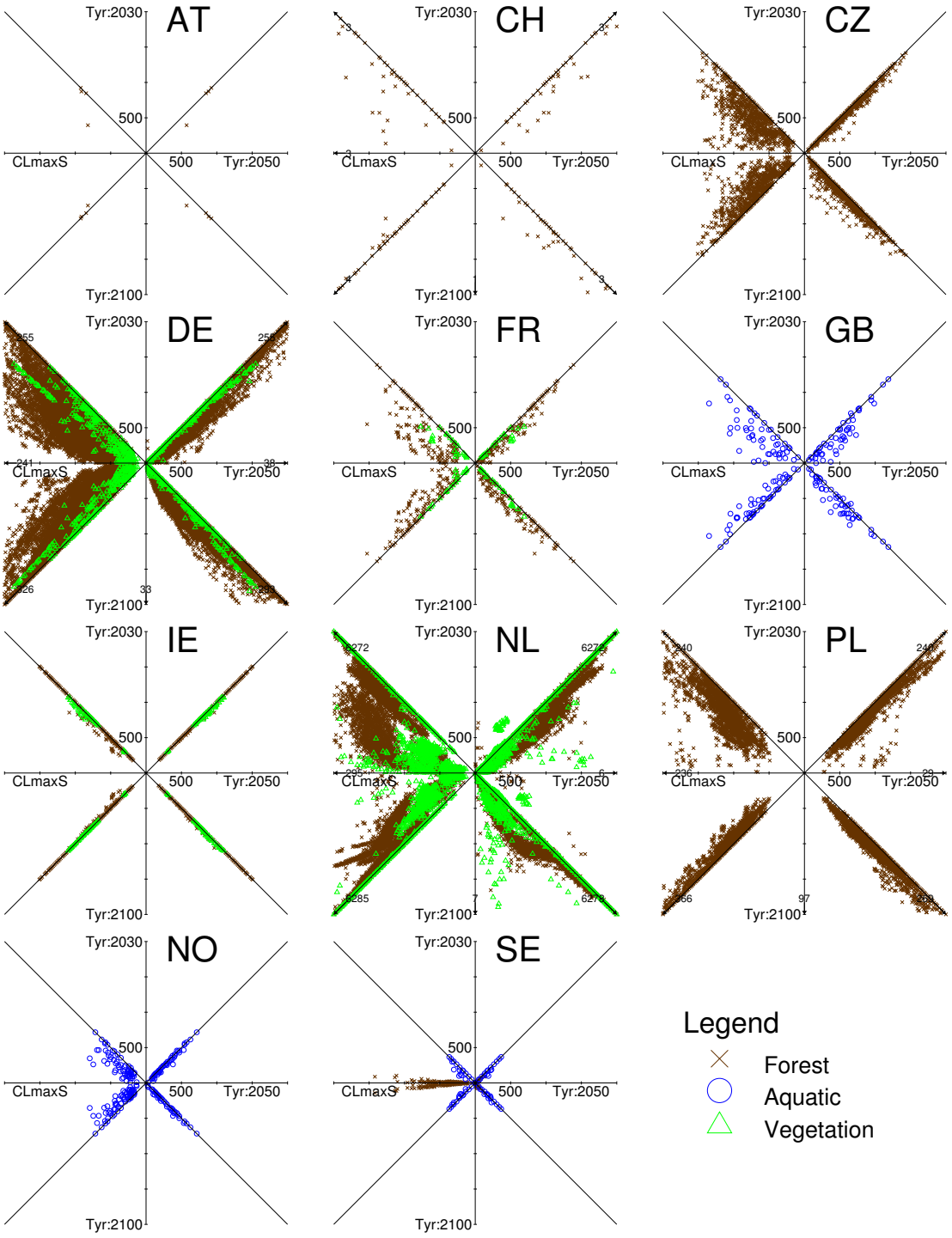

Figure 2-18. Correlations ('windmill plots') between the $TL_{max}(S)$ for the target years 2030, 2050 and 2100 and $CL_{max}(S)$ for 3 ecosystem classes and 11 countries for which TLFs have been computed.

3 The European Background Database

Maximilian Posch, Gert Jan Reinds*

*Alterra, Wageningen University and Research Centre, Netherlands

3.1 Introduction

A main task of the Coordination Center for Effects (CCE) is to collect and collate national data on critical loads and dynamic modelling, and to provide European maps and other databases to the relevant bodies under the LRTAP Convention, especially for the purpose of integrated assessment. Ideally, all those data are based on national data submissions, provided by National Focal Centres (NFCs) upon a call for data. However, if a country does not contribute national data, values from a European background database (EU-DB), which is held and updated by the CCE, can be used for those areas.

The previous version of the European background database has been described in the 2003 CCE Status Report (Posch et al., 2003). Over the last years new databases have become available, and thus the EU-DB has been updated. As before, only forests (forest soils) are considered in the European background database. Individual tree species are not identified, but a distinction is made between coniferous, broad-leaved (deciduous) and mixed forests. In deriving variables for the EU-DB which are not directly available in existing databases, the recommendations and transfer functions in the Mapping Manual (UBA, 2004) are followed as closely as possible.

In the following sections the data sources and procedures used for deriving the variables in the European background database are described. EU-DB contains the same data as were asked from NFCs in the last call for data (see Chapter 2). Some of the variables are displayed in map or graphical format.

3.2 Map Overlays

Input data for critical load calculations and dynamic modelling include parameters describing climatic variables, base cation deposition and weathering, nutrient uptake, N transformations and cation exchange. A combined map with the information to derive the required input data was constructed by combining the following maps/databases:

(a) The harmonised land cover map produced by the CCE and SEI by combining the Corine land cover map with the SEI land cover map (Posch et al., 2005).

(b) A soil map at scale 1:1,000,000 for all European countries (Eurosoil, 1999); except for Russia, Belarus, Ukraine and Moldova, for which the FAO 1:5,000,000 soil map (FAO, 1981) was used.

(c) Average forest growth derived from a updated data base of the European Forest Institute (EFI), which contains growth data a variety of species and age classes in about 250 regions in Europe (Schelhaas et al., 1999).

(d) A global map of detailed elevation data (on a 30"×30" grid) from NOAA/NGDC (Hastings and Dunbar, 1998).

(e) A map with EMEP grid cells of 50×50 km^2, in which S and N deposition data are provided.

Overlaying these maps and data bases, merging polygons within every EMEP50 grid cell differing only in altitude and discarding units smaller than 1 km^2 results in about 90,000 different forest-soil combinations.

The soil maps are composed of so-called soil associations, each polygon on the map representing one association. Every association, in turn, consists of several soil typological units (soil types) that each covers a known percentage of the soil association. The soil typological units on the maps are classified into more than 200 soil types (Eurosoil, 1999).

For each soil typological unit information is available, of which soil texture and drainage classes are used here to derive other input data. Six texture classes are defined from clay and sand content and listed in Table 5.12 in the

Mapping Manual. The drainage classes, which are used to estimate the denitrification fraction, are derived from the dominant annual soil water regime (Eurosoil, 1999; FAO, 1981).

Table 3-1 shows the distribution of forest over soil types in Europe for the 10 most common forest-soil types derived from the overlay of the soil- and forest map. Most forests are located on Podzols (about 25%), especially in the Nordic countries, and to a lesser extent on Podzoluvisols (about 15%), Cambisols (about 16 %), Luvisols (about 9%) and Lithosols (about 4%). Forest soils occur mainly on coarse (texture class 1) and medium textures (class 2). Forests on the fine textures (classes 3-5) are relatively rare. About 9% of European forests are located on peat soils (histosols).

Table 3-1. Area of the 10 most common forest-soil combinations in Europe.

Soil type	Area (km^2)	% Area
Podzols (P)	698246	25.2
Cambisols (B)	430280	15.6
Podzoluvisols (D)	421249	15.2
Histosols (O)	255690	9.2
Luvisols (L)	248140	9.0
Gleysols (G)	156363	5.7
Lithosols (I)	115961	4.2
Regosols (R)	103512	3.7
Arenosols (Q)	79445	2.9
Rendzinas (E)	69388	2.5

Some inaccuracy in these estimates exists, because the soil map consists of soil associations. The map overlay thus gives a forested area for each association, not for each soil type. Forests have been assigned evenly to all soil types within the association, which in reality will not always be the case.

3.3 Input data for critical loads and dynamic modelling

All calculations were done by assuming a soil depth (rooting zone) of 0.5 m.

Precipitation surplus and soil water content

To compute the concentration and leaching of compounds in the soil, the annual water flux through the soil has to be known. To this end meteorological data are needed. Long-term (1961-1990) average monthly temperature, precipitation and cloudiness were derived from a high resolution European data base (Mitchell et al., 2004) that contains monthly values for the years 1901-2001 for land-based grid-cells of 10'×10' (approximately 15×18 km in central Europe). For sites east of 32° a 0.5°×0.5° global database from the same authors was used.

Actual evapotranspiration was calculated according to a model used in the IMAGE global change model (Leemans and Van den Born, 1994) following the approach by Prentice et al. (1993). Potential evapotranspiration was computed from temperature, sunshine and latitude. Actual evapotranspiration was then computed using a reduction function for potential evapotranspiration based on the available water content in the soil, described by Federer (1982). Soil water content is in turn estimated using a simple bucket-like model that uses water holding capacity (derived from the available soil texture data) and precipitation data. A complete description of the model can be found in Annex 4 of Reinds et al. (2001).

These computations also yield the annual average soil water content θ.

The available water content (AWC) was estimated as a function of soil type and texture class according to Batjes (1996) who provides texture class dependent AWC values for FAO soil types based on an extensive literature review.

Base cation and chloride deposition

The total depositions of Ca, Mg, K and Na onto forests have recently been modelled by EMEP/MSC-W on the EMEP50 grid (Van Loon et al., 2005). Chloride deposition was assumed equal to the Na deposition.

Base cation weathering

Weathering of base cations, BC_w, was computed as a function of parent material class and texture class and corrected for temperature, as described in the Mapping Manual (UBA, 2004).

Weathering rates of Ca, Mg, K and Na as fractions of BC_w were estimated as a function of clay and silt content (in %) for texture classes 2 to 5 (Van der Salm, 1999) and as fixed fractions of total weathering for texture class 1 (De Vries, 1994).

Nutrient uptake

Net uptake of base cations and nitrogen was computed by multiplying the estimated annual average growth of stems and branches with the element contents of base cations and N in these compartments. Wood densities of 450 kg/m^3 and 650 kg/m^3 as well as branch-to-stem ratios of 0.15 and 0.20 for coniferous and deciduous trees, respectively, have been used. For mixed forests the average of these values were applied.

Forest growth was derived from the EFI database mentioned above (Schelhaas et al., 1999). Growth was assessed by taking from the database the average growth over all age classes for the combination of region and tree species group.

Contents of N, Ca, Mg and K in stems and branches of coniferous and deciduous forests are derived from Table 5.8 in the Mapping Manual UBA (2004), which is based on data from a literature study by Jacobsen et al. (2002). The average values of spruce and pine were assigned to conifers and the average of oak and beech to deciduous forests. Again, an average of these was used for mixed forests.

Denitrification and N immobilisation

The denitrification fraction, f_{de}, was computed as a function of drainage status, which is known for each soil type and is given in Table 5.9 of the Mapping Manual (UBA, 2004).

N immobilisation consists of a constant (time-independent) part, which is the same as used in critical load calculations (1 kg N ha^{-1}a^{-1}) and a time-dependent part, which is computed as a function of the prevailing C:N ratio of the top soil. This C:N ratio is estimated from a transfer function by Klap et al. (2002) which can also be found in the Mapping Manual (UBA, 2004). This transfer function computes the C:N ratio as a function of soil texture, forest type, climate variables and the N deposition of the relevant year (1995). The speed of change of the C:N ratio depends on the size of the C pool in the topsoil. This C pool for the top 20 cm is estimated from the organic carbon content (available for every soil type) and bulk density.

The bulk density ρ of the soil was computed from a transfer function using clay and organic carbon content, derived from data by Hoekstra and Poelman (1982) and Van Wallenburg (1988; see also UBA, 2004). Clay content is an attribute to the soil map, carbon content for each soil type was derived from a European database on forest soils (Vanmechelen et al., 1997).

Al-H relationship and organic acids

The Al concentration is computed from a gibbsite equilibrium (i.e. α=3) and the equilibrium constant is estimated from simultaneous measurements of [Al] and pH at about 150 forest monitoring plots as a function of soil texture class (De Vries et al., 2003).

Dissociation of organic acids was modelled by assuming them as mono-protic with a dissociation constant of pK=4.5 (see eqa.5.46 in UBA, 2004). The DOC concentration was estimated from a linear regression with soil pH and texture using data from European Intensive Forest Monitoring plots. A charge density m=0.023 mol/molC was used throughout.

Cation exchange capacity and base saturation

Cation exchange capacity (CEC) was computed as a function of clay content, organic carbon content and soil pH according to a transfer function by Helling et al. (1964; see also UBA, 2004).

Base saturation for the reference year (1995) was estimated from a transfer function derived by Klap et al. (2002; see also UBA, 2004). This transfer function computes the base saturation as a function of soil texture, forest type

as well as the S, N and base cation deposition. The base saturation values were used to calibrate the exchange constants of the H-Al-Bc exchange.

3.4 Results

The EU-DB obtained from the data(bases) and transfer functions described above can be used to compute critical loads of S and N acidity and nutrient N. Critical loads have been computed with the Simple Mass Balance (SMB) model, using a critical Al:Bc ratio of 1 mol mol^{-1} for all forests and soils, except for peat soils (Histosols), for which a critical molar Bc:H ratio is used (1 for conifers, 1/3 for deciduous forests and an average value of 2/3 for mixed forests). Several of the input variables as well as critical loads are displayed as cumulative distribution functions in Chapter 2, where they are compared to data from countries which have submitted national data in response to the recent call.

In Figure 3-1 the 5th percentiles of the maximum critical load of S acidity, $CL_{max}(S)$, and the critical load for nutrient N, $CL_{nut}(N)$, are displayed on the EMEP50 grid. The maps clearly show that in most grid cells (the 5th percentile of) the critical load for nutrient N is smaller than that of $CL_{max}(S)$.

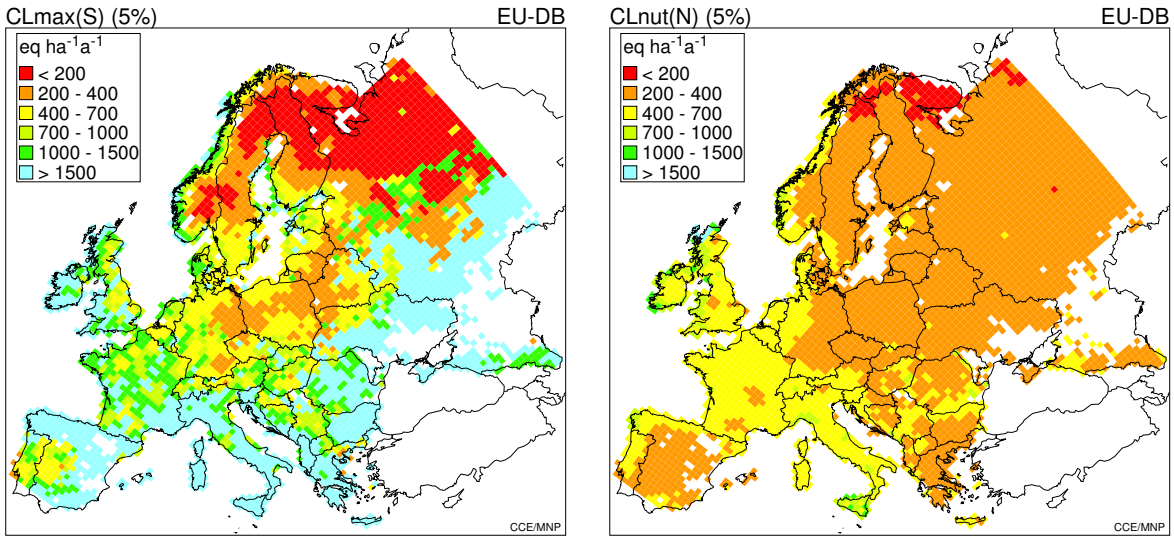

Figure 3-1. The 5th percentile of $CL_{max}(S)$ and $CL_{nut}(N)$ on the EMEP50 grid, computed from the European background database.

The exceedance of the acidity and nutrient N critical loads for the year 2010 is shown in Figure 3-2. In this scenario the implementation of the current legislation (the Gothenburg Protocol and the EU NEC Directive) is assumed. The forest-specific deposition has been provided by the EMEP/MSC-W (Tarrasón et al., 2004). As can be seen, acidification is a substantial problem only in some parts of central Europe, whereas eutrophication is a much more wide-spread and severe problem. These maps should be compared with the exceedance maps in Chapter 1.

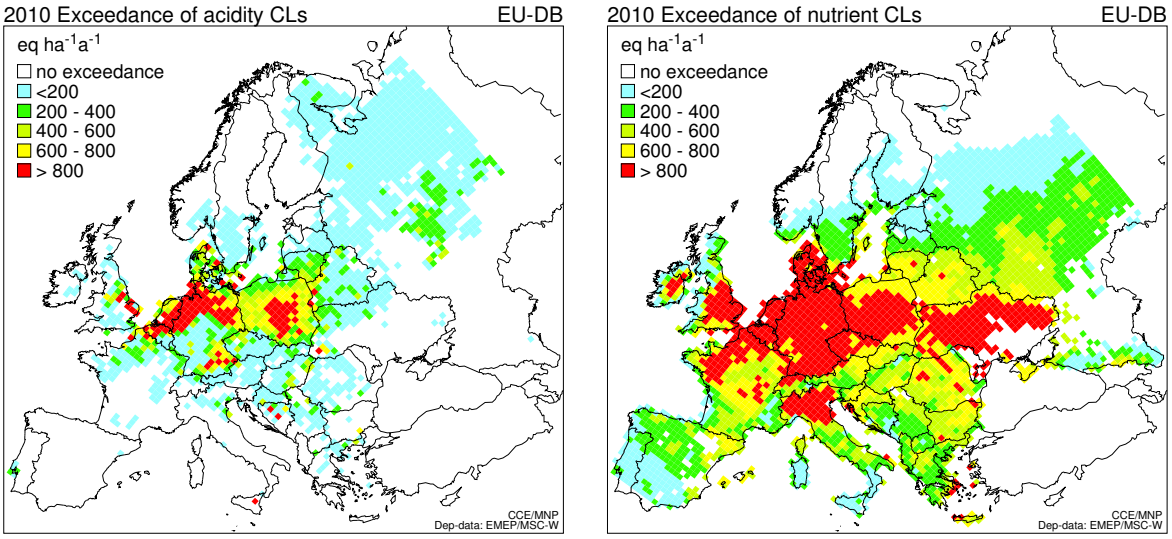

Figure 3-2. The average accumulated exceedance (AAE) of the acidity critical loads (left) and the critical loads of nutrient nitrogen (right), using the deposition to forests in 2010, assuming the implementation of current legislation (Gothenburg Protocol and EU NEC Directive).

Not only critical loads can be calculated with the European background database, also simulations with the dynamic soil acidification model VSD (Posch and Reinds, 2005), which has used by many European countries (see Part II), have been carried out. Figure 3-3 shows the temporal development of two major soil variables, pH and base saturation between 1990 and 2100 after running the VSD model on each of the circa 90,000 forest sites with S and N deposition constant after 2010 at 'Gothenburg level' (as used in Figure 3-2). The figure shows the temporal development of some percentiles ('percentile traces') of the distribution of those variables over the 110 years of simulation. As can be seen, the temporal development is rather unspectacular, which is not surprising for the pH, since for a constant deposition the soil solution concentrations will soon be in equilibrium with the deposited ions. Rather more surprising are the very minor changes occurring in the European distribution of base saturation, which is a slowly reacting soil variable. However, small changes in the distribution do not necessarily mean small changes at individual sites, decreases in some regions could be compensated by increases in others.

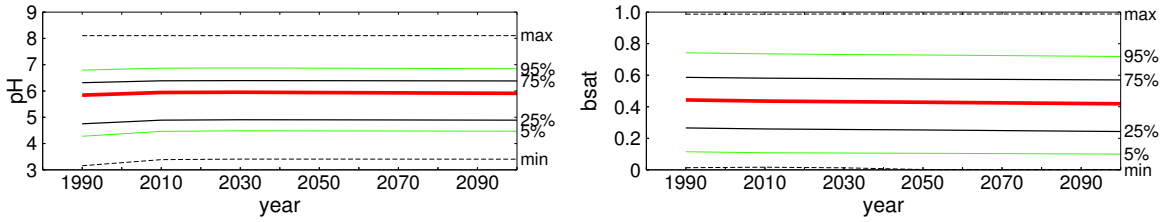

Figure 4-3. Temporal development (1990-2100) of some percentiles of pH (left) and base saturation (right) of the about 90,000 forest sites of the European background DB, when the VSD model is run with the 'Gothenburg deposition' after 2010.

Not only the variables themselves and their distributions are of interest, but also the relationship between them. Two key variables in any dynamic acidification model are the pH of the soil solution and the base saturation of the cation exchange complex. In Figure 3-4 the correlation between these two variables is shown for the year 2100, i.e. the last year of the simulation shown in Figure 3-3. The about 90,000 data points are shown in three colours, depending on the magnitude of the Gapon exchange constant for the Al-Bc exchange, K_{AlBc}. Since this is generally unknown, it is calibrated so that at every site a prescribed base saturation is obtained in 1995. The red dots in Figure 3-4 show sites for which $\log_{10}K_{AlBc}<0$, the blue dots sites for which $\log_{10}K_{AlBc}>2$, and the green ones with values between those two limits. Especially for sites with values of K_{AlBc} in the range between 0 and 2, the relationship between pH and base saturation shows an S-shaped pattern which has also been observed and/or modelled by Reuss (1983), Bloom and Grigal (1985) and De Vries et al. (1989).

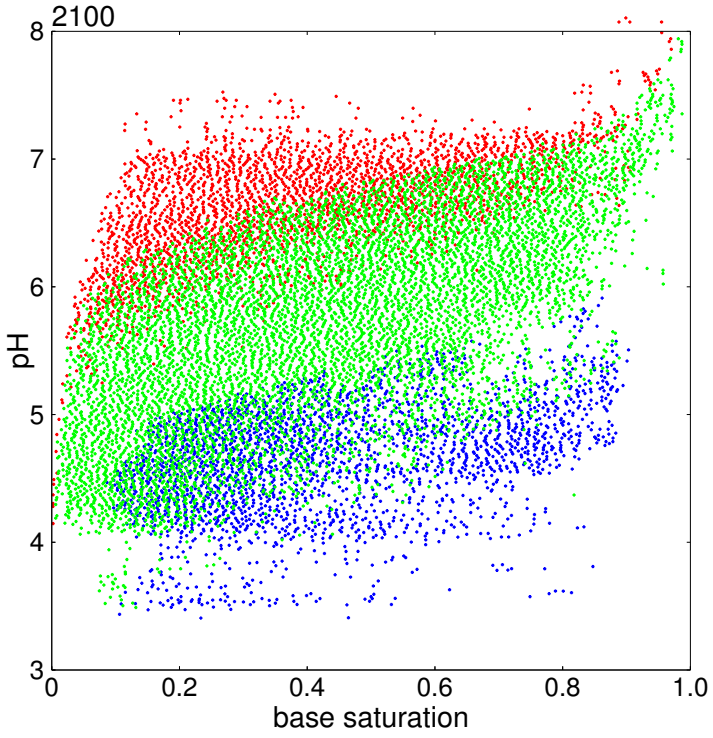

Figure 3-4. Correlation between base saturation and soil solution pH in 2100 for about 90,000 sites of the EU-DB. Red: sites with $log_{10}K_{AlBc}<0$, green: $0 \leq log_{10}K_{AlBc} \leq 2$, blue: $log_{10}K_{AlBc}>2$, where K_{AlBc} is the Al-Bc Gapon exchange constant.

In Figure 3-5 shows the correlation between two more pairs of variables at the end of the simulation of the about 90,000 European sites in 2100. The left panel illustrates, as expected, that high [Al]:[Bc] ratios are more likely to occur in soils with low base saturation; and the right panel confirms that the leaching of N is generally higher in soils with a low C:N ratio, i.e. soils which approach N saturation.

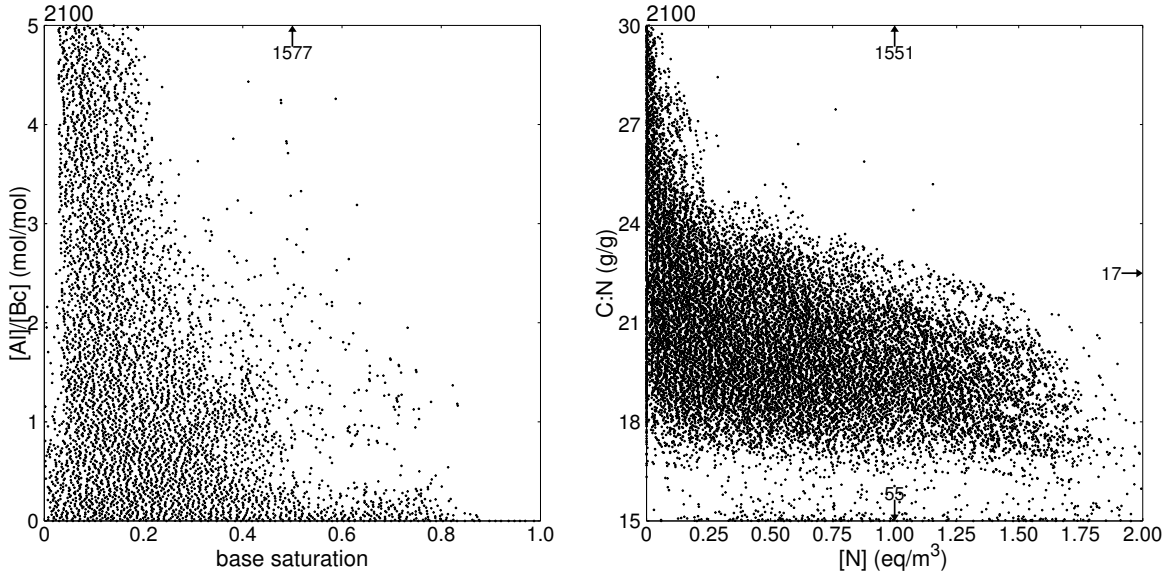

Figure 3-5. Correlation between base saturation and molar Al:Bc ratio (left) and between total N concentration in soil solution and the C:N ratio in the top soil layer (right) in 2100 for about 90,000 sites of the EU-DB.

The European background database has not only been used to compute critical loads and simulate the time development of the soils, but also to compute target loads and delay times. For acidification target loads are characterised not by a single number but by a function – very much like acidity critical loads. In Figure 3-6 the 5th percentile of the $TL_{max}(S)$ – the quantity of a target load function corresponding to $CL_{max}(S)$ in the critical load function – is displayed for the target years 2030 and 2050. By definition, a target load cannot be greater than a critical load, and for ecosystems for which no target load has to be calculated (e.g. an ecosystem which never experienced exceedance) the critical load function is, by definition, used a target load function. Thus the number of ecosystems in every grid cell is the same for critical load and target load statistics. The black-shaded grid cells in Figure 4-6 indicate cells in which for at least 5% of the ecosystem area no target loads can be calculated, i.e. even a reduction of the acidifying deposition to zero does not lead to a recovery of the ecosystem in the target year. Figure 3-6 should be compared to Figure 3-1 (left) to get an impression of the stringency of the target load as compared to the critical load.

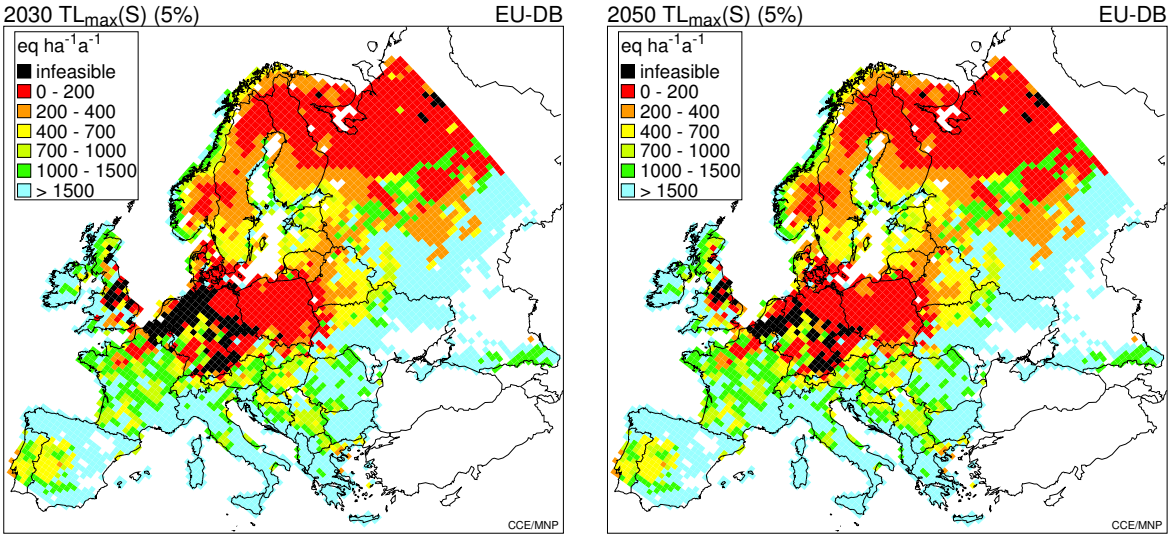

Figure 3-6. The 5th percentile of target loads $TL_{max}(S)$ for the years 2030 (left) and 2050 (right) on the EMEP50 grid, computed from the European background database.

3.5 Concluding remarks

The European background database (EU-DB) has been updated for use by the CCE to fill in gaps left by countries which do not deliver data as well as for possible studies on a European scale. The EU-DB includes the latest available data on a European scale for the calculation of critical loads and for running simple dynamic models. The database, however, is not a final product; it will be checked and updated, whenever inconsistencies in the existing data are found or new data become available.

References

Batjes NH (1996) Development of a world data set of soil water retention properties using pedotransfer rules. Geoderma 71: 31-52

Bloom PR, Grigal DF (1985) Modeling soil response to acidic deposition in nonsulfate adsorbing soils. Journal of Environmental Quality 14(4): 489-495

De Vries W, Posch M, Kämäri J (1989) Simulation of the long-term soil response to acid deposition in various buffer ranges. Water, Air and Soil Pollution 48: 349-390

De Vries W (1994) Soil response to acid deposition at different regional scales. Doctoral dissertation, Agricultural University Wageningen, Wageningen, Netherlands, 487 pp.

De Vries W, Reinds GJ, Posch M, Sanz MJ, Krause GHM, Calatayud V, Renaud JP, Dupouey JL, Sterba H, Vel EM, Dobbertin M, Gundersen P, Voogd JCH (2003) Intensive Monitoring of Forest Ecosystems in Europe. Technical Report 2003, EC-UNECE, Brussels and Geneva, 161 pp.

Eurosoil (1999) Metadata: Soil Geographical Data Base of Europe v. 3.2.8.0. Eurosoil, Ispra, Italy

FAO (1981) FAO-Unesco Soil Map of the World, 1:5.000.000; Volume V (Europe), Unesco, Paris, 199 pp.

Federer CA (1982) Transpirational supply and demand: Plant, soil, and atmospheric effects evaluated by simulation. Water Resour. Res. 18(2): 355-362

Hastings DA, Dunbar PK (1998) Development & assessment of the Global Land One-km Base Elevation Digital Elevation Model (GLOBE). ISPRS Archives 32(4): 218-221

Helling CS, Chesters G, Corey RB (1964) Contribution of organic matter and clay to soil cation exchange capacity as affected by the pH of the saturating solution. Soil Sci. Soc. Am. J. 28: 517-520

Hoekstra C, Poelman JNB (1982) Density of soils measured at the most common soil types in the Netherlands (in Dutch). Report 1582, Soil Survey Institute, Wageningen, Netherlands, 47 pp

Jacobsen C, Rademacher P, Meesenburg H, Meiwes KJ (2002) Element contents in tree compartments – Literature study and data collection (in German). Report, Niedersächsische Forstliche Versuchsanstalt, Göttingen, Germany, 80 pp

Klap JM, Brus DJ, De Vries W, Reinds GJ (2002) Assessment of site-specific estimates of critical deposition levels for nitrogen and acidity in European forest ecosystems using measured and interpolated soil chemistry. (in prep)

Leemans R, Van den Born GJ (1994) Determining the potential distribution of vegetation, crops and agricultural productivity. Water Air Soil Pollut. 76: 133-161

Mitchell TD, Carter TR, Jones PD, Hulme M, New M (2004) A comprehensive set of high-resolution grids of monthly climate for Europe and the globe: the observed record (1901-2000) and 16 scenarios (2001-2100). Tyndall Centre Working Paper 55, Norwich, United Kingdom, 30 pp.www.cru.uea.ac.uk/cru/data/hrg.htm

Posch M, Hettelingh J-P, Slootweg J, Downing RJ (eds) (2003) Modelling and mapping of critical thresholds in Europe. Status Report 2003, Coordination Center for Effects, RIVM Report 259101013, Bilthoven, Netherlands, iv+132 pp www.mnp.nl/cce

Posch M, Slootweg J, Hettelingh J-P (eds) (2005) European Critical Loads and Dynamic Modelling. Status Report 2005, Coordination Center for Effects, RIVM Report 259101016, Bilthoven, Netherlands, 171 pp www.mnp.nl/cce

Posch M, Reinds GJ (2005) VSD - User Manual of the Very Simple Dynamic soil acidification model. Coordination Center for Effects, MNP, Bilthoven, Netherlands (in prep.)

Prentice IC, Sykes MT, Cramer W (1993) A simulation model for the transient effects of climate change on forest landscapes. Ecol. Model. 65: 51-70

Reinds GJ, Posch M, De Vries W (2001) A semi-empirical dynamic soil acidification model for use in spatially explicit integrated assessment models for Europe. Alterra Report 084, Alterra Green World Research, Wageningen, Netherlands, 55 pp

Reuss JO (1983) Implications of the calcium-aluminum exchange system for the effect of acid precipitation on soils. Journal of Environmental Quality 12(4): 591-595

Schelhaas MJ, Varis S, Schuck A, Nabuurs GJ (1999) EFISCEN's European Forest Resource Database, European Forest Institute, Joensuu, Finland, www.efi.fi/projects/eefr/

Tarrasón L et al. (2004) Transboundary acidification, eutrophication and ground level ozone in Europe. EMEP Status Report 1/2004, Norwegian Meteorological Institute, Oslo. www.emep.int

UBA (2004) Manual on methodologies and criteria for modelling and mapping critical loads & levels and air pollution effects, risks and trends. Umweltbundesamt Texte 52/04, Berlin. www.icpmapping.org

Van der Salm C (1999) Weathering in forest soils. Doctoral dissertation, University of Amsterdam, Amsterdam, 288 pp

Vanmechelen L, Groenemans R, Van Ranst E (1997) Forest soil condition in Europe. Results of a large-scale soil survey. EC/UNECE, Brussels, Geneva, 261 pp

Van Loon M, Tarrasón L, Posch M (2005) Modelling base cations in Europe. EMEP/MSC-W & CCE Note 2/05, Norwegian Meteorological Institute, Oslo, 58 pp

Van Wallenburg C (1988) The density of peaty soils (in Dutch). Internal Report, Soil Survey Institute, Wageningen, Netherlands, 5 pp

4 Use of Critical Loads in Integrated Assessment Modelling

Maximilian Posch, Jean-Paul Hettelingh, Chris Heyes*

*Centre for Integrated Assessment Modelling (CIAM) at IIASA, Laxenburg, Austria

4.1 Introduction

Critical loads and their exceedances have been used in integrated assessment (IA) modelling since the negotiations leading to the Second Sulphur Protocol (Oslo, 1994). To be useable in IA models such as RAINS, the critical load information on the (currently) about 1.2 million ecosystems covering Europe has to be condensed and adapted. Since the deposition of sulphur and nitrogen species is computed on the EMEP grid, critical load information has been provided by the CCE in the form of protection and exceedance percentiles and isolines for this grid system. The methods for deriving such isolines are summarised in Chapter 8 of the Mapping Manual (UBA, 2004).

The change from the 150×150 to the 50×50 EMEP grid increased the number of grid cells by almost an order of magnitude. The distinction between different ecosystem classes (such as forests, semi-natural vegetation and surface waters) further enlarged the amount of data to be derived for IA modelling. This increase in the amount of data poses some problems for including critical loads in optimisation exercises carried out in IA modelling. Since it is not individual grids but countries that matter – after all, the grid system and size are to some extent arbitrary – , and since other pollutants (e.g. particulate matter) had to be included into the optimisation framework, the methodology for computing changes in exceedances due to changes in emissions has been simplified. The new approach has been inspired by the Life Cycle Impact Analysis (LCIA) community, which uses the simplest approach possible, i.e. a linear relationship between emission (change) and impact (change). We adopt this approach for including critical load and exceedance information into IA modelling, and in the following sections we define and derive the respective models and factors.

4.2 Methodology

In the IA modelling the average accumulated exceedance (AAE) has been used as the measure to compare emission reductions to critical load exceedances. The definitions and methods for calculating the AAE for acidity and nutrient N critical loads can be found in Chapter 7 of the Mapping Manual (UBA, 2004). And the simplest assumption (model) is that the change in the AAE for a receptor area (country) k is linearly related to the changes in all emissions of all pollutants involved, i.e.:

$$(1) \qquad AAE_{0,k} - AAE_k = f \cdot \sum_{p=1}^{P} \sum_{j=1}^{N_p} a_{p.k.j} \cdot \left(E_{0,p,j} - E_{p,j}\right), \quad k = 1,...K$$

where AAE_k is the AAE in receptor k for the new (or to be determined) emissions $E_{p,j}$ of pollutant p in emitter area j; $AAE_{0,k}$ is the AAE for the reference emissions $E_{0,p,j}$; N_p is the number of emitter regions for pollutant p, P is the number of pollutants, f is a unit conversion factor, and K is the number of receptor areas. Finally, $a_{p,k,j}$ are the coefficients determining the linear model, characterising the 'strength' of the relationship between emissions of pollutant p in country j and AAE in region k. We call the coefficients $a_{p,k,j}$ (region-to-country) *impact factors* (of pollutant p).

Eq.1 holds for the AAE of both nutrient N (eutrophication) critical loads and critical loads of acidity. In the first case the number of pollutants is P=2, namely NO_x and NH_3, whereas in the latter P=3, where the third pollutant is SO_2. Note that despite the fact that only total N deposition is needed in the calculation of exceedances, NO_x and ammonia emissions have to be considered separately, since they contribute in different ways to total N deposition (different sources and different behaviour in the atmosphere).

In mathematical terms, eq.1 is nothing but the linear term in the Taylor expansion of AAE_k, as a function of the emissions, around a given point ($\boldsymbol{E}_0$, $AAE_{0,k}$) with $\boldsymbol{E}_0=(E_{0,1,1}, \ldots, E_{0,P,Np})$. Thus the expression is, by definition, exact for $\boldsymbol{E}=\boldsymbol{E}_0$, and the smaller the deviations in the emissions from $\boldsymbol{E}_0$ the better the approximation will be. The task is (a) to select proper reference points ($\boldsymbol{E}_0$, $AAE_{0,k}$), (b) to derive the set of impact factors $a_{p,k,j}$, and (c) to determine the range of applicability of the model, i.e. estimate the error made in comparison to exceedance calculations with the exact model.

Before carrying out these steps, the relationship to the factors used in LCIA shall be shortly discussed: In LCIA one is interested in the overall (ideally: global) impact of the change in one unit of emission. Here this would be the change in AAE in the whole of Europe which is obtained by summing over all K countries:

$$AAE = \sum_{k=1}^{K} AAE_k \qquad (2)$$

and AAE_0 is defined analogously. Summing over k in eq.1 yields then:

$$AAE_0 - AAE = f \cdot \sum_{p=1}^{P} \sum_{j=1}^{N_p} c_{p.j} \cdot \left(E_{0,p,j} - E_{p,j}\right) \qquad (3)$$

where we have defined the coefficients:

$$c_{p,j} = \sum_{k=1}^{K} a_{p,k,j} \qquad (4)$$

and it is these coefficients the LCIA community is interested in. These coefficients are variably called (site-dependent) 'characterisation', 'damage' or 'impact' factors. A recent example, using the accumulated exceedance (AE) as 'impact category indicator', can be found in Seppälä et al. (2005). Keeping in mind the definition of a critical load, the most obvious indicator would be ecosystem area protected, and it has been studied as well (e.g., Krewitt et al., 2001; Hettelingh et al., 2005). However, it turns out that the linearity assumption is not always fulfilled in this case, and caution should be exercised when using a linear model for 'protected ecosystem area' as impact category indicator. See Appendix B for a description of impact factors that could be considered by experts in the field of Cost Benefit Analaysis including preliminary results with respect to dynamic modelling.

4.3 Results

The choice of reference emissions $\boldsymbol{E}_0$ for the linear model is limited: It has to be emissions for which the (ecosystem-specific) deposition fields have been computed with the full atmospheric transport model, the Unified Model of EMEP/MSC-W in this case (see Tarrasón et al., 2004), thus allowing AAE_0 to be computed exactly. And the emissions should not be too far away from the expected (new) emissions, for which the model is used, in order to increase the probability that the linear model is a good approximation of 'reality'. Therefore we used the country emissions for the year 2010 from the so-called baseline scenario 'current legislation' ('BL_CLE'), which has been prepared for the EU's Clean Air for Europe (CAFE) programme (Amann et al., 2005). The impact factors $a_{p,k,j}$ are then computed by changing the emission of pollutant p in source region j, leaving the emissions of the other pollutants and all other source regions unchanged. With this special emission vector the corresponding exceedances AAE_k are computed. Then this special case is inserted into eq.1, leaving only a single term on the right-hand side, from which the impact factors for every receptor country k can be obtained as:

$$a_{p,k,j} = \frac{AAE_{0,k} - AAE_k}{E_{0,p,j} - E_{p,j}}, \quad k = 1,\ldots,K \qquad (5)$$

For every such emission change the corresponding AAE_k's have to be computed, and this means running the exact atmospheric transport model, or having an approximate version available, such as the source-receptor matrices in case of the old EMEP lagrangian model. Due to the inherent non-linearities in the Unified Model, no such general source-receptor matrices exist. But the Unified Model has been run for a 15% emission reduction for each pollutant in each of the 51 source regions. And thanks to this database the impact coefficients can be computed without approximations. It should be noted, that the (weak) cross-correlations, e.g., the change in ammonium

deposition due to changes in sulphur emissions have been neglected here (although there is no principal problem to include them).

Since there are critical loads data for 36 receptor countries, the calculations result in (51+46+51)×36= 5328 impact coefficients for acidification and (51+46)×36=3492 coefficients for nutrient N. Tabulating these almost 9,000 values with sufficient precision, would result in quite unwieldy tables, making a comparison and interpretation almost impossible. However, this is facilitated with the aid of the graphical representations shown in Figures 4-1 and 4-2. Every cell in the matrices represents an impact coefficient for the respective source-receptor combination for the chosen pollutant and effect. The colour represents the size class (see legend in Figure 4-2) with darker/redder colours indicating higher values. The cells are identified by the ISO 3166 2-letter country codes (ISO, 2005); the 3-letter codes ASI and NOA are for the remaining Asian and African areas within the EMEP modelling domain, respectively; and 5 sea areas: ATL=Atlantic, BAS=Baltic Sea, BLS=Black Sea, MED=Mediterranean, NOS=North Sea. The coefficients are in meq $ha^{-1}kt^{-1}$, i.e. if emissions are given in kt a^{-1} of NO_2, NH_3 or SO_2, respectively, one has to set $f=10^{-3}$ in eq.1 to obtain the AAE in the customary units of eq $ha^{-1}a^{-1}$.

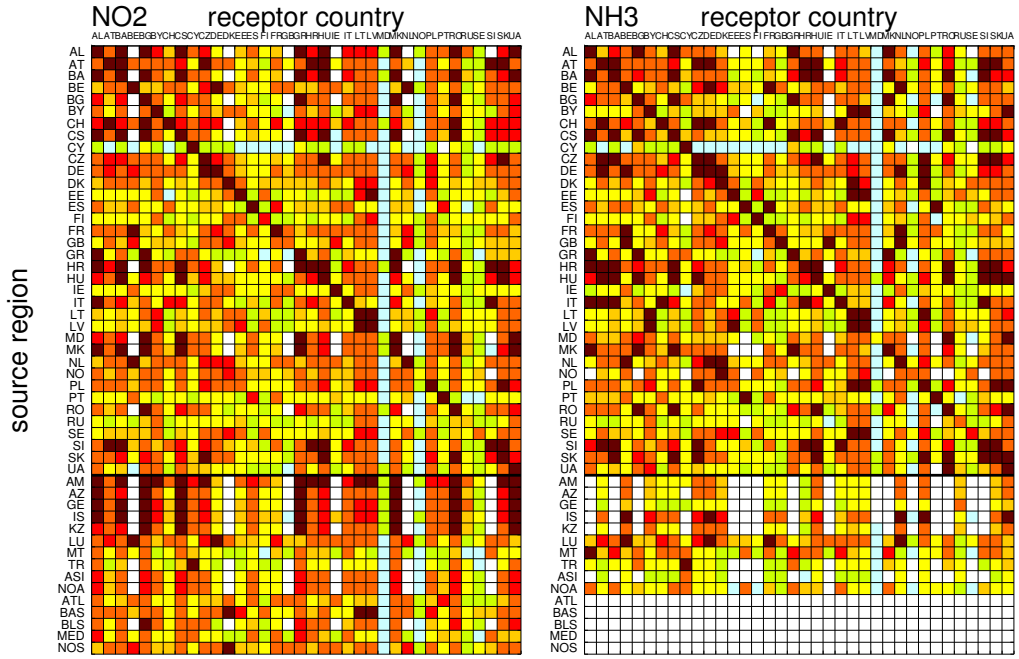

*Figure 4-1. Graphical representation of the impact factors for **eutrophication** for the emissions of NO_2 and NH_3. The upper square represents the source-receptor relationship for the alphabetically ordered 36 countries for which critical loads data are available (see Figure 5-2 for the legend and the text for the codes).*

The generally more reddish colour of the eutrophication panels (Figure 4-1) compared with the acidification panels (Figure 4-2) clearly indicates that exceedances of nutrient N are higher and more widespread than exceedances of acidity critical loads, which is confirmed by the maps in Chapter 1. A white column indicates that critical loads are not (any more) exceeded in that country in the reference year (here: 2010). The upper square delimited by the thick horizontal line in Figures 4-1 and 4-2 represents the AAE source-receptor relationship for the 36 countries for which critical loads data are available. Since these countries are sorted alphabetically both vertically and horizontally, the diagonal-dominance – i.e. the darker colours in the diagonal from upper left to lower right – shows that generally most of the contribution to its exceedance comes from the countries themselves. But also other sources can have a large contribution to a country's exceedance: e.g. the SO_2 emissions from international shipping in the North Sea to the exceedance of acidity critical loads in the Netherlands.

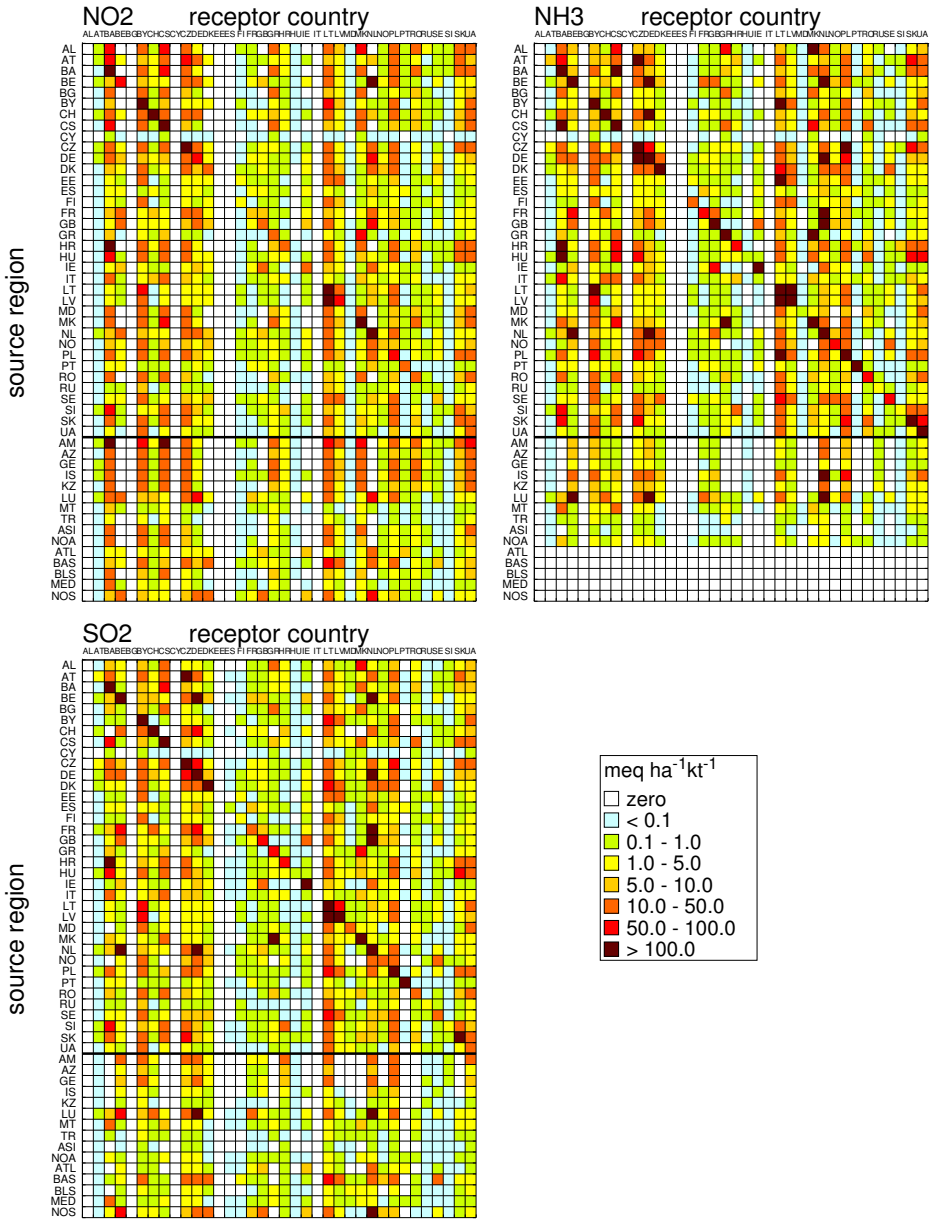

*Figure 4-2. Graphical representation of the impact factors for **acidification** for the emissions of NO_2, NH_3 and SO_2. The upper square represents the source-receptor relationship for the alphabetically ordered 36 countries for which critical loads data are available (see the text for the codes).*

4.4 How good are the linear approximations?

The use of the linear model derived above, e.g. in the optimisation mode of the RAINS model, inevitably raises the question of how much it deviates from exact calculations (within the foreseeable range of application). First we investigate how much the exceedance in a country differs from linearity as a function of the emission changes in a single source region. This is done by computing the AAE with the full model and check 'how linear' the results are. This is illustrated in Figure 4-3; for two countries it shows the AAE as a function of the reduction in a single pollutant (NO_2 and NH_3 in the case of eutrophication, SO_2 in addition for acidification) in one source region. It can be seen that for emission reductions up to 50% the relationship is quite linear. In fact, in all cases displayed each correlation coefficient for the ten sets of 51 data points is above –0.999.

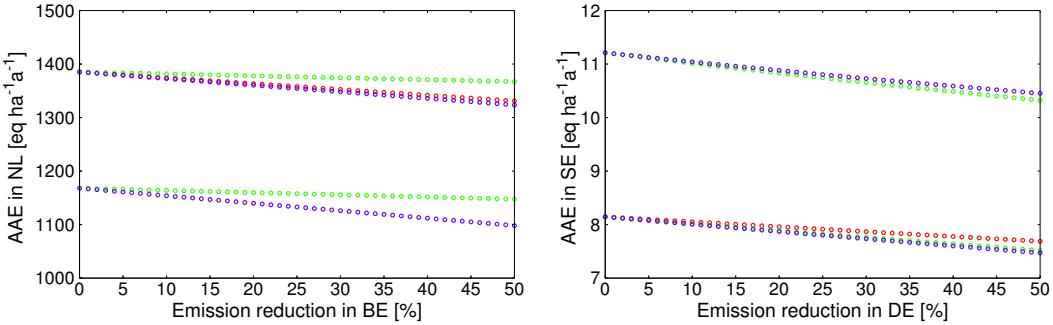

Figure 4-3. Acidification and eutrophication AAE in the Netherlands (left) and Sweden (right) as a function of emission changes in Belgium and Germany, resp. Calculations are shown in steps of 1% reduction of SO_2 (red circles), NO_2 (green) and NH_3 (blue). The data points strongly suggest in all cases a linear relationship over the whole range shown.

Changing the emissions in a single source region (as shown in Figure 4-3) is, in general, a small overall change and thus linearity might be expected for these so-called marginal changes. A sterner test of the linearity assumption is to change the emissions in *all* source regions simultaneously. Figure 4-4 shows the AAE for acidification and eutrophication in the United Kingdom and Europe as function of simultaneous percent emission reductions in all source regions. Also shown are the straight lines resulting from the linear model derived in this chapter. The graphs indicate that for reductions up to at least 20% the linear model provides a very good approximation. It is also clear from general considerations – and the graphs support this – that the linear model fails if one gets closer to zero exceedance: While the exact calculations will never yield a negative AAE, the linear model intersects at some point with the x-axis, and thus for all reduction beyond that point would yield a negative AAE. To avoid negative values, the left-hand side of eq.1 has to be set to zero if AAE_k becomes greater than $AAE_{0,k}$.

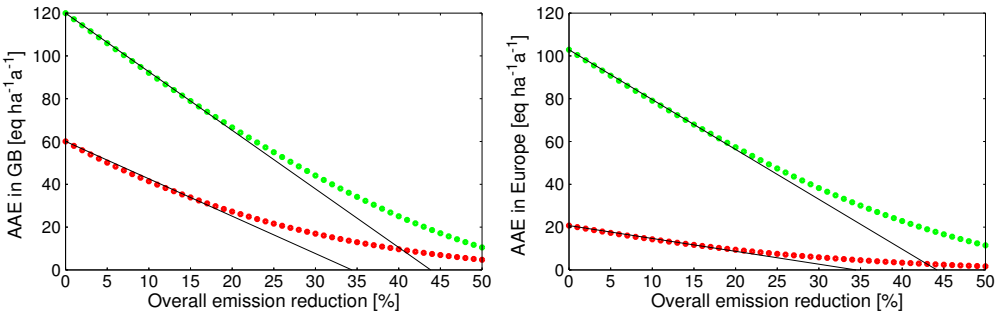

Figure 4-4. AAE in the United Kingdom (left) and Europe (right) for acidification (red) and eutrophication (green) as a function of equal percent emission reductions in all source regions and for all pollutants. The black straight lines show the linear model derived above.

4.5 Future work

The linear model to compute the AAE in European countries for emission reduction scenarios turns out to be a very good approximation as long as the reductions stay below 20%, and are still acceptable in many cases for higher reduction percentages. However, to gain more confidence, and possibly improve the model, the following points should be considered:

- To make optimal use of the model, the reference case ($\boldsymbol{E}_0$, AAE_0) should be taken as close as possible to investigated scenarios, thus minimising the error made due to the linearization. E.g., one could take

emissions which are, say, 20% below the 2010 emissions as reference case. Any expected change from 2010 emissions would then probably be close to this reference case.

- The investigation of the error made by the linearization should be made more systematic, i.e. all source-receptor relationship should be investigated.
- The inclusion of cross-correlations between the pollutants, i.e. the influence of a reduction in X on the deposition of Y, should be considered.
- To better capture the approach to zero AAE, one could investigate some simple non-linear (e.g. second-order) model. However, any such increase in complexity has to be carefully balanced with its impact on the optimisation routines used in integrated assessment.

It should be kept in mind that the linear model for calculating exceedances will always result in approximations. Thus it is strongly recommended to check any final result by an *ex-post* calculation using the exact procedures.

References

Amann M, Bertok I, Cabala R, Cofala J, Heyes C, Gyarfas F, Klimont Z, Schöpp W, Wagner F (2005) A final set of scenarios for the Clean Air For Europe (CAFE) Programme. Final Report to the European Commission, International Institute for Applied Systems Analysis, Laxenburg, Austria, 103 pp. www.iiasa.ac.at/rains

Hettelingh J-P, Posch M, Potting J (2005) Country-dependent characterisation factors for acidification in Europe – A critical evaluation. International Journal of Life-Cycle Assessment 10(3):177-183 <DOI: http://dx.doi.org/10.1065/lca2004.09.182>

ISO (2005) www.iso.org/iso/en/prods-services/iso3166ma/02iso-3166-code-lists/list-en1.html

Krewitt W, Trukenmüller A, Bachmann TM, Heck T (2001) Country-specific damage factors for air pollutants: a step towards site dependent life cycle impact assessment. International Journal of Life-Cycle Assessment 6(4): 199-210

Seppälä J, Posch M, Johansson M, Hettelingh J-P (2005) Country-dependent characterisation factors for acidification and terrestrial eutrophication based on accumulated exceedance as an impact category indicator. International Journal of Life-Cycle Assessment, OnlineFirst <DOI: http://dx.doi.org/10.1065/lca2005.06.215>

Tarrasón L et al. (2004) Transboundary acidification, eutrophication and ground level ozone in Europe. EMEP Status Report 1/2004, Norwegian Meteorological Institute, Oslo. www.emep.int

UBA (2004) Manual on methodologies and criteria for modelling and mapping critical loads & levels and air pollution effects, risks and trends. Umweltbundesamt Texte 52/04, Berlin. www.icpmapping.org

Appendix A Instructions for the Call for Data

This Appendix is a reprint of the instructions as it was sent to the national focal centres with the call for data.

Instructions for Submitting Critical Loads and Dynamic Modelling Data

Coordination Center for Effects (CCE), Bilthoven, November 2004

1. Introduction

This document contains the instructions for the submission of data to the CCE on critical loads of acidity and eutrophication as well as dynamic modelling output.

Your submission should contain the following key outputs:

(1) Updated critical loads; and input variables to allow consistency checks and inter-country comparisons (Table 1; and Table 4 for surface waters)

(2) Target load functions for target years 2030, 2050 and 2100; and a damage or recovery delay time (Table 2)

(3) Values of chemical variables (e.g. Al concentration) in 1990, 2010 and in the target years for two different scenarios (Table 3)

(4) A document describing the sources and methods used to produce the data.

Please note:

- The deadline for the submissions is **28 February 2005**.
- The preferred file format of the data is an Access database file (mdb), but also files with formats of DBase, Excel, or comma separated ASCII files are accepted. The easiest way to comply with the requested format is to use an Access database that is made available by the CCE.
- Please email your submission to jaap.slootweg@rivm.nl . The data can be attached to the email, but large data files can also be uploaded using ftp to ftp://ftp.mnp.rivm.nl/cce/incoming/. If you have used ftp, please inform J. Slootweg with an email.
- Target load functions are asked for the **target years 2030, 2050 and 2100**[3], all with the **implementation year 2020**[1], in which deposition reductions after the **protocol year 2010** are fully implemented (see last section for details).
- Historic depositions of nitrogen and sulphur up to the Gothenburg protocol, and depositions originating from natural sources (background) are available from the CCE upon request.
- All information is also available on our website under ***News***: www.rivm.nl/cce

[3] The Working Group on Strategies and Review at its 36th session (Geneva, 13-16 September 2004) confirmed the choice of the implementation and target years. However, it noted that the target year 2100 should be used for scientific purposes only.

2. Most important changes since the last call for data:

- The implementation year has changed from 2015 to **2020**[1].
- The target load functions are **NOT** to be minimised with the critical load function.
- The values of output variables that are related to criteria for acidification are requested. for 5 years, using (1) deposition values following the Gothenburg protocol in 2010 keeping them constant for years thereafter (this scenario is abbreviated **Go** in the remainder of these Instructions) and (2) a deposition scenario based on EMEP MSC-W background values (**Bg)** as of the implementation year (see Table 3).
- The structure of Table 2 has been simplified, now containing a single row for each site.
- The status variables used as indicators for dynamic modelling are more clearly defined.
- New VSD features, e.g. calibration also for Gaines-Thomas exchange and arbitrary exponent *expAl*.
- The computation of Damage Delay Times (DDT) and Recovery Delay Times (RDT)
- The software provided by the CCE now enables you to perform consistency checks on your critical load database. Therefore it is important to use 'null' (i.e. 'nothing') to indicate missing or no value, and ***not***, e.g., '-1' or '-999' or '0'.

3. Data structure

The data structure is summarized in Tables 1 to 4 described below.

The easiest way to assemble and submit data is to use either of the two template **Access** databases that are provided by the CCE**,** one for VSD users (**VSD05NS.mdb**) and the second for NFCs that use other software/models (**call05NS.mdb**).

Both VSD05NS.mdb and call05NS.mdb contain 3 Tables, '*inputs*', '*targetloads*' and '*scenvars*', resp., with the attributes listed and described in Tables 1-3 of these Instructions respectively. VSD05NS.mdb is the ACCESS version of the VSD model, tailored for this call. After activation it automatically fills Tables 2 and 3. The file call05NS.mdb cannot automatically fill Tables 2 and 3, since results depend on the dynamic model(s) used by the NFC. It also includes Table 4 for the convenience of surface water modellers.

Finally, both VSD05NS.mdb and call05NS.mdb include software which allows you to perform consistency checks on your data. These checks can be carried out (see operating details provided on the CCE site or when receiving VSD05NS.mdb) and will generate screen messages.

The database call05NS.mdb and a more detailed description on how to make use of its features can be downloaded from our website www.rivm.nl/cce under 'News'.

Upon request of an NFC the CCE will provide the Access file VSD05NS.mdb including the deposition pathways 'Go' and 'Bg' for EMEP50-grid cells covering the requesting country. Scenario 'Go' includes grid average, semi-natural vegetation and forest specific deposition values; and the default for VSD will be set to forest specific deposition (if you wish to use VSD also for semi-natural vegetation, you will have to replace the deposition).

The CCE recommends using deposition files generated by the CCE in collaboration with EMEP MSC-W. However, these deposition files have to be requested from the CCE, if you do not use VSD (in which case they are contained in VSD05NS.mdb).

Every ecosystem within an EMEP50-grid cell for which critical loads are provided is represented in the Table 1 by one line (record), and every record has 47 entries, holding site information on critical loads, and input data for

CLs and dynamic modelling[4]. Records for which no dynamic modelling results are calculated should contain the value '–1' in the column 'DMstatus'. The target load functions themselves are to be submitted according to the structure given in Table 2. Finally, Table 3 contains the values of 7 chemical variables for 5 years obtained by running the dynamic model with the 2010 (Gothenburg) depositions kept constant afterwards ('Go') or reduced to depositions from natural sources only ('Bg'). Entries for Tables 1–4 are described in more detail below.

3.1 Data structure of critical loads and input data:

Table 1. Attributes of the table 'inputs' (47 columns; for surface waters see Table 4).

Variable	**Explanation**	Note
SiteID	Identifier for the site	1)
Lon	Longitude (decimal degrees)	2)
Lat	Latitude (decimal degrees)	2)
I50	EMEP50 horizontal coordinate	3)
J50	EMEP50 vertical coordinate	3)
EcoArea	Area of the ecosystem within the EMEP grid cell (km^2)	4)
CLmaxS	Maximum critical load of sulphur (eq ha^{-1} a^{-1})	
CLminN	Minimum critical load of nitrogen (eq ha^{-1} a^{-1})	
CLmaxN	Maximum critical load of nitrogen (eq ha^{-1} a^{-1})	
CLnutN	Critical load of nutrient nitrogen (eq ha^{-1} a^{-1})	
nANCcrit	The quantity $-ANC_{le(crit)}$ (eq ha^{-1} a^{-1})	5)
Nleacc	Acceptable nitrogen leaching (eq ha^{-1} a^{-1})	
crittype	Chemical criterion used: 1: molar [Al]:[Bc]; 2: [Al](eq/m^3); 3: base sat.(-); 4: pH; 5: [ANC](eq/m^3); 6: molar[Bc]:[H]; 7: molar [Bc]:[Al]; 0: empirical; –1: other	
critvalue	Critical value for the chemical criterion (given in *crittype*)	
thick	Thickness (root zone!) of the soil (m)	
bulkdens	Average bulk density of the soil (g cm^{-3})	
Cadep	Total deposition of calcium (eq ha^{-1} a^{-1})	6)
Mgdep	Total deposition of magnesium (eq ha^{-1} a^{-1})	6)
Kdep	Total deposition of potassium (eq ha^{-1} a^{-1})	6)
Nadep	Total deposition of sodium (eq ha^{-1} a^{-1})	6)
Cldep	Total deposition of chloride (eq ha^{-1} a^{-1})	6)
Cawe	Weathering of calcium (eq ha^{-1} a^{-1})	6)
Mgwe	Weathering of magnesium (eq ha^{-1} a^{-1})	6)
Kwe	Weathering of potassium (eq ha^{-1} a^{-1})	6)
Nawe	Weathering of sodium (eq ha^{-1} a^{-1})	6)
Caupt	Net growth uptake of calcium (eq ha^{-1} a^{-1})	6) 7)
Mgupt	Net growth uptake of magnesium (eq ha^{-1} a^{-1})	6) 7)
Kupt	Net growth uptake of potassium (eq ha^{-1} a^{-1})	6) 7)
Qle	Amount of water percolating through the root zone (mm a^{-1})	6)
lgKAlox	Equilibrium constant for the Al-H relationship (log_{10}) (The variable formerly known as Kgibb)	8)
expAl	Exponent for the Al-H relationship (=3 for gibbsite equilibrium)	8)

[4] NFCs who wish to make more detailed analyses of individual sites can use the "VSDStudio" software, developed in collaboration with Alterra and available on the CCE website.

pCO2fac	Partial CO_2-pressure in soil solution as multiple of the atmospheric CO_2 pressure (-)	6)
cOrgacids	Total concentration of organic acids (m*DOC) (eq m^{-3})	6)
Nimacc	Acceptable nitrogen immobilised in the soil (eq ha^{-1} a^{-1})	9)
Nupt	Net growth uptake of nitrogen (eq ha^{-1} a^{-1})	6)7)
Fde	Denitrification fraction (0<=fde<1) (-)	6)10)
Nde	Amount of nitrogen denitrified (eq ha^{-1} a^{-1})	6)10)
CEC	Cation exchange capacity (meq kg^{-1})	DM)
Bsat	Base saturation (-)	DM)
yearbsat	Year in which the base saturation was determined	DM)
lgKAlBc	Exchange constant for Al vs Bc (log_{10})	DM)
lgKHBc	Exchange constant for H vs Bc (log_{10})	DM)
Cpool	Amount of carbon in the topsoil (g m^{-2})	DM)
CNrat	C/N ratio in the topsoil (g/g)	DM)
yearCN	Year in which the CNrat and Cpool were determined	DM)
DMstatus	–1: no dynamic modelling for this site 0: non-violation of criterion & non-exceedance at present 1: Target Load information is given in Table 2	
EUNIScode	EUNIS code, max. 4 characters	11)

Notes on Table 1 (see last column):

1) Use integer values only (4-bytes)!
2) The geographical coordinates of the site or a reference point of the polygon (sub-grid) of the receptor under consideration (in decimal degrees, i.e. 48.5 for 48°30', etc.)
3) Indices (2-byte integers) of the 50km x 50km EMEP-grid cell in which the receptor is located. It is the grid with North Pole at (8,110) as described in the 2003 CCE Status Report, Appendix A, p.127.
4) Please remove spurious records with an ecosystem area smaller than 0.01 km^2.
5) The **negative** Acidity Neutralising Capacity, equal to $Al_{le(crit)} + H_{le(crit)} - HCO_{3,le(crit)}$ [$-OrgAcids_{le(crit)}$].
6) Values used in the critical load calculations.
7) These are net uptakes equal to the annual average amount removed from the site by harvesting.
8) From the equation $[Al]=KAl_{ox}\cdot[H]^{expAl}$ (with [Al] and [H] in mol/L). For help with unit conversions see Appendix C of the 2003 CCE Status Report.
9) In general this will *not* be the amount immobilised at present! If data permit calculate Nimacc as $N_i+N_{fire}+N_{eros}+N_{vol}-N_{fix}$ (see Mapping Manual at www.icpmapping.org).
10) These two are mutually exclusive, i.e. one of them has to be null!
11) You can find all the information on EUNIS codes at http://eunis.eea.eu.int/eunis/index.jsp

DM) These variables are used for dynamic modelling only.

3.2 Data structure for Target Load Functions and Delay Times:

Table 2 is automatically filled by VSD05NS.mdb for ecosystem sites for which in Table 1 the attribute 'DMstatus' is equal to 1, i.e. for which target loads exist.

A Target Load Function (TLF) in a target year consist of **4 nodes** (combinations of N and S depositions) of which the first is the (N,S) combination in year *y* (*y*=2030, 2050, 2100) with zero N deposition, i.e. (0,depS1_*y*) and the

last for zero S deposition, i.e. (depN4_*y*,0). More than four nodes cannot be accepted. If the TLF consists of 3 nodes only, i.e. (0, depS1_*y*), (depN2_*y*, depS2_*y*) and (depN3_*y*,0), then (0,0) should be inserted for (depN4_*y*,depS4_*y*).

The Recovery Delay Time (RDT) and Damage Delay Time (DDT) is the year after 2010 and before 2100, generated with the deposition scenario **Go**. If recovery takes place before 2010 the RDT attribute should be set to 0; and if recovery occurs after 2100 then the RDT attribute should be 9999. Analogously, 0 and 9999 should be used when DDT is before 2010 or after 2100, respectively. Please note that it is not possible that for a single site both DDT and RDT exist simultaneously. However, it is possible that a site does not have any delay time. The concept of Recovery Delay Time (RDT) and Damage Delay Time (DDT) are further explained in a final section of this document and described in more detail in the CCE Dynamic Modelling Manual or Chapter 6 of the Mapping Manual.

Table 2. Attributes of the table 'targetloads' (30 columns).

Variable	**Explanation**
SiteID	Identifier for the site (relates to Table 1)
Status_2030	0: Non-exceedance in 2010 & no reduction required in target year 1: TL function present 2: Target load not feasible
Status_2050	
Status_2100	
RDT	Recovery Delay Time (a year)
DDT	Damage Delay Time (a year)
depN1_2030	N-value of first node of TLF for 2030 (should be 0!) (in eq ha^{-1} yr^{-1})
depS1_2030	S-value of first node of TLF for 2030
depN2_2030	N-value of second node of TLF for 2030
depS2_2030	S-value of second node of TLF for 2030
…	...
depN4_2100	N-value of the last node of the targetload for 2100
depS**4**_2100	S-value of the last node of the targetload for 2100 **(should be 0!)**

3.3 Data structure for scenario output:

In order to see the changes over time of the chemical status of ecosystems the following seven variables for year *a* (*a*=1990, 2010) and deposition scenario *dep* (*dep*=Go2030, Go2050, Go2100, Bg2030, Bg2050, Bg2100) are requested (concentrations are from the soil solution or, when aquatic systems are modelled, in surface water) for **all** ecosystems:

1. $[Al^{3+}]$ [eq m^{-3}] (Al_*a*; Al_*dep*)
2. [Ca+Mg+K] [eq m^{-3}] (Bc_*a*; Bc_*dep*)
3. pH (pH_*a*; pH_*dep*)
4. ANC concentration [eq m^{-3}] (ANC_*a* ; ANC_*dep*)
5. base saturation [-] (bsat_*a*; bsat_*dep*)
6. C:N ratio [g g^{-1}] (CNrat_*a* ; CNrat_*dep*)
7. Nitrogen (= $[NO_3]$ + $[NH_4]$) concentration in [eq m^{-3}] (cN_*a*; cN_*dep*)

These variables are independent of the scenario in 1990 and 2010, while for the years thereafter a distinction is required between the **Go** or **Bg** deposition scenario.

The extremes of the changes of variable values over time are assumed to be captured by the **Go** scenario (highest future depositions without emission reductions beyond what is already agreed in the Gothenburg protocol) and the **Bg** scenario (lowest possible depositions caused by non-anthropogenic emissions only). The **Bg** deposition scenario starts in 2020, and in the period 2010 and 2020 depositions are linearly interpolated between **Go** and **Bg.**

Table 3. Attributes of the table 'scenvars' (57 columns).

Variable	*Explanation*
SiteID	Identifier for the site (relate to Table 1)
Al_1990	Aluminium concentration in 1990
Al_2010	Aluminium concentration in 2010
Bc_1990	Base cation concentration in 1990
…	…
cN_2010	Nitrogen concentration in 2010
Al_Go2030	Aluminium concentration in 2030 under the **Go** scenario
Al_Go2050	Aluminium concentration in 2050 under the **Go** scenario
Al_Go2100	Aluminium concentration in 2100 under the **Go** scenario
…	…
cN_Go2100	Nitrogen concentration in 2100 under the **Go** scenario
Al_Bg2030	Aluminium concentration in 2030 under the **Bg** scenario
…	…
cN_Bg2050	Nitrogen concentration in 2050 under the **Bg** scenario
cN_Bg2100	Nitrogen concentration in 2100 under the **Bg** scenario

3.4 Aquatic ecosystems:

For aquatic ecosystems Table 1 should be replaced by Table 4 below; Tables 2 and 3 remain unchanged.

Table 4. Attributes of the table 'h2oinputs'.

Variable	**Explanation**
SiteID	Identifier for the site
Lon	Longitude (decimal degrees)
Lat	Latitude (decimal degrees)
I50	EMEP50 horizontal coordinate
J50	EMEP50 vertical coordinate
EcoArea	Area of the ecosystem(whole catchment) within the EMEPgrid (km^2)
CLmaxS	Maximum critical load of sulphur (eq ha^{-1} a^{-1})
CLminN	Minimum critical load of nitrogen (eq ha^{-1} a^{-1})
CLmaxN	Maximum critical load of nitrogen (eq ha^{-1} a^{-1})
CLnutN	Critical load of nutrient nitrogen (eq ha^{-1} a^{-1})
crittype	Criterion used: 6: [ANC](eq/m^3); 0: other
critvalue	Value of the criterion used
SoilYear	Year for soil measurements
ExCa	Exchangeable pool of calcium in given year (%)
ExMg	Exchangeable pool of magnesium in given year (%)
ExNa	Exchangeable pool of sodium in given year (%)
ExK	Exchangeable pool of potassium in given year (%)
thick	Thickness of the soil (m)
Porosity	Soil pore fraction (%)
bulkdens	Bulk density of the soil (g cm^{-3})

Nimacc	Acceptable amount of nitrogen immobilised in the soil (eq ha^{-1} a^{-1})
CEC	Cation exchange capacity (meq kg^{-1})
HlfSat	Half saturation of SO4 ads isotherm (µeq L^{-1})
Emx	Maximum SO4 ads capacity (meq kg^{-1})
Nitrif	Nitrification in the catchment (meq m^{-2} a^{-1})
Denitrf	Denitrification rate in catchment (meq m^{-2} a^{-1})
Cpool	Amount of carbon in the topsoil in the given yearCN(g m^{-2})
Npool	Amount of nitrogen in the topsoil in the given yearCN(g m^{-2})
CNRange	The C/N ratio range where N accumulation occurs
CNUpper	The upper limit of C/N ratio where N accumulation occurs
CaUpt	Net growth uptake of calcium (meq m^{-2} a^{-1})
MgUpt	Net growth uptake of magnesium (meq m^{-2} a^{-1})
KUpt	Net growth uptake of potassium (meq m^{-2} a^{-1})
NaUpt	Net growth uptake of sodium (meq m^{-2} a^{-1})
SO4Upt	Net growth uptake of sulphate (meq m^{-2} a^{-1})
NH4Upt	Net growth uptake of ammonia (meq m^{-2} a^{-1})
DepYear	Year for deposition measurements
Cadep	Total deposition of calcium (eq ha^{-1} a^{-1})
Mgdep	Total deposition of magnesium (eq ha^{-1} a^{-1})
Kdep	Total deposition of potassium (eq ha^{-1} a^{-1})
Nadep	Total deposition of sodium (eq ha^{-1} a^{-1})
Cldep	Total deposition of chloride (eq ha^{-1} a^{-1})
NH4dep	Total deposition of ammonia (eq ha^{-1} a^{-1})
NO3dep	Total deposition of nitrate (eq ha^{-1} a^{-1})
LakeYear	Year for lake measurements
Calake	Measured concentration of calcium in lake(µmol L^{-1})
Mglake	Measured concentration of magnesium in lake(µmol L^{-1})
Nalake	Measured concentration of sodium in lake(µmol L^{-1})
Klake	Measured concentration of potassium in lake(µmol L^{-1})
NH4lake	Measured concentration of ammonia in lake(µmol L^{-1})
SO4lake	Measured concentration of sulphate in lake(µmol L^{-1})
Cllake	Measured concentration of chloride in lake(µmol L^{-1})
NO3lake	Measured concentration of nitrate in lake(µmol L^{-1})
RelArea	The area of the lake relative to the catchment (%)
RelForArea	The area of the forest relative to the catchment (%)
RetTime	Retention time in the lake (a)
Qs	Annual runoff flux (m a^{-1})
expAl	Exponent for the Al-H relationship ()
pCO2	Partial CO_2-pressure in the lake in relation to the atmospheric CO_2 pressure (%atm)
DOC	DOC concentration in the lake (µmol L^{-1})
Nitriflake	Nitrification in the lake (%)
Cased	Sedimentation velocity of calcium in the lake (m a^{-1})
Mgsed	Sedimentation velocity of magnesium in the lake (m a^{-1})
Nased	Sedimentation velocity of sodium in the lake (m a^{-1})
Ksed	Sedimentation velocity of potassium in the lake (m a^{-1})
NH4sed	Sedimentation velocity of ammonia in the lake (m a^{-1})
SO4sed	Sedimentation velocity of sulphate in the lake (m a^{-1})
Clsed	Sedimentation velocity of chloride in the lake (m a^{-1})
NO3sed	Sedimentation velocity of nitrate in the lake (m a^{-1})
UptNH4lake	Uptake of ammonia in the lake (in % of measured value)
UptNO3lake	Uptake of Nitrate in the lake (in % of measured value)
DMstatus	–1: no TL is calculated 0: non-violation of criterion & non-exceedance at present 1: Target load information is given in Table 2
EUNIScode	EUNIS code (C1=standing waters; C2=running waters)

4. Documentation:

Please provide the CCE with documentation to substantiate and justify sources and methods applied in response to the call for data. It is strongly recommended to apply agreed methods as described in the Mapping Manual (www.icpmapping.org) and explicitly list and describe the deviations from the Manual.

You are requested to structure the contents of your documentation following the outline applied in the CCE progress report 2004. However, please do not apply 2-column or other layout features. The RIVM reporting requirements are currently best served with a plain single-column WORD layout.

Target Loads and Delay Times

The simplest and most straightforward use of a dynamic model is so-called *scenario analysis*. After the input data files, including (historical) deposition sequences, for a site are assembled and poorly known parameters are calibrated against observations, the model can be used to analyse the consequences of different future deposition (and land use) scenarios by comparing how selected soil chemical parameters develop over time.

Scenario analysis (in the context of dynamic modelling) is the computation of a future value of a chemical parameter for a chosen/given deposition trend as driving force, i.e., the future deposition is determined first, and then the (chemical) consequences for the soil/water are evaluated. This process could be repeated until an acceptable deposition reduction is achieved; however, this can be a lengthy trial and error process. To speed up this process, a so-called ***target load*** could be determined by back-calculating a suitable deposition path from a prescribed future value of a chemical variable, i.e. a target load is the deposition (path) which ensures that a prescribed chemical criterion (e.g., the Al/Bc ratio) is met in a given year. If it exists at all, there exists an infinite variety of deposition paths, i.e. target loads. To bring order into this multitude and to make results comparable, a target load is a deposition path characterised by three numbers (years): (i) the protocol year, (ii) the implementation year, and (iii) the target year (see Fig.1).

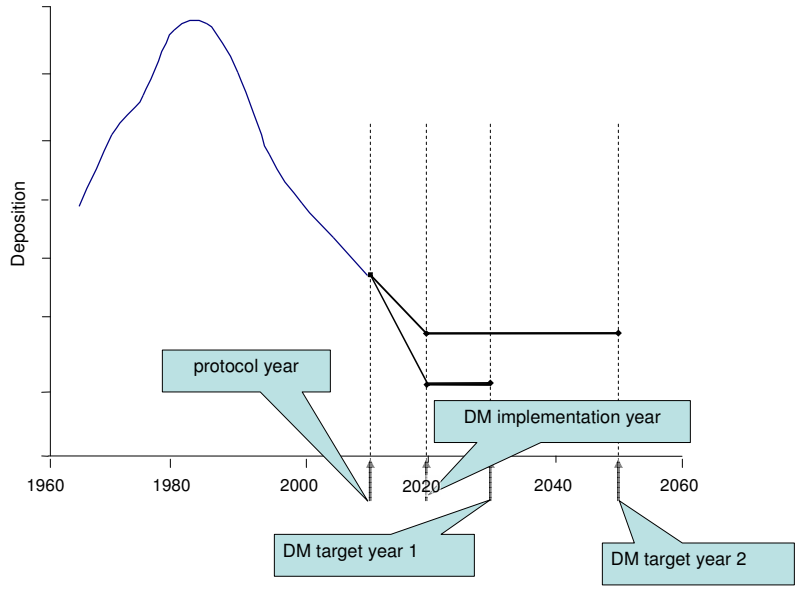

*Figure 1: Schematic representation of deposition paths leading to target loads by dynamic modelling (DM), characterised by three key years. (i) The year up to which the (historic) deposition is fixed (**protocol year**); (ii) the year in which the emission reductions leading to a target load are implemented (**DM implementation year**); and (iii) the years in which the chemical criterion is to be achieved (**DM target years**).*

The ***protocol year*** for dynamic modelling is the year up to which the deposition path is assumed to be known and cannot be changed. This can be the present year or a year in the (near) future, for which emission reductions are already agreed. An example is the year 2010, for which the Gothenburg Protocol, the EU NEC Directive and other (national) legislation is (soon expected to be) in place.

The ***implementation year*** for dynamic modelling is the year in which all reduction measures to reach the final deposition (the target load) are assumed to be implemented. Between the protocol year and the implementation year deposition are assumed to change linearly (see Fig.1). To avoid confusion with the term 'implementation year' as used by integrated assessment modellers, we (occasionally) prefix it with 'DM' for 'dynamic modelling'.

Finally, the ***target year*** for dynamic modelling is the year in which the chemical criterion (e.g., the Al/Bc ratio) is met (for the first time). Again, 'DM' is prefixed to emphasise the use of the term in dynamic modelling.

In summary, the above three special years and the accompanying prescriptions define a unique deposition path that is (also) referred to as target load.

In the Dynamic Modelling Manual and in Chapter 6 of the Mapping Manual it was argued and illustrated that ***a target load is the deposition for which a pre-defined chemical or biological status is reached in the target year and maintained (or improved) thereafter.*** This implies, *inter alia*, that a target load has always to be smaller (or equal) to the corresponding critical load. In addition, unnecessary calculations can be avoided by observing the following steps for calculating target loads: If at present the critical load is not exceeded and the (chemical) criterion is not violated, the site is 'safe' and no target load needs to be calculated (DMstatus=0 in Table 1). Otherwise the steps outlined in Fig.2 should be followed:

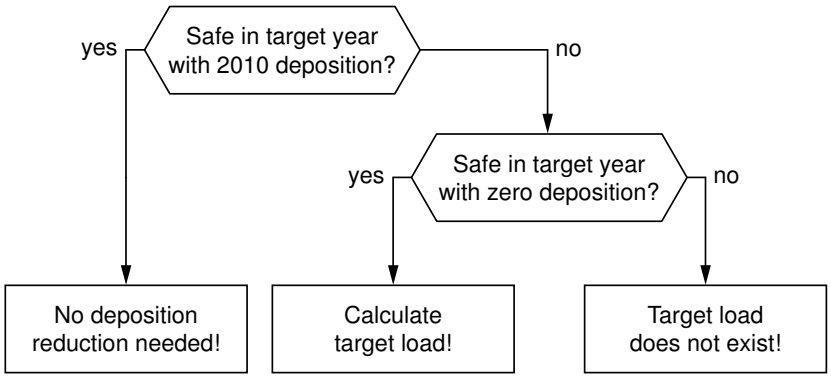

Figure 2: Decision tree for determining whether a target load has to be calculated. Note that 'Safe' means that there is non-exceedance of the critical load and non-violation of the criterion.

The above steps are automatically carried out in the VSD implementations in Access and the VSDStudio software.

So far, only a single pollutant has been considered. In the case of acidification, however, the deposition of both N and S contribute to the problem. Thus, pairs of N and S deposition have to be determined which result in the desired chemical status in the target year. And all pairs define the so-called ***target load function*** (TLF) in the (N_{dep},S_{dep}) plane, in the same way as critical loads define the critical load function. Of course, different TLFs are obtained for different target years, approaching the critical load function (CLF) when the target year moves towards infinity. Obviously, only a finite number of such pairs can be computed, and in most cases a small number will suffice. In this call for data, only 4-node TLFs are accepted by the CCE.

Examples of 4-node TLFs (for different target years) are shown in Fig.3. Due to the finite buffers in the soil, such as time-dependent immobilisation, a TLF can intersect with the CLF for certain values of the depositions (see Fig.3). To ensure that the chemical criterion is also met *after* the target year, the minimum of the TLF and the CLF has to be determined, but these computations will be carried out at the CCE.

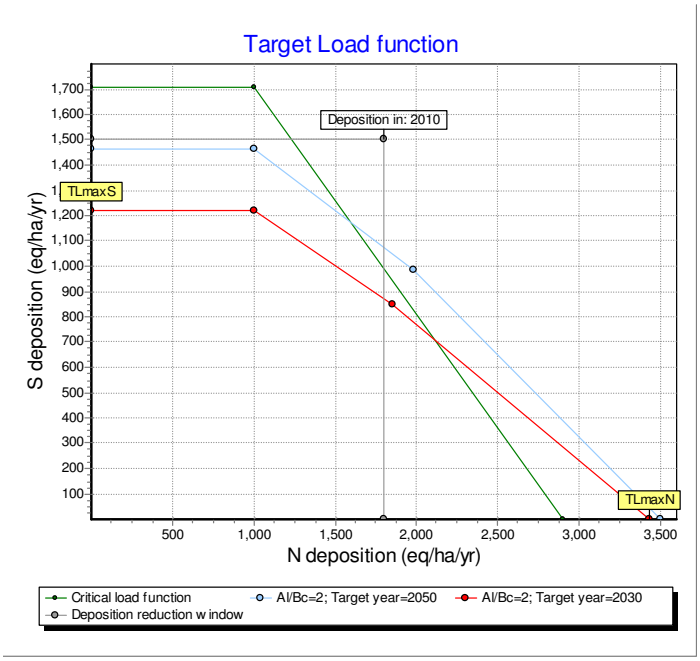

Figure 3: Examples of a 4-node target load functions for different target years (VSD-Studio output). Also shown is the corresponding critical load function (top line). The computations to determine the minimum of the TLF and the CLF will be carried out at the CCE.

Damage and Recovery Delay Times

It is often assumed that when attaining non-exceedance, i.e. when reducing deposition to (or below) critical loads, the risk of 'harmful effects' is immediately removed, i.e. the chemical criterion (e.g. the Al/Bc-ratio) that links the critical load to the effect(s), immediately attains a non-critical ('safe') value. But the reaction of soils, especially their solid phase, to changes in deposition is delayed by (finite) buffers (such as the cation exchange capacity). These buffer mechanisms can delay the attainment of a critical chemical parameter, and it might take decades or even centuries, before a desired state is reached. Only with a dynamic model can the times by computed that are involved in attaining a certain chemical state in response to given deposition scenarios. The time between the first exceedance of the critical load and the first violation of the criterion is called the Damage Delay Time (DDT), whereas the time between achieving non-exceedance and obtaining non-violation of the criterion is called Recovery Delay Time (RDT).

In this call for data the CCE asks (in Table 2) for the computation of damage and recovery delay times – or rather the year in which damage or recovery occurs – for the special case of constant S and N deposition after the protocol year (2010), i.e. for the case in which no further deposition reductions are carried out beyond the Gothenburg protocol.

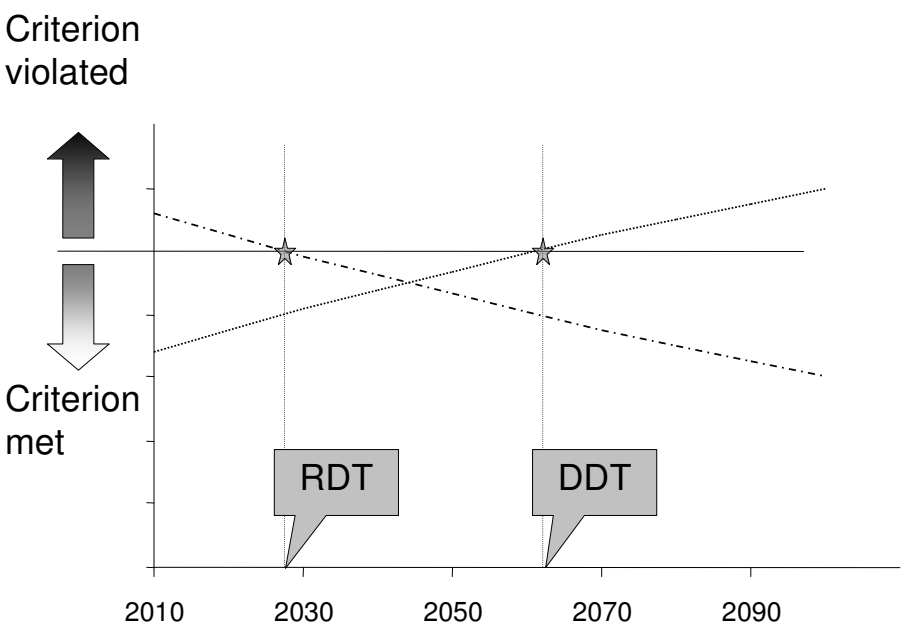

Figure 4: 'Typical' developments of a soil chemical variable (e.g. Al/Bc-ratio) in comparison to its criterion. The dashed-dotted line shows the development in case the deposition is below the critical load, whereas the dotted line shows the development for depositions exceeding critical loads. The year, in which the criterion is met [violated] for the first time, defines the Recovery Delay Time (RDT) [the Recovery Delay Time (RDT)] of the system. Note that for a criterion for which high values are 'good', the labels 'RDT' and 'DDT' have to be interchanged.

Note that:

- a damage delay exists only if there is exceedance of critical loads in the specified year (in this call 2010) , but non-violation of the chemical criterion; and
- recovery can only occur if there is non-exceedance of critical loads in the specified year, but the criterion is still violated.

In the other two possible cases – (c) exceedance and violation of the criterion, and (d) non-exceedance and non-violation – the system is 'damaged' or 'safe', respectively.

Appendix B. Exploring marginal impact coefficients for use in Integrated Assessment and Cost-effectiveness Analysis

B.1 Introduction

Economic evaluation of costs and benefits is generally based on relationships between changes in driving forces and pressures (and related costs) and changes in impacts (and related benefits). This memo focuses on marginal coefficients that establish relationships involving relative changes of pressure and impact indicators. While some have been developed and used already, other indicators described in this memo require testing and review with counterparts in the field of Integrated Assessment and Cost Benefit Analysis. This memo aims to contribute to this debate.

Impact indicators for use in integrated assessment (the RAINS model) have focused on the use of critical loads for acidification and eutrophication. They are based on the ecosystem specific comparison between atmospheric deposition and critical loads. This comparison can yield ecosystem specific information on non-exceedances and the related area of protection. This information can and has been be provided on a variety of spatial resolutions, an EMEP50 grid cell, a country, or (pan) Europe, and differentiated according to ecosystem type (EUNIS classification).

Critical load values remain constant over time while the magnitude of depositions varies with the temporal development of national emissions,. Thus the magnitude of (non) exceedance varies with emissions over time as well. This change over time of exceedances has consequences for the response time of ecosystems to recover (in case of non-exceedance) or to become damaged. Damage to an ecosystem will occur at some point in time after deposition exceeds critical loads (exceedance). By using a dynamic model for acidification we can quantify the number of years that it will take for damage (i.e. violation of the underlying critical limit value) to occur. This time lag is called Damage Delay Time (DDT). Conversely, protection will occur after critical loads are no longer exceeded. Similarly, we can quantify the number of years that it will take for an ecosystem to recover, i.e. the critical limit value to be achieved. This time delay is called the Recovery Delay Time (RDT).

The relationship between emission changes and resulting changes of exceedances has been exploited in RAINS simulations (scenario analysis and optimization) in support of the Oslo protocol (1994), the Gothenburg protocol (1999) and the NEC directive (2001). The temporal component of protection or damage has not yet been incorporated in such assessments.

The question addressed in this memo is whether quantifiable indicators can be developed that are based on the relationship between changes of national emissions and the response in terms of (non)exceedances, (non)protection or (non)recovery in time. The background is to provide further ecosystem specific information that can be useful in applications of RAINS and Extended-CBA.

Results in this memo are based on an analysis using CCE's Very Simple Dynamic (VSD) model applied to the CCE background database described in chapter 3.

While computation is not foreseen under the Service-Contract, preliminary marginal impact coefficients have been computed for illustrative purposes on the basis of critical loads and target loads. The quantification of coefficients based on other dynamic modelling concepts, such as Damage Delay Time (DDT) and Recovery Delay Time (RDT) requires additional conceptual development. For the latter coefficients a tentative description has been included in this appendix.

B.2 Marginal impact coefficients based on critical load data

The response to the latest CCE call for data includes critical loads for acidification and eutrophication for forests, semi-natural vegetation and surface waters. The EUNIS classification has been used to enhance cross border compatibility of ecosystem definition. A summary of the result of the call for data has been presented at the 15th CCE workshop and 21st meeting of the Task Force on Modelling and Mapping. Results (see CCE Status Report 2005)

This section focuses on the derivation of marginal coefficients related to critical loads and ecosystem area protection.

Marginal Ecosystem-area Protection (Marginal-EP)

The change of the area of protected ecosystems caused by the change of 1 kton of acid emissions in a country will be termed marginal ecosystem-area protection (marginal- EP). The marginal EP can be computed for (groups of) ecosystems, in (groups of) EMEP50 grid cells , in a country, or in Europe (EU25).

$$\Delta EP(e_i) = \frac{\partial(EP)}{\partial(e_i)} \qquad (1)$$

where $\Delta EP(e_i)$ is the marginal-Ecosystem area protection (e.g. in the EU25) and e_i the emission of country *i.*

The method for deriving marginal-EP coefficients has been developed, implemented and published (Hettelingh et al., 2005).

Marginal Average Accumulated Exceedance

The change of Average Accumulated Exceedance (AAE) caused by the change of 1 kton of acid emissions in a country will be termed marginal Average Accumulated Exceedance (marginal AAE). The marginal AAE can be computed for an ecosystem, in EMEP50 grid cells, in a country or in Europe (EU25) where the critical load is exceeded, as follows:

$$\Delta AAE(e_i) = \frac{\partial(AAE)}{\partial(e_i)} \quad (2)$$

whe*re $\Delta AAE(e_i)$ is the marginal AAE in the EU25 and e_i the emission of country *i*.

Table B-1 gives preliminary values for $\Delta AAE(e_i)$ using critical loads for acidification, emissions of each of the acidifying polluters and the EMEP transfer matrices used for the support of CAFE. The last two columns apply display the Marginal Average Accumulated Exceedances with respect to eutrophication. With respect to acidification it can be seen (column 3) that 1 kt of SO_2 emission reduction in Luxenburg yields a reduction by 3669 meq ha^{-1} a^{-1} of the Average Accumulated Exceedance of sensitive ecosystems in the EU25. The Marginal Average Accumulated Exceedance of ammonia of the Netherlands (column 7) is about 10228 meq ha^{-1} a^{-1}. The marginal AAE with respect to eutrophication is higher for all countries than the marginal AAE for acidification. The reason is that critical loads for eutrophication are exceeded significantly in ecosystems of most countries of the EU25.

Table B-1: Preliminary Marginal Average Accumulated Exceedance coefficients for acidifying and eutrophying pollutants, using critical loads from the CCE background database (see chapter 3).

	Acidification						Eutrophication	
	SO_2 (kt)	d(AAE)/d(SO_2) (meq $ha^{-1}a^{-1}$)	NO_2 (kt)	dAAE/d(NO_2) (meq $ha^{-1}a^{-1}$)	NH_4 (kt)	dAAE/d(NH_3) (meq $ha^{-1}a^{-1}$)	dAAE/d(NO_2) (meq $ha^{-1}a^{-1}$)	dAAE/d(NH_3) (meq $ha^{-1}a^{-1}$)
AT	30,4	401,76	159,9	181,979	56,1	667,503	1374,533	6465,44
BE	98,5	3068,043	232,2	534,031	79,4	4509,385	1394,131	11388,16
DK	17,9	1096,7	146,7	409,409	81,3	3768,27	938,842	6319,577
FI	61,3	63,653	151,3	63,579	33,8	81,865	269,7	450,058
FR	414,3	551,571	1089,4	208,237	733,3	466,93	818,155	1982,582
GR	168,1	65,469	266,4	33,416	53,6	202,725	441,632	2707,857
HU	265,7	421,483	135,3	205,596	82,5	821,945	1092,415	4390,835
IE	32,9	154,551	99	135,758	128,8	165,637	807,265	4865,667
IT	375,7	54,688	1006,1	43,851	420,8	101,794	611,705	2182,736
LU	2,8	3669,294	28,1	946,608	6,1	10211,25	3157,783	41096,73
NL	60,1	5726,59	315,4	655,095	144,4	10227,65	1272,664	12241,44
PL	1046,2	478,331	615,5	276,348	327,9	1031,945	845,358	2408,206
PT	102,7	192,682	213,6	64,641	69,2	183,81	827,841	3671,985
ES	416,4	49,204	970,3	37,733	381,7	49,986	500,611	1282,747
SE	59,1	177,496	200,5	158,046	51,3	286,517	508,732	1223,531
GB	366,3	368,371	1085,3	229,67	322,6	440,143	673,818	1690,295
EE	43,6	98,518	27,6	107,429	10,8	286,236	540,325	3133,237
LV	10,9	428,89	28,9	222,283	13,9	914,629	877,899	5111,5
LT	33,4	1078,75	41,2	349,188	55,2	2873,519	863,232	5868,168
CZ	120,5	719,089	187,1	319,83	68,3	1374,306	1287,147	5593,066
SK	53,6	453,527	72,1	231,808	32	1256,378	1140,545	6448,236
SI	22,2	158,049	39,4	106,882	19,9	186,991	1971,311	12964,7
CY	17,2	0,637	21,1	0,759	6,3	0,757	5,935	8,948
MT	11,7	20,53	5,9	9,064	1,4	26,776	134,403	310,928
DE	449,7	952,98	1182,2	340,758	623,8	1451,369	1055,738	3489,624

The CCE provided preliminary country specific marginal AAE coefficients to CIAM for implementation in the optimization algorithm of RAINS. These were based on the submission of critical loads data by Member States. Results were applied in the support of the Thematic Strategy on Air Pollution

Similarly the marginal Accumulated non-Exceedance (marginal AnE) can be computed for areas where critical loads are not exceeded as follows:

$$\Delta AnE(e_i) = \frac{\partial(AnE)}{\partial(e_i)} \qquad (3)$$

Recently the CCE provided preliminary country specific marginal AAE coefficients to CIAM for implementation in the optimization algorithm of RAINS.

A description of the method to derive $\Delta AAE(e_i)$ can be found in Seppälä (2005).

B.3 Marginal impact coefficients based on dynamic modelling data

The response of dynamic modelling data includes information on target loads (TL), target years, RDT and DDT. A target load is the deposition (path) which in the CAFÉ assessment starts in 2020 (the implementation year), and which ensures recovery by having the prescribed chemical (or, ideally, biological) criterion (e.g., the Al:Bc ratio) be met in a given year and maintained thereafter. Target loads (to be implemented with 2020 emissions) were computed to achieve critical chemical values in 2030, 2050 or 2100. RDT and DDT values were computed on the basis of a deposition path according to Base Line Current Legislation Emissions (BL-CLE) in 2010 and kept constant thereafter (until 2100).

This section focuses on the derivation of marginal coefficients related to dynamic modelling indicators.

Marginal Average Accumulated Non-Achievement (marginal-ANA)

Similar to the AAE based on critical loads, it is possible to compute Average Accumulated Non-Achievement (ANA) based on target loads. Non-Achievement means that a deposition exceeds target loads. The change of ANA caused by the change of 1 kton of acid emissions in a country will be termed marginal Average Non-Achievement coefficient (marginal ANA). The marginal-ANE can be computed for a year for which a target load can be computed. A target load becomes higher when the period becomes longer for an ecosystem to recover. When officially submitted data is used the marginal-ANA is relevant for a subset of ecosystems for which dynamic modelling data is received. When the CCE background database is used, the marginal-ANA can be computed for all forest-ecosystems for which critical loads are exceeded and the critical limit value violated "now" (which we define to be 2000). The marginal-ANA is written as follows:

$$\Delta ANA(e_i) = \frac{\partial(ANA)}{\partial(e_i)} \qquad (4)$$

The method for deriving $\Delta ANA(e_i)$ coefficients and (the meaningfulness of the) results need to be established and tested. As a first exercise the marginal-ANA was computed using the CCE backgrounddatabase.

Table B-2 illustrates results for $\Delta ANA(e_i)$ using critical loads for acidification, emissions of each of the acidifying polluters and the EMEP transfer matrices used for the support of CAFE.

Table B-2: Preliminary Marginal Average Accumulated Non-achievement coefficients for acidifying pollutants, using results of the CCE's Very Simple Dynamic model when applied to the CCE background database (see chapter 3).

Marginal Average Accumulated Non-Achievement (marginal-ANA)

	Reduction of Non-achievement (meq ha^{-1} a^{-1}) caused by 1 kt of SO_2 in 2030,2050 and 2100			Reduction of Non-achievement (meq ha^{-1} a^{-1}) caused by 1 kt of NO_2 in 2030,2050 and 2100			Reduction of Non-achievement (meq ha^{-1} a^{-1}) caused by 1 kt of NH_3 in 2030,2050 and 2100		
	2030	**2050**	**2100**	**2030**	**2050**	**2100**	**2030**	**2050**	**2100**
AT	244,388	234,038	219,055	250,189	250,042	249,676	857,994	858,424	859,033
BE	3005,158	2691,26	2467,667	716,083	712,784	705,51	6178,089	6153,88	6110,499
DK	837,958	324,498	166,735	526,084	518,595	511,985	4699,29	4623,567	4532,275
FI	25,451	22,127	21,002	92,724	92,32	91,931	161,68	161,394	161,06
FR	480,83	438,633	395,278	288,039	286,427	284,904	646,353	643,564	642,444
GR	18,489	18,206	17,947	46,59	46,587	46,585	263,829	263,868	263,858
HU	289,871	285,303	280,919	283,929	284,924	285,528	1167,117	1169,63	1175,28
IE	107,425	75,524	69,334	178,289	174,313	170,732	235,856	232,544	228,792
IT	31,619	30,388	28,544	64,426	64,464	64,381	165,965	166,084	166,023
LU	3274,292	3219,587	2981,853	1303,74	1302,284	1298,722	14261,64	14257,23	14233,23
NL	5598,92	5276,657	5012,832	784,97	780,446	775,593	11216,7	11194,88	11163,77
PL	350,195	335,142	326,008	364,044	362,822	361,667	1303,922	1302,44	1299,13
PT	100,862	99,327	97,975	83,509	83,374	83,101	259,61	259,485	259,089
ES	37,163	32,858	29,034	58,563	58,36	57,974	98,013	97,869	97,471
SE	107,501	75,713	57,959	211,943	210,101	208,485	411,835	409,264	406,882
GB	335,867	269,527	245,449	299,162	292,545	286,992	611,863	582,003	545,279
EE	40,265	32,755	31,795	155,137	154,413	153,781	495,896	495,336	494,799
LV	98,008	90,691	88,487	303,914	303,336	302,827	1346,135	1345,93	1345,68
LT	299,748	290,441	286,847	437,301	436,67	436,172	3561,186	3563,116	3564,319
CZ	593,583	575,876	548,296	447,145	446,308	445,124	2000,211	1998,441	1994,005
SK	336,934	331,291	326,716	316,23	316,128	316,093	1790,649	1792,454	1790,791
SI	96,893	93,523	87,9	149,188	149,444	149,361	265,562	267,15	267,632
CY	0,476	0,474	0,467	0,968	0,962	0,958	0,882	0,883	0,883
MT	13,141	12,751	11,835	12,708	12,691	12,649	37,131	37,205	37,128
DE	791,755	716,775	647,056	465,858	463,391	460,829	1959,362	1950,612	1940,513

Table B-2 shows that marginal-ANA coefficients decrease from 2030 to 2100. This stands to reason because recovery is likely to require lower depositions as the simulation period becomes longer. Thus 1 kton of SO_2

reduction in the Netherlands will lead to a reduction of the non-achievement of target loads by about 5599, 5277 and 5012 meq ha^{-1} a^{-1} in 2030, 2050 and 2100 respectively.

Marginal Damage Delay Time

The change of Damage Delay Time caused by the change of 1 kton of acid emissions in a country will be termed marginal Damage Delay Time. The marginal-DDT is to be explored and computed for ecosystems for which dynamic modelling data is submitted, and critical loads are exceeded. This subset includes ecosystems for which critical limits are both violated and non-violated. Considering the importance of the gap-closure concept – which maintains exceedances – in the support of both the Gothenburg protocol and NEC directive, it is argued that this indicator is likely to be (more) important.

To derive marginal DDT two steps have to be taken. Firstly, for years *y* (*y = 2021,…,2100),* or a subset thereof the DDT of ecosystems is related to the AAE of the same ecosystems. From this the change of DDT relative to the change of AAE can be established as follows:

$$\Delta DDT(AAE) = \frac{\partial(DDT)}{\partial(AAE)} \quad (5)$$

Secondly, from equation 2, we can obtain the marginal DDT by:

$$\Delta DDT(e_i) = \Delta DDT(AAE) \times \Delta AAE(e_i) = \frac{d(DDT)}{\partial(e_i)} \quad (6)$$

The method for deriving $\Delta DDT(e_i)$ coefficients and (the meaningfulness of the) results need to be established and tested.

Marginal Recovery Delay Time

The change of Recovery Delay Time caused by the change of 1 kton of acid emissions in a country will be termed marginal Recovery Delay Time. The marginal-RDT is to be (tentatively) computed for a subset of ecosystems for which dynamic modelling data were received from National Focal Centres. This subset regards ecosystems for which critical loads are <u>not</u> exceeded and the critical limit value still violated in 2000 (“now”). This situation occurs when the critical load stopped being exceeded in an historical year, while the system has been stressed for too long for the critical limit value to be achieved already. We only see the situation “now”, i.e. non exceedance while not safe, without knowing when critical loads stopped being exceeded. This situation can apply to broad parts of Europe.

The area in question for which data is available is rather small because the majority of ecosystems for which dynamic modelling has been performed turns out to address areas where critical loads are exceeded.

To derive marginal-RDT two steps have to be taken. Firstly, for each year *y* (*y =2021,…,2100)* the RDT of ecosystems is related to the AnE of the same ecosystems. From this the change of RDT relative to the change of AnE can be established as follows:

$$\Delta RDT(AnE) = \frac{\partial(RDT)}{\partial(AnE)} \quad (7)$$

Secondly, from equation 3, we can obtain the marginal RDT by:

$$\Delta RDT(e_i) = \Delta RDT(AnE) \times \Delta AnE(e_i) = \frac{\partial(RDT)}{\partial(e_i)} \quad (8)$$

The method for deriving $\Delta RDT(e_i)$ coefficients and (the meaningfulness of the) results need to be established and tested.

References

Hettelingh J-P, Posch M, Potting J (2004) Country-dependent characterisation factors for acidification in Europe – A critical evaluation. International Journal of Life-Cycle Analysis, OnlineFirst <DOI: http://dx.doi.org/10.1065/lca2004.09.182>

CCE Status Report 2005, Posch M, Slootweg J, Hettleingh JP (eds.), MNP Report 259101016/2005, 171 pp.

Hettelingh J-P, Posch M, Potting J (2005) Country dependent characterisation factors for acidification in Europe, Int.J.LCA 10(3): 177-184.

Seppälä J, Posch M, Johansson M, Hettelingh J-P (2005): Country-dependent Characterisation Factors for Acidification and Terrestrial Eutrophication Based on Accumulated Exceedance as an Impact Category Indicator. Int J LCA, Accepted, OnlineFirst <DOI: http://dx.doi.org/10.1065/lca2005.05.209>